Journal of the National Academy of Forensic Engineers®

Vol. 33 No. 1 June 2016

National Academy of Forensic Engineers®

Journal Staff

Technical Review Process

The Technical Review Committee Chair chooses the reviewers for each Journal manuscript from amongst the members and affiliates of the NAFE according to their competence and the subject of the paper, and then arbitrates as necessary during the review process. This confidential process concludes with the acceptance of the finished paper for publication or its rejection or withdrawal. The name(s) of authors are included with their published works. However, unpublished drafts together with the names and comments of reviewers are entirely confidential during the review process and are excised upon publication of the finished paper.

National Academy of Forensic Engineers®

Board of Directors

President
John P. Leffler, P.E.
Senior Member

President-Elect
Michael D. Leshner, P.E.
Fellow

Senior Vice President
Martin Gordon, P.E.
Senior Member

Vice President
Klas Haglid, P.E.
Senior Member

Treasurer
Jerry S. Ogden, P.E.
Fellow

Secretary
Paul Swanson, P.E.
Senior Member

Past Presidents

Jeffrey D. Armstrong, P.E.
Fellow

E. Ross Curtis, P.E.
Life Member

Paul R. Stephens, P.E.
Fellow

Directors at Large

John Certuse, P.E.
Fellow

Marvin M. Specter, P.E., L.S.
Life Member

Executive Director
Arthur E. Schwartz, Esq.

Submitting Proposed Papers to NAFE for Consideration

A concise abstract of approximately 100 words shall be sent to the Journal Editor for initial consideration. Upon approval of the abstract, the author will be scheduled to present their work at one of the semi-yearly NAFE Technical Conferences. A 90% complete draft copy of the manuscript shall be submitted to the Journal Editor for review and approval no later than 30 days before the conference.

For complete details about requirements for authors, visit:
www.nafe.org/assets/docs/journalcontents.pdf

For the NAFE Bylaws content "Responsibilities of, Obligations of and Guidelines for Authors, the Journal Editor, Technical Review Committee Chair, and Technical Reviewers," visit:
www.nafe.org/assets/docs/journalguidelines.pdf

Copies of the Journal

The Journal of the National Academy of Forensic Engineers® contains papers that have been accepted by NAFE. In most cases, papers have been presented at NAFE seminars. Members and affiliates receive a copy of the Journal as part of their annual dues. To obtain additional copies, the costs are as follows: $15.00 for members and correspondents of the NAFE; $30.00 for members of the NSPE not included in NAFE membership; $45.00 for all others. Requests should be sent to Arthur Schwartz, Executive Director, NAFE, 1420 King St., Alexandria, VA 22314-2794. Individual Journal papers may also be purchased and downloaded from the NAFE website at www.nafe.org.

Editor's Note

Some graphics reproduced in the black and white print edition are more clearly represented in the electronic version, which displays graphics in full color.

Comments by Readers

Comments by readers are invited, and, if deemed appropriate, will be published.
Send to: Arthur Schwartz, Esq., Executive Director, 1420 King St., Alexandria, VA 22314-2794.
Comments can also be sent via email to journal@nafe.org.

Material published in this Journal, including all interpretations and conclusions contained in papers, articles, and speeches, are those of the specific author or authors and do not necessarily represent the view of the National Academy of Forensic Engineers® (NAFE) or its members.

Table of Contents

Forensic Engineering Analysis of Unvented Gas Appliances in High Altitudes 1
By James A. Petersen, PE (NAFE 631S)

Advanced Forensic Engineering Analysis of a School Bus/Tractor-Trailer Crash. 9
By Richard M. Ziernicki, PhD, PE (NAFE 308F) and
William H. Pierce, PE (NAFE 846C)

Forensic Engineering Analysis of a Shopping Mall Explosion 25
By Jerry R. Tindal, PE (NAFE 642M)

Forensic Considerations Regarding Traction and Tribometry of Bathing Surfaces 37
By John Leffler, PE (NAFE 709S) and
Mark Blanchette, PhD

Preliminary Analysis of Roadway Accident Rates for Deaf and Hard-of-Hearing Drivers — Forensic Engineering Application 47
By Martin E. Gordon, PE (NAFE 699S) and
Justin J. Pearson

Forensic Engineering Analysis of a Sequence of Power Infrastructure Failures Atop an Office Building. 53
By Mauricio Cueva-Eguiguren, PE (NAFE 776S)

Forensic Engineering Investigation of PVC Piping Failure in a Multistory Condominium Building. 63
By John Certuse, PE (NAFE 708F)

Forensic Engineering Analysis of Failed UTV Roll Cages 69
By Olof H. Jacobson, MS, PE (NAFE 496F)
Stephen A. Batzer, PhD, PE (NAFE 677M)
Mark H. Kittel, PE (NAFE 757M)
Jesse A. Grantham, PhD, PE (NAFE 597S)
Guy J. Barbera, PE (NAFE 732M) and
Allen Molitoris, PE (NAFE 464C)

Forensic Engineering Technology Solutions for Highway Work Zone Temporary Traffic Control Investigations. 85
By Daniel J. Melcher, PE (NAFE 711S) and
Rachel E. Keller, PE (NAFE 873M)

All papers in this edition were presented at the NAFE seminar held 1/23/16 in Tampa, FL.

Forensic Engineering Analysis of Unvented Gas Appliances in High Altitudes

By James A. Petersen, PE (NAFE 631S)

Abstract

A family moves into a house about 4,000 feet above sea level. They use a refrigerator powered by LP gas. A short time after the refrigerator was installed, they notice and complain about smells and soot. They take their 9-month-old to a hospital in response to persistent crying. A short time later, they notify the refrigerator manufacturer, which examines and tests the refrigerator. They find the refrigerator's burner venturi blocked, generating high levels of carbon monoxide. Twelve years later, the parents bring a lawsuit against the installers of the refrigerator. At that time, the appliance is not available, and the house has been remodeled. A forensic engineering study is assigned to determine the effect high altitude has on this particular appliance design.

Keywords

CO, carbon monoxide, LP-gas, LPG, propane, refrigerator, high altitude, unvented appliance, derating

Introduction

This paper is a discussion of the generation of carbon monoxide (CO) from a naturally aspirated and unvented gas appliance (not derated) installed at a high altitude. The appliance type is a refrigerator, using a small LP-gas fueled flame to power an ammonia absorption system. **Figure 1** shows the subject model refrigerator and its gas train components.

Figure 1
LP-gas refrigerator, front and back.
Lower photo shows gas train components.

CO is a product of incomplete combustion. Extended exposure above certain levels is toxic. **Figure 2** shows exposure limits from several sources; however, many variations are available. Most organizations agree that an 8-hour exposure of ~9 ppm is acceptable for most of the population.

Unvented gas appliances have low input (gas) ratings. They take combustion air from the living space and discharge their combustion products into that same space. Since the appliances have low gas usage, the amount of CO generated is usually not a health concern. For the most part, unvented heaters are a concern, but cooking appliances (and, in this case, refrigerators) would also be in this category of unvented gas appliances. For comparison, unvented heaters are rated at a maximum of 40,000 BTU/hr[1] while gas refrigerators are much lower. In this situation, they are rated at 2,200 BTU/hr. Gas refrigerators are used in recreational vehicles or remote locations where electricity is not available.

James A. Petersen, PE, 1301 Spruce Street, Texarkana, TX 75501; (903) 793-8581; c3h8pete@gmail.com

Organization	Period	CO level	Notes
ASHRAE	8 hrs	9 ppm	From Standard 62.2-2013
USEPA	8 hrs 1 hr	9 ppm 35 ppm	NAAQS (outdoor air) NAAQS (outdoor air)
ACGIH	8 hrs	25 ppm	Threshold Limit Value (*)
NIOSH	8 hrs 15 min	35 ppm 200 ppm	Recommended Exp. Limit (*) Short-term Exposure Limit (*)
OSHA	8 hrs	50 ppm	Permissible Exposure Limit (*)
WHO	24 hrs 8 hrs 1 hr 15 min	6 ppm 9 ppm 30 ppm 87 ppm	indoor air indoor air indoor air indoor air
(*) above indicates a standard for an occupational situation			

Figure 2
Typical exposure duration chart.

Two lawsuits were brought by the homeowners. The first, which was later dismissed, was against the appliance manufacturer. A second lawsuit was brought 12 years later against the gas company that installed the refrigerator. In the period between the first and second lawsuit, the refrigerator was lost, and the residence was rebuilt.

Issues for the forensic engineer on the second case included unvented appliances in general, the derating of those appliances for altitude concerns, and the CO generated — if the appliance is not derated.

Background and Timeline

The family moved to a mountain state in July of 1992. There, they built a cabin in the hills at an altitude of about 4,280 feet above sea level. The cabin did not have running water or electrical service. **Figure 3** shows the cabin about two years after the exposure.

Figure 3
Family cabin about two years after the exposure.

Initially, the cabin was heated by kerosene heaters. This was later supplemented with a wood-burning stove. The family would crack the windows to ventilate the extra heat from the wood stove, and they cooked on an LP-gas oven/range. An LP-gas fuel refrigerator was installed in September of 1992. They would use a gas-powered generator to supply electricity for one to two hours in the evening.

The gas company serviced the refrigerator in October of 1992, answering a complaint about a smell and headaches. They cleaned soot from the refrigerator flue and advised the family to use it but shut it off if they smelled anything again. This refrigerator was swapped out for a new refrigerator about this time.

The mother took her infant son to the hospital in November of 1992 because he was waking up in the night crying. The hospital tested both mother and son for exposure to carbon monoxide and released them. They were advised to shut off the possible source of the CO, so they shut off the LP-gas refrigerator. No records of any hospital tests were available when the second lawsuit was filed. The possible sources of CO included:

- LP-gas fueled refrigerator, ~2200 BTU/hr, (0.86 SCFH), 700 BTU/hr pilot light
- The candles, lanterns (light)
- Kerosene heaters (rating/usage unknown)
- Wood-burning stove
  (removing combustion air from residence)
- LP-gas oven/range (rating/usage unknown)
- Gasoline-powered generator
  (outside, evening only — rating unknown)
- Vehicles

The general timeline is as follows:

- July 1992 — family moved into home the summer of 1992
- September 1992 — refrigerator installed
- October 1992 — complained of smell and soot

- October 1992 — refrigerator replaced, but smell/soot persisted

- November 1992 — 9-month-old infant taken to hospital concerning the crying
  - Hospital tested and released infant
  - Records not available

- March 1993 — initial lawsuit filed; refrigerator tested at residence by manufacturer's expert
  - ~3,500 ppm CO recorded at stack
    - before cleaning dog hair from venturi
    - ~4 minutes after startup
  - High reading after cleaning (shortly after)

- November 2005 — The author was retained on behalf of the appliance installer.
  - Subject refrigerator not available
  - Subject home substantially changed

Preliminary Investigation

In response to the initial lawsuit, the subject refrigerator was tested onsite by an expert for the refrigerator manufacturer. He first tested the refrigerator, as found, and recorded a high CO reading in the flue (~3,500 ppm). An examination revealed the venturi* was blocked with dog hair, and the vent was coated in soot. In addition, he determined the appliance had not been adjusted for high altitudes. He cleaned the venturi and vent, restarted the refrigerator, and recorded a CO reading of more than 2,000 ppm immediately after startup.

The discussion/negotiation between the plaintiff and refrigerator manufacturer is unknown. However, the third-party certification of the appliance design to a national standard (ANSI/AGA Z21.19, *Refrigerators Using Gas Fuel* [2]) was likely disclosed. The plaintiff's explanation was that the high CO reading, after cleaning, was due to the refrigerator not being derated for the altitude. The "as-found" CO reading was due to a lack of derating and the obstruction of the venturi.

The refrigerator manual included instructions for derating the refrigerator. These amounted to increasing the regulated pressure to the appliance†. Additionally, a high-altitude burner orifice (smaller diameter) was available, although not mentioned in the manual. These findings were apparently not disputed by the plaintiff's expert. The first lawsuit was dismissed.

Twelve years later, a lawsuit was filed against the gas company that had installed the refrigerator and did not derate the appliance for altitude. The plaintiff's expert had adopted the manufacturer's expert opinions and further opined that properly operating gas appliances would not generate any CO. He had not done any further testing or research. As mentioned above, the refrigerator was not available, and the residence had been rebuilt.

A literature search turned up the following related documents:

- *National Fuel Gas Code* NFPA 54 – ANSI/AGA Z223.1-1988 [3]

- National Propane Gas Association NPGA #404-1992; *Safety Warning for Operating and Servicing Propane Refrigerators* [4]

- Refrigerator literature

(All literature above circles back to NFPA 54.)

Litigation document production included sales and service records for the subject appliance. These verified that the refrigerator had not been derated for high altitude. NFPA 54, adopted as Code by the state, required that appliances be derated when installed above 2,000 feet per Code or per manufacturer's instructions.

***National Fuel Gas Code* NFPA 54 – ANSI/AGA Z223.1-1988**

"8.1.2 High Altitude. Ratings of gas utilization equipment are based on sea level operation and shall not be changed for operation at elevations up to 2,000 feet (600 m). For operation at elevations above 2,000 feet (600 m), equipment ratings shall be reduced at the rate of 4 percent for each 1,000 feet (300 m) above sea level before selecting appropriately sized equipment.

Exception: As permitted by the authority having jurisdiction."

* The venturi premixes air with the gas to a level below the flammable limit. Combustion occurs after the mixture exits the venturi and burner.

† Initially, this is counterintuitive because increased pressure would result in higher gas flow. The resulting increase in gas velocity; however, draws more air into the venture, diluting the mixture.

Manufacturer's Instructions Regarding Altitude

"…The specified fuel is propane, and the supply pressure is 11 inches of water column at sea level. At higher altitudes, we recommend that the pressure be increased according to the following table:"

ALTITUDE	PRESSURE
0' – 3,280'	11" WC
3,280' – 6,560'	11.8" WC
6,560' – 9840'	13" WC

From a technical (FE) perspective, this second lawsuit did not appear to have a great deal of merit because the subject appliance was identical to the refrigerators in recreational vehicles. These RVs regularly travel to altitudes beyond 4,300 feet and have no instructions regarding derating of any of the appliances. Nevertheless, since the injured party was young, a Code violation existed, and CO poisoning was vaguely familiar to the general public, the client decided to develop information that could be used for this and future cases. The information could be general in nature or specific to the matter at hand. This would include the effect of altitude on CO generation, unvented appliances, and the derating of appliances for altitude.

Basic subjects (questions) were developed to focus the work for this matter:

- How does altitude affect CO production in general?
- How does altitude affect CO production for this particular appliance?
- How does clogging of the venturi on this appliance affect CO production?
- What was the dilution of CO due to normal ventilation of the residence?
- Why was the CO reading so high after cleaning of the subject appliance?

How Does Altitude Affect CO Production in General?

NFPA 54 is rather specific in its formula for derating naturally aspirated appliances: 4% for each 1,000 feet above sea level (after 2,000 feet). This requirement is independent of the appliance type of or its native rating. The requirement had been in NFPA 54 for decades and likely supported by testing; however, that information was not discovered.

Instead, it was decided to conduct testing at various altitudes to obtain data for CO production. Few areas offer the range of altitudes that would allow tests to be conducted and limit variations due to local weather. The Big Island of Hawaii is one of those locations — where 0 to 6,300 feet above sea level is easily realized, and 0 to 9,000/13,000 feet above sea level is possible. Here, tests were conducted at 0, 2,000, 4,000, and 6,300 feet above sea level. A small butane stove was used for the tests, primarily because it was easily moved between tests. **Figure 4** shows the Big Island with test locations.

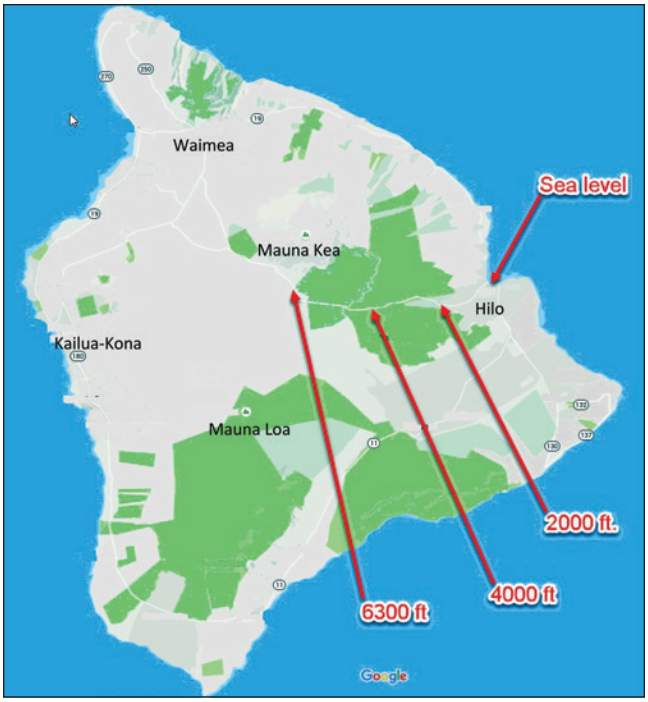

Figure 4
Island of Hawaii, showing test locations.

The methodology followed a field test developed by R. J. Karg and Associates[5]. This procedure was developed, reflecting the requirements for ANSI/CSA Z21.1-2012, *Household Cooking Gas Appliances*[6]. The stove was operated on high for ~5 minutes before collecting the sample so that a "steady-state" mixture would be realized. The combustion products were collected in a 9-inch flower pot, rather than a "hot pot" in the Karg protocol[7]. Combustion products were collected in a bag and analyzed with a standard CO monitor. The results were measurable — ranging from 13 to 28 ppm — and were repeatable, going up and down the mountain. The test setup and results are shown in **Figure 5**.

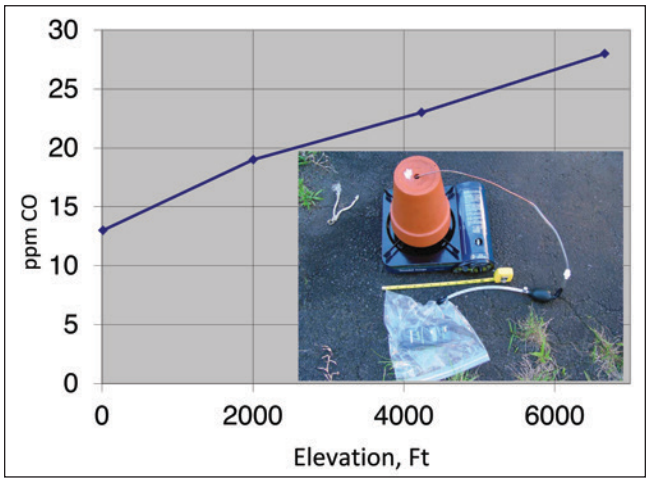

Figure 5
Test setup and chart, showing recorded CO values.

How Does Altitude Affect CO Production for This Particular Appliance?

An exemplar refrigerator was obtained, along with a high-altitude orifice. The refrigerator was mounted in a covered trailer so that it could be easily transported to a high altitude site. A combustion gas analyzer was also obtained to sample directly from refrigerator's flue (a Testo model 325XL). This gas analyzer reports CO content (O_2%, CO_2%) and temperature as well as other values.

Tests were conducted at Texarkana, TX (~280 feet) and Clovis, NM (~4300 feet). Test variables included gas supply pressure and venturi obstruction. The high altitude tests added the high altitude orifice. Results of those tests are shown in Appendices A and B. At low altitude, the CO recorded was quite low until the venturi was fully obstructed. The tests at the higher altitude were higher but still nominal until the venturi was fully obstructed. **Figure 6** shows the rear of the refrigerator and test equipment.

What Was the Dilution of CO Due to Normal Ventilation of the Residence?

The CO readings from the tests above were taken from the flue of the refrigerator. The combustion products included some amount of excess air. This excess air is necessary to ensure complete combustion and eliminate sooting. Once these combustion products leave the flue of the refrigerator, they dilute further with the air in the residence.

To determine the CO content in the living space, the undiluted CO from the flue analysis must be determined. This, in combination with the appliance rating, residence volume, and residence ventilation, can be used to determine the CO exposure.

Figure 6
Rear of refrigerator, sample location and test equipment.

Note: It would have been easier to simply operate the subject appliance as installed in the home and record the ambient CO. Since this is not possible, the flue analysis is needed to model the CO exposure.

The author started with the basic combustion equation for propane:

$$C_3H_8 + 5\ O_2 \rightarrow 3\ CO_2 + 4\ H_2O$$

Considering the nitrogen content in air:

$$C_3H_8 + 5\ O_2 + 20\ N_2 \rightarrow 3\ CO_2 + 4\ H_2O + 20\ N_2$$

The volumetric relationship for this expanded equation:

$$1 + 5 + 20 \rightarrow 3 + 4 + 20 = 27$$

Burning 1 cubic foot of propane results in 27 cubic feet of combustion products. This relationship is needed to relate the appliance rating to the volume of combustion products exhausted. For propane, 1 cubic foot of gas at standard temperature and pressure is about equal to 2,500 BTU. The orifice for the tested

refrigerator flowed, by test, at 0.869 SCFH at 11 in. WC. A higher pressure of 13 in. WC would have resulted in a flow rate of 0.945 SCFH‡.

The CO content is not significant in this combustion equation, being in the order of parts per million. From the flue analysis, the undiluted CO content can be calculated, using the CO reading and the O_2% content:

$$CO_{\text{undiluted}} = (20.9/(20.9 - O_2\%)) \times CO_{\text{ppm}}$$

The results of these calculations are shown in Appendices A and B; e.g., an analysis of 5 ppm CO with a 10.3% O_2 content would result in an undiluted 11 ppm, (App. A, top line)§.

The living area volume was calculated from measurements taken by the initial investigators. To be conservative — and eliminate arguments over closed doors impeding mixing — only the common area of the kitchen and living room was calculated. The volume for these two rooms was ~3800 ft^3. Additionally, the refrigerator was assumed to be running continuously.

For this 3800 ft^3 living area, some amount of air changes per hour (ACH) had to be assumed. These values may range from 0.5 for a very tight construction to 1.25 for a very loose construction. Based on the testimony and production, an ACH value of 1.0 was assumed for the model.

Knowing the flue flow rate (FFR), undiluted CO, interior volume (IV) and air changes per hour (ACH), the CO in the living area could be calculated as follows:

$$CO_{\text{living area}} = CO_{\text{undiluted}} \times \left(\frac{FFR}{ACH \times IV}\right)$$

The calculated levels of CO in the living area are shown in Appendices A and B. Values of less than 0.5 ppm are shown as "0."

The calculated values also assume the appliance would be operating continuously — a conservative assumption. Operating at some lower duty cycle would result in lower CO values.

Why Was the CO Reading So High After Cleaning of the Subject Appliance?

High CO readings, especially those beyond the specified range for the instrument, can saturate the sensor. The instrument must be purged with fresh air to "zero" it out. This purging process can take several minutes and is not well discussed in the instrument manuals. For normal technician work, this is not an issue because they operate at relatively low values, allowing the instrument to recover quickly.

At the initial inspection and test, the best explanation for the high readings after the venturi was cleaned is that the instrument was not zeroed out. The initial high reading may have been taken before the appliance had warmed up, creating a higher-than-normal amount of CO.

Opinions and Conclusions

After this testing and analysis, this author developed the following opinions:

- The refrigerator will generate CO, regardless of altitudes, orifices, or pressures at issue in this matter**.
- For this model refrigerator, the levels of CO generated at ~4,000 feet above sea level are not excessive.
- The CO readings measured in the earlier test by others were not due to a failure to derate the refrigerator.
- The CO readings, measured in the earlier test by others, would have been substantially reduced when diluted by the volume of the kitchen and living room.
- The failure to derate the refrigerator did not appreciably contribute to an increased generation of CO.

The matter settled soon after, and the details were not disclosed.

‡ At low pressures, the flow rate through an orifice is a function of the square root of the differential pressure. See Appendices A and B for other flow rates.

§ The Testo model used would calculate undiluted CO automatically.

** ANSI Z21.19, Section 2.4 permits a maximum of 0.03% (or 300 ppm) carbon monoxide in an air free (undiluted) sample of the flue gases.

This paper is not intended to suggest that gas appliances should not be derated for altitude. The lack of adjustment in this matter was not proximate to the generation of an abnormal amount of CO. In investigating CO incidents, it would be preferable to test the subject appliance in its "as-found" condition and settings[8]. Vented appliances may have different results. Variations of the methods described may be used to test other gas appliances. Finally, don't ignore other potential CO contributors.

References

1. ANSI/CSA Z21.11.2-2013. Gas-fired room heaters, volume II, unvented room heaters. Washington DC; American National Standards Institute.

2. ANSI/AGA Z21.19-1990. Refrigerators using gas fuel. Washington DC; American National Standards Institute.

3. ANSI/AGA Z223.1-1988. National fuel gas code. Quincy, MA; National Fire Protection Association.

4. NPGA #404-1992. Safety warning for operating and servicing propane refrigerators. Washington DC; National Propane Gas Association.

5. Field protocol for gas range carbon monoxide emissions testing. For the Chicago Regional Diagnostics Working Group; July 2001. http://www.karg.com/pdf/CO_Field_Protocol_annotated.pdf

6. ANSI/CSA Z21.1-2012. Household cooking gas appliances. Washington DC; American National Standards Institute.

7. RJ Karg Associates/WxWare Diagnostics. CO hot pot assembly instructions. Topsham, MA. http://www.karg.com/pdf/CO%20Hot%20Pot/CO_Hot_Pot_Assembly_Instructions.pdf

8. ASTM E2292-2014. Standard guide for field investigation of carbon monoxide poisoning incidents. West Conshohocken, PA; ASTM International.

Appendix A

Gas Refrigerator Test
Model XXXXX; Fabricated 9-11-2004
7-Sep-06
Texarkana, TX; 280 feet above sea level
Barometric pressure; 29.98 → 29.96

Venturi port condition	Reg. Input Press. IN WC	Orifice[4] ID	Calibrated Orifice Flow @ 11" WC SCFH	Actual Orifice Flow @ Actual press.[1] SCFH	Flue Temp. °F	Amb. Temp °F	O_2 %	CO (diluted) ppm	CO_2 %	CO af (undiluted)[2] ppm	Undiluted flow rate into area[3] SCFH	Equivalent CO diluted in 3837 FT3/HR ppm*
Clear	11.0	370	0.869	0.869	304.5	68	10.3	5	7.1	**11**	23.5	0
Clear	10.5	370	0.869	0.849	322.6	68	10.4	5	7	**10**	22.9	0
Clear	10.0	370	0.869	0.829	323.4	68	10.8	5	6.7	**10**	22.4	0
1/2 clogged	11.0	370	0.869	0.869	333.5	68	9.7	4	7.4	**7**	23.5	0
1/2 clogged	10.5	370	0.869	0.849	345.2	68	9.5	4	7.5	**8**	22.9	0
1/2 clogged	10.0	370	0.869	0.829	366.1	68	9.5	4	7.5	**8**	22.4	0
Fully clogged	11.0	370	0.869	0.869	342.6	68	7.9	508	8.6	**814**	23.5	5
Fully clogged	10.5	370	0.869	0.849	308.5	68	8.3	241	8.3	**400**	22.9	2
Fully clogged	10.0	370	0.869	0.829	291.1	68	7.8	355	8.7	**563**	22.4	3

[1]Actual flow = Calibrated flow x SQRT($P_{act.}/P_{cal.}$)
[2]CO_{af} = CO x 21 ÷ (21 – O_2)
[3]This flow rate is 27 times the actual propane input in SCFH
[4] Orifice marked '370' is the standard orifice.

*Kitchen & living room volume @ 1 change per hour
'0' ppm means less than 0.5 ppm

Mass equations:

$C_3H_8 + 5\ O_2 \longrightarrow 3\ CO_2 + 4\ H_2O$ Basic combustion equation

$C_3H_8 + 5\ [O_2 + 4\ N_2] \longrightarrow 3\ CO_2 + 4\ H_2O$ Basic equation considering nitogen content in air

$C_3H_8 + 5\ O_2 + 20\ N_2 \longrightarrow 3\ CO_2 + 4\ H_2O + 20\ N_2$ Expanded basic equation

Volumetric relationship:

$C_3H_8 + 5\ O_2 + 20\ N_2 \longrightarrow 3\ CO_2 + 4\ H_2O + 20\ N_2$ Expanded basic equation

$1 + 5 + 20 \longrightarrow 3 + 4 + 20 = 27$ (26 cubic feet of fuel plus air yields 27 cubic feet of combustion products)

E.G. Burning 1 cubic foot of propane yields 27 feet of undiluted flue gas

Appendix B

Gas Refrigerator Test
Model XXXXX; Fabricated 9-11-2004
16-Jul-06
Clovis, NM; 4300 Feet above sea leval
Barometric pressure; 26.13 → 26.07

Venturi port condition	Reg. Input Press. IN WC	Orifice[4] ID	Calibrated Orifice Flow @ 11" WC SCFH	Actual Orifice Flow @ Actual press.[1] SCFH	Flue Temp. °F	Amb. Temp °F	O_2 %	CO (diluted) ppm	CO_2 %	CO af (undiluted)[2] ppm	Undiluted flow rate into area[3] SCFH	Equivalent CO diluted in 3837 FT3/HR ppm*
Clear	11.0	370	0.869	0.869	173.7	91.3	7.4	7	8.9	**11**	23.5	0
Clear	11.8	370	0.869	0.900	189.0	91.3	6.9	8	9.3	**11**	24.3	0
Clear	13.0	370	0.869	0.945	195.7	91.3	6.0	9	9.8	**13**	25.5	0
1/2 clogged	11.0	370	0.869	0.869	197.1	91.3	6.8	12	9.3	**17**	23.5	0
1/2 clogged	11.8	370	0.869	0.900	209.9	91.3	6.1	7	9.8	**10**	24.3	0
1/2 clogged	13.0	370	0.869	0.945	219.3	91.3	5.8	9	10	**13**	25.5	0
Fully clogged	11.0	370	0.869	0.869	212.7	91.3	6.4	1739	9.6	**2501**	23.5	15
Fully clogged	11.8	370	0.869	0.900	211.6	91.3	5.2	2584	10.4	**3440**	24.3	22
Fully clogged	13.0	370	0.869	0.945	203.5	91.3	3.0	>4000	11.9	**>4000**	25.5	>27
Clear	11.0	382	0.623	0.623	214.6	95.2	7.9	7	8.6	**11**	16.8	0
Clear	11.8	382	0.623	0.645	274.4	95.2	7.7	8	8.8	**12**	17.4	0
Clear	13.0	382	0.623	0.677	280.1	95.2	6.5	8	9.6	**11**	18.3	0
1/2 clogged	11.0	382	0.623	0.623	296.6	95.2	16.6	2	2.9	**10**	16.8	0
1/2 clogged	11.8	382	0.623	0.645	306.4	95.2	9.6	6	7.5	**12**	17.4	0
1/2 clogged	13.0	382	0.623	0.677	334.6	95.2	7.3	15	9	**24**	18.3	0
Fully clogged	11.0	382	0.623	0.623	328.7	95.2	9.2	743	7.8	**1317**	16.8	6
Fully clogged	11.8	382	0.623	0.645	294.5	95.2	8.2	1079	8.4	**1777**	17.4	8

[1]Actual flow = Calibrated flow x SQRT($P_{act.}/P_{cal.}$)
[2]$CO_{af} = CO \times 21 \div (21 - O_2)$
[3]This flow rate is 27 times the actual propane input in SCFH
[4] Orifice marked '370' is the standard orifice. CR-212-1M is marked '382'

*Kitchen & living room volume @ 1 change per hour
'0' ppm means less than 0.5 ppm

Mass equations:

$C_3H_8 + 5\ O_2 \longrightarrow 3\ CO_2 + 4\ H_2O$	Basic combustion equation
$C_3H_8 + 5\ [O_2 + 4\ N_2] \longrightarrow 3\ CO_2 + 4\ H_2O$	Basic equation considering nitogen content in air
$C_3H_8 + 5\ O_2 + 20\ N_2 \longrightarrow 3\ CO_2 + 4\ H_2O + 20\ N_2$	Expanded basic equation

Volumetric relationship:

$C_3H_8 + 5\ O_2 + 20\ N_2 \longrightarrow 3\ CO_2 + 4\ H_2O + 20\ N_2$	Expanded basic equation
$1 + 5 + 20 \longrightarrow 3 + 4 + 20 = 27$	(26 cubic feet of fuel plus air yields 27 cubic feet of combustion products)
E.G. Burning 1 cubic foot of propane yields 27 feet of undiluted flue gas	

Advanced Forensic Engineering Analysis of a School Bus/Tractor-Trailer Crash

By Richard M. Ziernicki, PhD, PE (NAFE 308F) and William H. Pierce, PE (NAFE 846C)

Abstract

This paper presents advanced techniques used to reconstruct a motor vehicle accident involving a fully loaded tractor-trailer and school bus with 30 young students. The accident investigation included analysis of the physical evidence using photogrammetry and high-definition laser scanning, application of engine control module (ECM) and global positioning system (GPS) data, and analyzing onboard video footage from the bus. Momentum-based crash simulation software (PC-Crash) was used to simulate the accident. The simulation data was compared with National Transportation Safety Board (NTSB) data and with the onboard bus video footage. Further, rigid-body kinematic equations were used to determine occupant kinematics (velocities) and dynamics (accelerations). Multiple graphics are used to demonstrate the accident reconstruction and occupant kinematics and dynamics.

Keywords

School bus, tractor-trailer, on-board video, photo-match, rigid-body kinematics, PC-Crash, point clouds, photogrammetry, high-definition scanning, interactive animation, event data recorder

Introduction

A school bus loaded with 30 children was traveling westbound on a four-lane divided highway. The school bus proceeded to turn left across the eastbound lanes of the divided highway, approaching a two-lane divided road. However, the bus was crossing the eastbound lanes of the divided highway into the path of a tractor-trailer, which was carrying a load of sod.

The semi driver applied the brakes, but was unable to avoid colliding with the rear right side of the school bus. As a result of the collision, the school bus spun clockwise (approximately 180 degrees in yaw) prior to coming to rest near the northbound lane of the divided two-lane road. The semi came to rest in a ditch east of the school bus with the semi-tractor rolling a quarter turn and semi-trailer rolling a half turn.

According to the National Transportation Safety Board (NTSB), 11 children sustained minor injuries, eight children sustained major injuries, and there was one fatality. The lead author of this paper was retained to reconstruct the accident by the law firm representing the family of the child that was fatally injured.

In addition, 21 of the 29 surviving children on the bus responded to a general accident questionnaire issued by the NTSB. All of those 21 children reported wearing lap belts at the time of the accident. Further, there was evidence that the fatally injured child was wearing his seatbelt at the time of the accident. However, the fatally injured occupant's lap belt unlatched during the incident, and his seat cushion became detached. The victim was found in the aisle near the rear of the bus.

This paper presents several technologies and methodologies used to reconstruct and animate the accident. The reconstruction of the accident involved reviewing NTSB's accident investigation; analysis of physical evidence; estimating impact speeds and post-impact speeds from NTSB investigation, on-board school bus video footage, school bus global positioning data, and the semi's engine control module; simulating the accident using PC-Crash; verifying the simulation data using on-board school bus video; determining the kinematics throughout the school bus; and finally creating photo-realistic animation and interactive animation of the accident.

NTSB Investigation Summary

During the accident investigation, the NTSB performed high-definition scanning of the accident site, the semi, and the school bus, evaluated the injuries sustained by all of the passengers on the school bus, and conducted an occupant kinematics study to evaluate the

Richard Ziernicki, PhD, PE, and William Pierce, PE, 7185 South Tucson Way, Englewood, CO 80112-3987
(303) 925-1900; rziernicki@knottlab.com, wpierce@knottlab.com

effectiveness of lap belts using Mathematical Dynamic Models (MADYMO) software.

The authors of the paper expanded upon NTSB's investigation by determining impact configuration, reconstructing speeds of both vehicles prior to, during, and after the collision, simulating the accident, and preparing an occupant kinematics model without relying on expensive MADYMO software.

Physical Evidence

Reconstruction of the accident first involved plotting the physical evidence. The Florida Highway Patrol (FHP) surveyed the accident scene, which included several tire marks. The authors of this paper identified additional evidence on the roadway using scene photographs. After identifying the additional evidence, photogrammetry was performed using police photographs to identify the locations of the physical evidence (**Figure 1**). **Figure 2** shows the evidence placed on a scaled diagram.

Figure 1
Photogrammetry of tire marks.

Figure 2
Physical evidence overlaid on aerial diagram.

After plotting the physical evidence, the authors determined the impact configuration. First, photographs were taken around the perimeter of the school bus. Photogrammetry software (Photomodeler Scanner) was used to create a 3-dimensional model of the damaged school bus in virtual space (**Figure 3**). Further, the geometry of the semi-tractor was captured using a high-definition 3-D laser scanner, in which 3 million points of the semi-tractor were captured (**Figure 4**).

Figure 3
Point Cloud of exterior of subject school bus.

Figure 4
Point Cloud of exterior of subject semi.

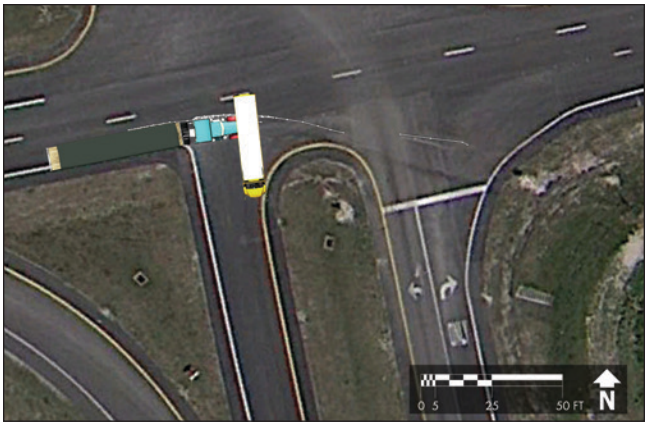

Figure 5
Impact configuration overlaid on physical evidence diagram.

Next, the virtual bus and semi-tractor models were aligned such that their crush profiles matched, thus establishing the impact configuration. The bus and semi-tractor impact configuration were then overlaid on top of the physical evidence diagram (**Figure 5**).

Figure 6
School bus GPS data plotted on aerial image.

The physical evidence shows at least 14 feet of skid marks left by the semi-tractor's left rear tires prior to impact, indicating that the semi-tractor had locked brakes before impact. After impact, scrub marks were left by the rear wheels of the school bus, showing rotational yaw motion of the school bus. The left-side bus tires dug into the grassy median as the bus spun, as evidenced by the deep furrow marks. The semi-trailer overturned as the semi-tractor entered the ditch on the southeast corner of the intersection, as evidenced by the sod dirt and gouges in the road.

Impact Speed Analysis

The pre-impact speeds of the school bus and the semi were approximated using data obtained by the FHP and NTSB. The pre-impact speeds determined through this analysis were used as starting points during momentum-based simulation of the accident using PC-Crash. More accurate pre-impact speeds of the school bus and semi were determined through the simulation of the accident, which will be discussed later in the paper.

The school bus had an onboard global positioning system (GPS) that recorded the location and instantaneous speed of the bus every 15 seconds. The authors used the GPS data to plot the position and corresponding instantaneous speed of the school bus every 15 seconds in the one minute prior to the collision (**Figure 6**). The last recorded GPS data point occurred near the point of impact. At this point, the bus was traveling at 15 mph. Therefore, the speed of the bus in the vicinity of the impact was 15 mph. The spatial resolution of the GPS introduces some error. However, this speed was used as a starting point during simulation of the accident in PC-Crash.

In order to approximate the pre-impact speed range of the semi, the authors relied on both the semi's event data recorder (EDR) and the onboard school bus camera that was pointed near the steps of the bus.

One of the onboard school bus cameras was pointed toward the steps of the bus recording at 15 frames per second. Five frames prior to noticeable movement due to impact, the semi came into frame near the southwest corner solid edge line of the roadway (**Figure 7**). Based on the frame rate, the semi came into frame between 0.26 and 0.33 seconds prior to impact. The impact configuration diagram shown in **Figure 5** was used to determine that the semi was 20.8 feet from the impact location between 0.26 and 0.33 seconds prior to impact.

Figure 7
Semi comes into view of bus camera five frames prior to impact.

Further, skid marks indicate that the semi was braking at least 14 feet prior to impact, and the EDR data indicated that the semi was decelerating at a rate of 0.316 g's prior to impact. Using the distance, time range, and deceleration rate of the semi, the authors were able to determine the impact speed range of the semi.

The impact speed range of the semi was determined to be 42 to 53 mph using this analysis (calculations shown in **Appendix A**). The impact speed range of the semi was further refined by incorporating the semi's EDR data, which recorded the semi speed in one-second intervals.

Based on the EDR data (**Figure 8**), the semi had the brakes applied and decelerated at an average constant rate of 0.319 *g* to 49 mph or less. The constant average deceleration rate with application of brakes is consistent with braking and no impact. Between 37 and 49 mph, the average deceleration rate increased to 0.546 *g*, consistent with the semi impacting the bus between 37 and 49 mph.

The EDR data showed that impact occurred after the semi decelerated to 49 mph or less, and the video analysis showed the semi's pre-impact speed was at least 42 mph. Therefore, the range of the semi's pre-impact speed was between 42 and 49 mph.

Post-Impact Speed Analysis

Next, the post-impact speeds — or the speeds of both the semi and the school bus after maximum engagement — were approximated. The post-impact speeds were later refined during simulation of the accident using PC-Crash. The authors used the NTSB video analysis bus position data to approximate the post-impact speeds of both the school bus and the semi.

First, the school bus speeds were plotted by differentiating the NTSB bus position data (**Figure 9**). Using this method, the bus separation speed was determined as approximately 28 mph. After estimating the school bus post-impact speed, the semi's post-impact speed was determined from the NTSB bus position data.

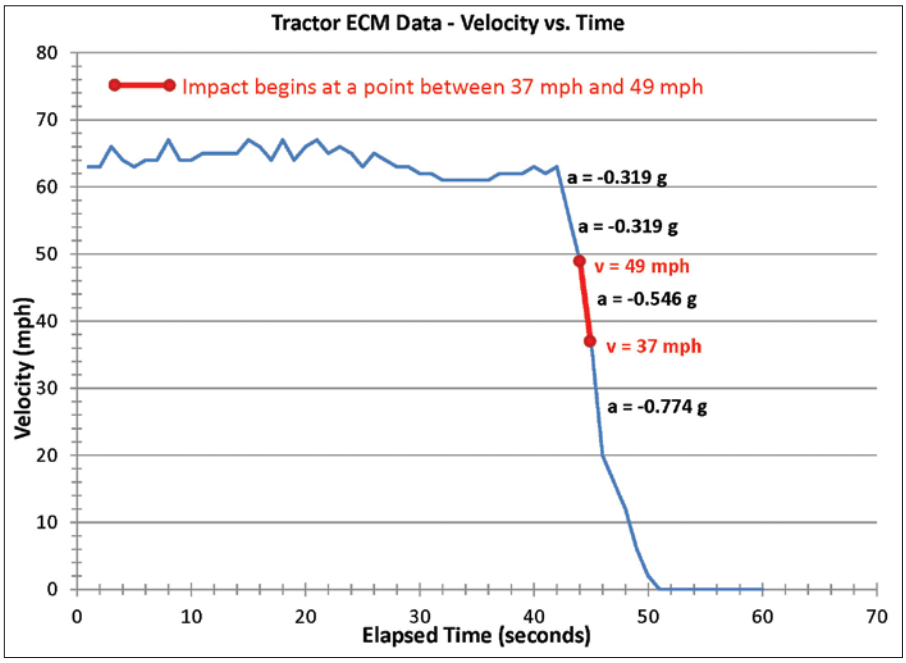

Figure 8
Plotted semi EDR data.

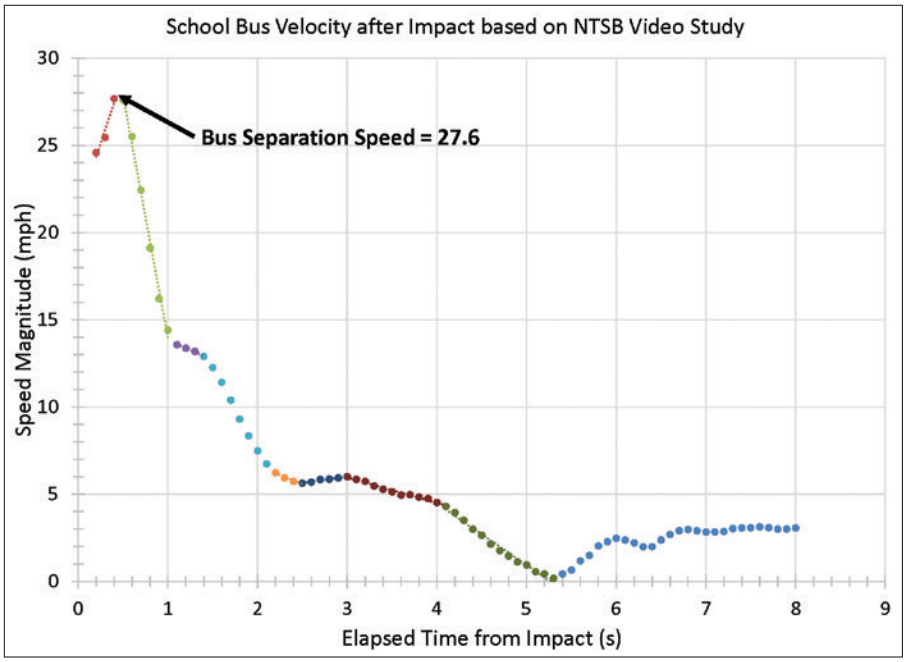

Figure 9
Post-impact bus speed determined from NTSB position data.
(The various colors shown are arbitrary.)

To calculate the semi's post-impact speed, the school bus position data from NTSB's video analysis was used to plot the location of the bus every 0.1 seconds through the impact sequence. The location of the point of maximum engagement on the bus was also plotted in 0.1-second intervals (**Figure 10**). This location corresponds to the approximate position of the front of the semi through impact. By differentiating the position data around the point of maximum engagement, the authors determined that the separation speed of the semi was approximately 36 mph.

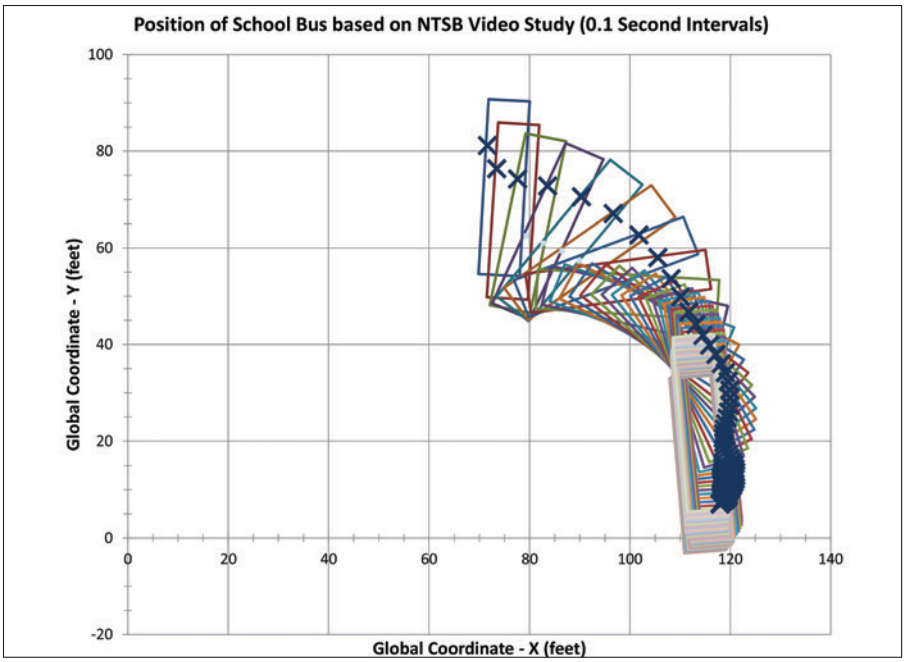

Figure 10
Bus position (0.1-second intervals) plotted from NTSB data.

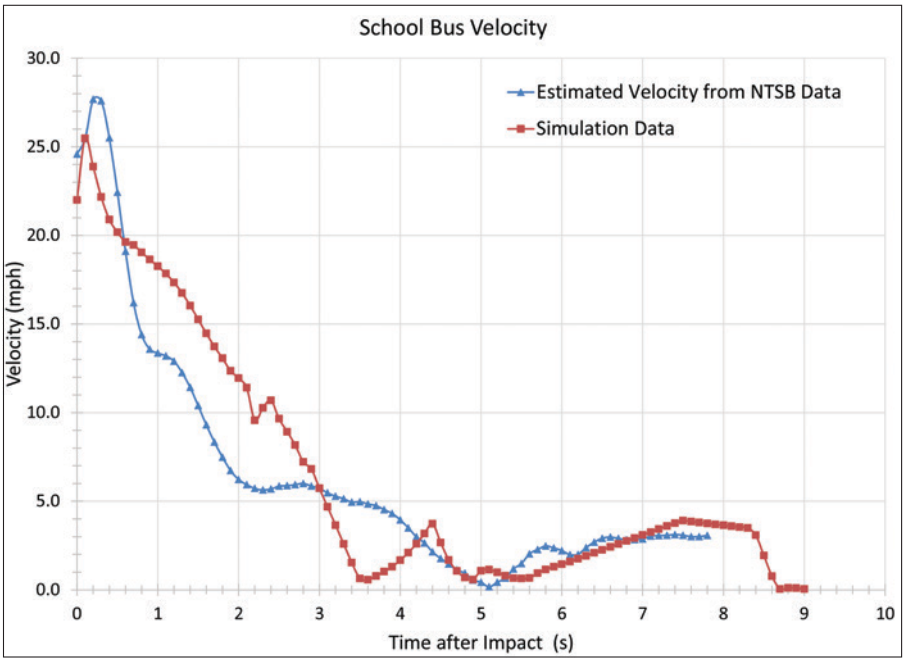

Figure 11
Bus post-impact speeds simulated in PC-Crash compared to NTSB video study.

PC-Crash Simulation

After determining the approximate pre- and post-impact speeds of both the school bus and the semi, the authors simulated the collision using momentum-based simulation software (PC-Crash).

The simulation process involved first determining the inertial parameters of both the school bus and semi as well as roadway friction properties. Virtual roadway terrain, physical evidence, and impact configuration were also input into PC-Crash.

After setting up the physical parameters and accident scene evidence in PC-Crash, the authors used the approximate pre-impact speeds of both the school bus and the semi as a starting point in the simulation process. The pre-impact speeds of both the school bus and the semi were refined by simulating the motion of both the school bus and semi until the motion of the school bus and the semi best matched the physical evidence and the approximated post-impact speeds of both the school bus and semi.

The PC-Crash simulation was used to determine a pre-impact speed of the school bus of 22 mph and the pre-impact speed of the semi of 45 mph. The simulation data further showed a post-impact speed of the school bus of 26 mph and a post-impact speed of the semi of 39 mph.

The PC-Crash speed of the school bus was then compared to the speeds determined through analysis of the NTSB data (**Figure 11**). Further, the PC-Crash

simulation roll rate of the school bus was also compared to the roll rate obtained by the NTSB through video analysis. There was a high rate of consistency between the authors' PC-Crash simulation and the NTSB video analysis. As a further check for consistency, the simulation motion was applied to virtual models of the school bus and semi. A virtual school bus camera was placed in the location of the onboard school bus camera that was directed toward the steps and the door of the school bus. The simulated motion of the school bus and semi (as viewed through the virtual camera) closely matched the motion of the school bus and semi (as observed through the onboard school bus camera), thus further verifying the reliability of the PC-Crash simulation data.

Calculation of Delta-V at Seat of Fatally Injured

After simulating the accident, the authors investigated the delta-V vector — or change in velocity vector — at the seat of the fatally injured occupant.

The semi struck the side of the bus offset far from the bus's center of gravity, resulting in the bus sustaining a large post-impact rotational velocity. Due to the extended length of the bus, the authors hypothesized that the change in tangential velocity associated with the bus's rotational velocity had a significant effect on the overall change in velocity sustained by the bus near the seat of the fatally injured occupant, who was sitting near the rear of the bus.

In order to account for the change in rotational velocity at the seat position of the fatally injured occupant when determining overall delta-V, the principles of rigid body kinematics were applied.

The PC-Crash simulation data was used to determine the delta-V of the combined bus and bus occupants center of gravity (ΔV_B) and the change in rotational speed about the center of gravity ($\Delta\omega$). The distance vector from the bus's center of gravity to the fatally injured occupant seat position was also measured using a scaled bus schematic ($r_{A/B}$). The magnitude and direction of delta-V at the seating location of the fatally injured occupant was then calculated using the equation for rigid body kinematics:

$$\Delta V_A = \Delta V_B + \Delta\omega \times r_{A/B} \quad (1)$$

Figure 12 shows the graphical representation of the application of equation (1). The velocity components associated with roll and pitch rotational velocities were determined insignificant and therefore neglected. **Figure 13** shows the summary of the velocity components and magnitudes of both the CG and the location where the fatally injured occupant was sitting (roll and pitch rotational velocities neglected).

For reference, calculations (including roll and pitch rotational velocities) are provided in **Appendix B**. When accounting for roll and pitch rotational velocities, the magnitude of the delta-V for the location of the fatally injured occupant was 61.7 mph or 2.2 percent higher than when roll and pitch rotational velocities were neglected.

Figure 13 shows that the change in velocity of the center of gravity was only 22.5 mph whereas the change in velocity at the seating position of the fatally injured was significantly higher (60.3 mph). Therefore, the authors' hypothesis that the change in rotational velocity significantly affected the overall change in velocity at the seat location of the fatally injured was proven valid.

Variation of Delta-V throughout Bus

The authors also calculated (with the assistance of computing software) the magnitude of delta-V throughout the bus at seat level by applying equation (1) to thousands of points equally spaced at seat level height. The computing software was also used to create a color-coded diagram showing the delta-V throughout the bus at seat level. Further, the authors overlaid the NTSB occupant injury severity data over the color-coded delta-V diagram (**Figure 14**).

Figure 14 shows that the delta-V near the front of the bus was nearly 0 mph, whereas the delta-V increased approaching the rear of the bus with the rear of the school bus sustaining a delta-V near 70 mph. As expected, the general injury severity as categorized by the NTSB also increased toward the rear of the school bus. The significant variation in delta-V throughout the bus shows that the effects of rotation in offset collisions involving extended length passenger vehicles, such as buses or long vans, cannot be neglected.

Alternative Graphical Method to Determine Delta-V

After determining the delta-V vectors for two points using the equation of rigid body kinematics, a simple graphical method can be applied to quickly determine the speed and direction of the delta-V at any

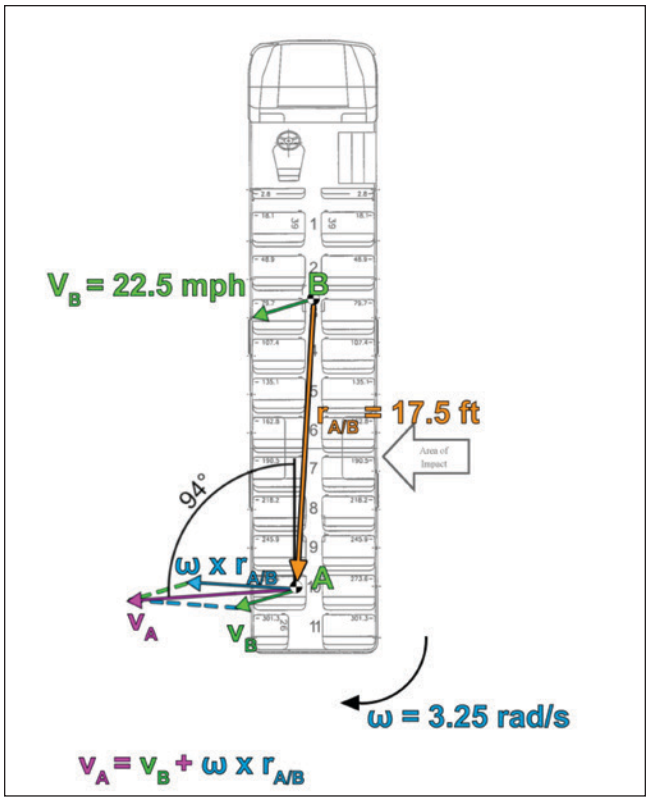

Figure 12
Graphical representation of rigid body kinematic calculations.

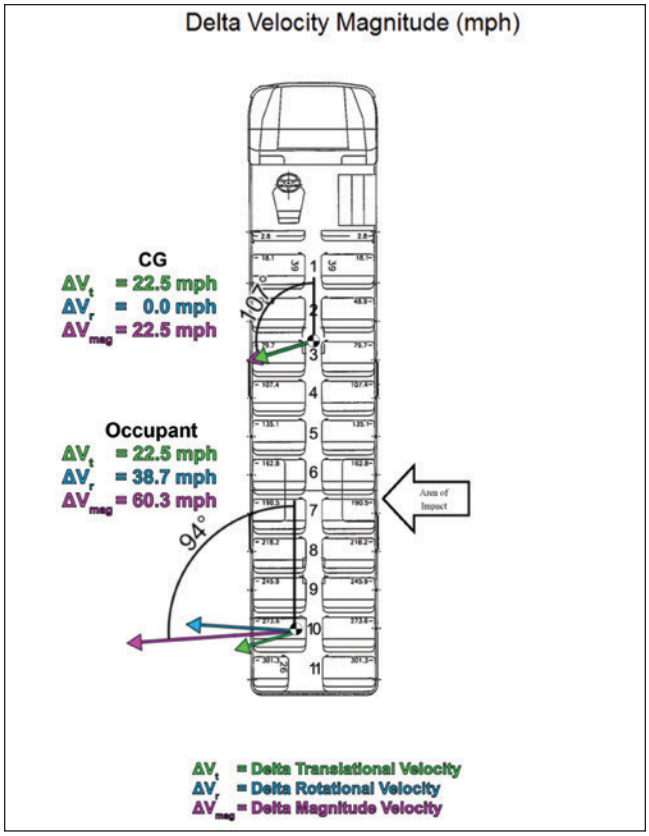

Figure 13
Summary of the velocity components of CG and seat of fatally injured occupant.

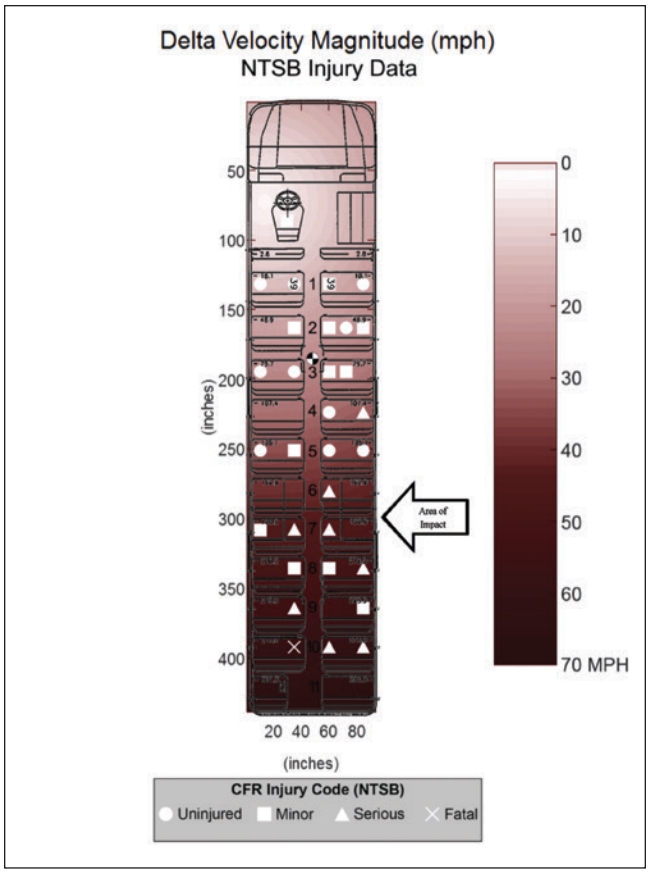

Figure 14
Magnitude of delta-V and reported injury severity.

point on the school bus in two-dimensional space. This graphical method neglects effects of the roll and pitch rotational velocities and therefore can only be used when the roll and pitch rotational velocities can be neglected, such as in this case study. The analysis first involves determining the instant center — or location on the bus in two-dimensional space — that sustained a delta-V of 0 mph. The instant center is determined by drawing perpendicular lines from the delta-V magnitude vectors of the CG and the fatally injured occupant. The point where the lines intersect is considered the instant center (**Figure 15**).

After determining the instant center, the delta-V vector at any section of the bus could be calculated. As an example, the delta-V sustained by the bus driver's seat was calculated; first the magnitude was determined. In order to calculate the magnitude of the delta-V, the distance from the instant center to the bus driver seat, $d_{drivers}$, and the distance from the instant center, d_{CG}, were determined (**Figure 16**). The magnitude of the delta-V for the bus driver seat was calculated using equation (2). The application of quantities in equation (2) is shown in equation (3).

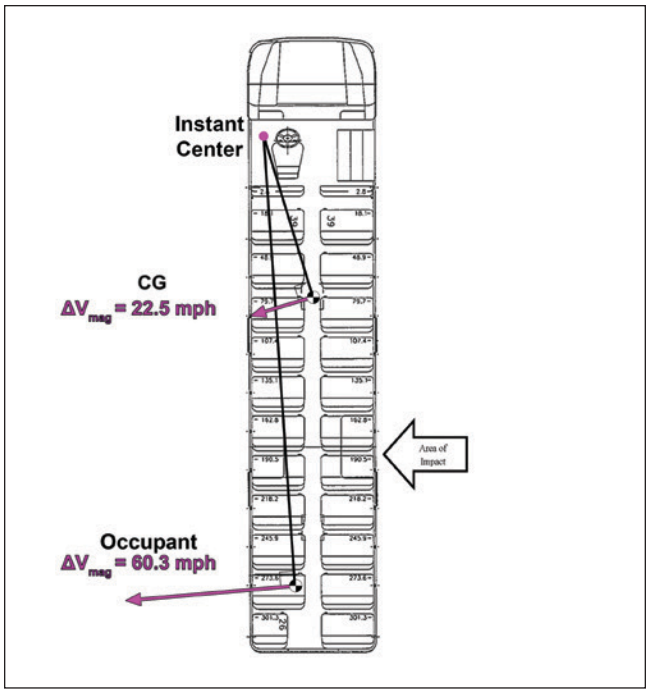

Figure 15
Diagram showing location of instant center.

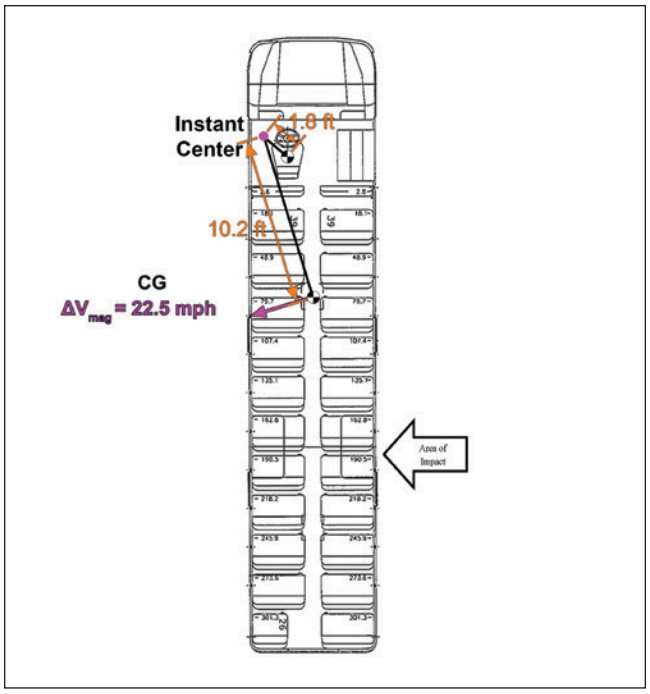

Figure 16
Diagram showing distances d_{driver} and d_{CG}.

$$\Delta V_{driver} = \frac{d_{driver}}{d_{CG}} * \Delta V_{CG} \quad (2)$$

$$\Delta V_{driver} = \frac{1.8\ ft}{10.2\ ft} * 22.5\ mph = 4.0\ mph \quad (3)$$

The direction of the delta-V vector for the bus driver's seat is perpendicular to the line drawn from the instant center to the bus driver's seat in the direction of the rotation as shown in **Figure 17**.

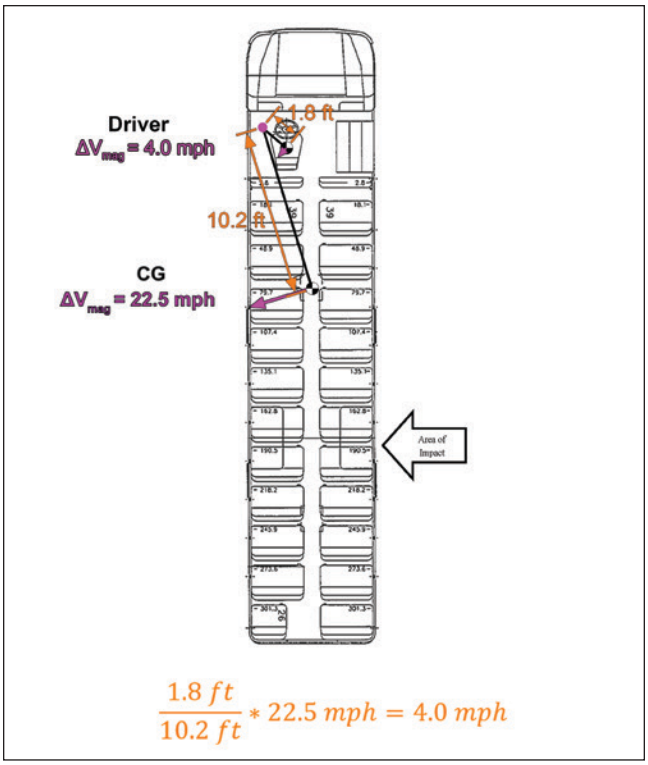

Figure 17
Direction of delta-V is perpendicular to line drawn from instant center.

Occupant Kinematics

After determining the delta-V at the seat location of the fatally injured occupant, the occupant kinematics of the fatally injured occupant were determined.

During the impact phase of the collision, the restrained portions of the occupant would have traveled in the direction of the bus seat, while the unrestrained portions of the occupant would have traveled in the opposite direction relative to the bus seat. However, during impact, the fatally injured occupant's seatbelt became unlatched, and the seat cushion became detached. Therefore, the occupant became completely unrestrained and traveled in the opposite direction relative to the bus seat (shown as dotted line in **Figure 18**).

The mean and peak accelerations sustained by the bus in the vicinity of the occupant were calculated using a Haversine model of crash pulse shown in equations (4) and (5).

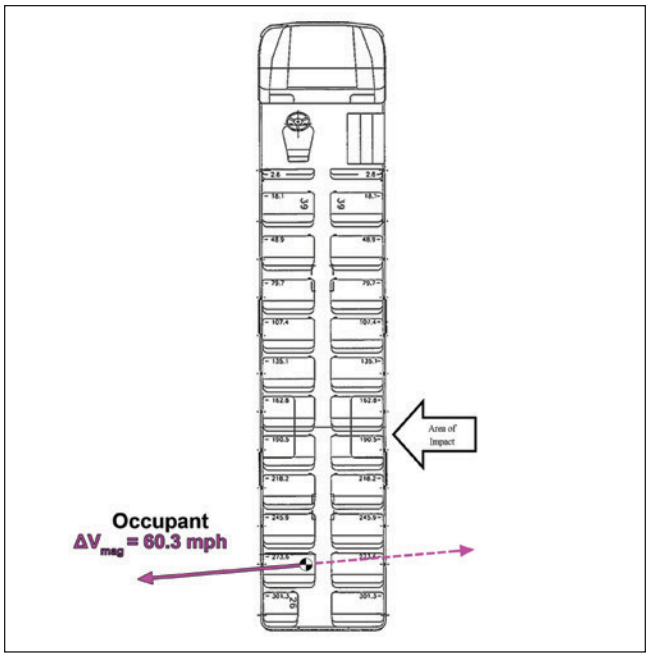

Figure 18
Direction of unrestrained occupant movement depicted by dashed line.

$$a_{occupant,mean} = \frac{\Delta V_{occupant}}{\Delta t} \quad (4)$$

$$a_{occupant,peak} = \frac{2*\Delta V_{occupant}}{\Delta t} \quad (5)$$

The change in velocity of the occupant ($\Delta V_{occupant}$) was calculated as 60.3 mph. The impulse time (Δt) was estimated using published school bus side impact crash test data as 0.1 seconds. Through application of equations (4) and (5), the respective mean and peak accelerations of the bus in the vicinity of the occupant were calculated as approximately 27.5 g and 54.9 g.

Animation

The PC-Crash simulation data was applied to computer-generated models of the school bus and the semi within virtual space to produce traditional, linear, photo-realistic animations as well as an interactive environment of the accident.

The authors utilized a process that combines computer-generated, virtual vehicles and Google Street View Imagery (**Figure 19**) to produce linear animations of the accident that are photo-realistic in quality. The process involves matching the 3D scene's virtual camera with the background image or "backplate" (**Figure 20**) and compositing the rendered vehicles and signage over the backplate image (**Figure 21** and **Figure 22**).

Figure 19
Google Street View Imagery used as "backplate" background for animation.

Figure 20
Virtual CG Scene (blue) matched to backplate image.

Figure 21
Backplate image before compositing.

Figure 22
Still frame from composited, photo-realistic animation.

In addition to the traditional linear animations, the authors also produced an interactive virtual visualization of the accident scene. This interactive format allows the user to move around the virtual accident scene to view the accident from any vantage point in time and space. Many other parameters can also be adjusted interactively to allow the user to present a variety of views together with overlaid information, such as real-time vehicle speeds and occupant delta velocities (**Figure 23**).

Figure 23
Interactive visualization interface displaying vehicle speeds and occupant delta velocities.

Conclusion

This case study demonstrates the use of various technologies and methodologies during the reconstruction of a collision between a school bus and a semi. Such technologies and methodologies can be useful when investigating other vehicle collisions.

This paper also demonstrates the use of both analytical and graphical methods to approximate the delta-V vectors at any point on the bus. The analysis showed the delta-V near the front of the bus was only about 4 mph whereas the delta-V near the rear of the bus was approximately 70 mph. Therefore, this case study demonstrates that when investigating occupant delta-Vs in offset collisions that induce rotation in extended length passenger vehicles, such as buses or long vans, the effects of rotation cannot be neglected.

Finally, high-end rendered animations were created using data from the PC-Crash simulation. Further, an interactive animation was created, allowing the user to maneuver a virtual camera within the virtual scene. Therefore, the interactive animation allowed the user to view the accident from various vantage points around the intersection.

Bibliography

Bedford A, Fowler, W. 2008. Engineering Mechanics DYNAMICS. 5th edition. Upper Saddle River, NJ: Pearson Education, Inc. p. 476-480.

Bolte K, Jackson L, Czech B, Lack S, Barson A, Summers S. Simulations of large school bus crashes. SAE Technical Paper 2000-01-0469. Warrendale, PA: Society of Automotive Engineers; 2001.

Bolte K, Lack S, Jackson L. Large school bus side impact stiffness factors. SAE Technical Paper 2002-01-0554. Warrendale, PA: Society of Automotive Engineers; 2002.

Breen K, Anderson C. The application of photogrammetry to accident reconstruction. SAE Technical Paper 861422. Warrendale, PA: Society of Automotive Engineers; 1986.

Callahan M, LeBlanc B, Vreeland R, Bretting G. Close-range photogrammetry with laser scan point clouds. SAE Technical Paper 2012-01-0607. Warrendale, PA: Society of Automotive Engineers; 2012.

Cliff W, Montgomery D. Validation of PC-Crash – a momentum-based accident reconstruction program. SAE Technical Paper 960885. Warrendale, PA: Society of Automotive Engineers; 1996.

Cliff W, Moser A. Reconstruction of twenty staged collisions with PC-Crash's optimizer. SAE Technical Paper 2001-01-0507. Warrendale, PA: Society of Automotive Engineers; 2001.

Coleman C, Tandy D, Colborn J, Ault N. Applying camera matching methods to laser scanned three dimensional scene data with comparisons to other methods. SAE Technical Paper 2015-01-1416. Warrendale, PA: Society of Automotive Engineers; 2015.

PC-CRASH Accident-Simulation Program version 9.1. Linz, Austria; Dr. Steffan Datentechnik GmbH: 2012.

Photomodeler 2014.1.1. Vancouver, BC; Eos Systems Inc.: 2014.

Fancher P, Ervin R, Winkler C, Gillespie T. A factbook of mechanical properties of the components for single-unit and articulated heavy trucks. Report number UMTRI-86-12. Ann Arbor, MI: The University of Michigan Transportation Research Institute; 1986.

Fay R, Robinette, Deering D, Scott J. Using event data recorders in collision reconstruction. SAE Technical Paper 2002-01-0535. Warrendale, PA: Society of Automotive Engineers; 2002.

Fenton S, Kerr R. Accident scene diagramming using new photogrammetric technique. SAE Technical Paper 970944. Warrendale, PA: Society of Automotive Engineers; 1997.

Fenton S, Neale W, Rose N, Hughes W. Determining crash data using camera matching photogrammetric technique. SAE Technical Paper 2001-01-3313. Warrendale, PA: Society of Automotive Engineers; 2001.

Grimes W, Dickerson C, Smith, C. Documenting scientific visualizations and computer animations used in accident reconstruction. SAE Technical Paper 980018. Warrendale, PA: Society of Automotive Engineers; 1998.

Messerschmidt W, Muttart J. A statistical analysis of data from heavy vehicle event data recorders. SAE Technical Paper 2009-01-0880. Warrendale, PA: Society of Automotive Engineers; 2009.

Neale W, Fenton S, McFadden S, Rose N. A video tracking photogrammetry technique to survey roadways for accident reconstruction. SAE Technical Paper 2004-01-1221. Warrendale, PA: Society of Automotive Engineers; 2004.

Pepe M, Sobek J, Huett G. Three dimensional computerized photogrammetry and its application to accident reconstruction. SAE Technical Paper 890739. Warrendale, PA: Society of Automotive Engineers; 1989.

Pepe M, Sobek J, Zimmerman D. Accuracy of three-dimensional photogrammetry as established by controlled field tests. SAE Technical Paper 930662. Warrendale, PA: Society of Automotive Engineers; 1993.

Steffan H, Moser A. The Collision and trajectory models of PC-Crash. SAE Technical Paper 960886. Warrendale, PA: Society of Automotive Engineers; 1996.

Steffan H, Moser A. How to use PC-Crash to simulate rollover crashes. SAE Technical Paper 2004-01-0341. Warrendale, PA: Society of Automotive Engineers; 2004.

Switzer D, Candrlic T. Factors affecting the accuracy of non-metric analytical 3-D photogrammetry, using Photomodeler. SAE Technical Paper 1999-01-0451. Warrendale, PA: Society of Automotive Engineers; 1999.

Tandy D, Coleman C, Colborn J, Hoover T, Bae J. Benefits and methodology for dimensioning a vehicle using a 3D scanner for accident reconstruction purposes. SAE Technical Paper 2012-01-0617. Warrendale, PA: Society of Automotive Engineers; 2012.

Varat M, Husher S. Vehicle impact response analysis through the use of accelerometer data. SAE Technical Paper 2000-01-0850. Warrendale, PA: Society of Automotive Engineers; 2000.

Ziernicki R, Danaher D. Forensic engineering use of computer animations and graphics. Journal of the National Academy of Forensic Engineers. 2006;23(2):1-9.

Ziernicki R, Danaher D, Ball J. Forensic engineering evaluation of physical evidence in accident reconstruction. Journal of the National Academy of Forensic Engineers. 2007;24(2):1-10.

Ziernicki R, Pierce W, Leiloglou A. Forensic engineering usage of surveillance video in accident reconstruction. Journal of the National Academy of Forensic Engineers. 2014;31(2):9-19.

Appendix A

First equations (1) and (2) were applied to determine the semi's average velocity range over the time range of 0.263 and 0.33 seconds.

$$V_{avg,min} = \frac{d}{t_{max}} = \frac{20.8 \text{ ft}}{0.33\ s} = 63.0\ \frac{ft}{s} \quad (1)$$

$$V_{avg,max} = \frac{d}{t_{min}} = \frac{20.8\ ft}{0.263\ s} = 79.1\ \frac{ft}{s} \quad (2)$$

Next, the range of speed reduction, ΔV, due to braking was calculated using (3) and (4)

$$\Delta V_{min} = a * t_{min} = 0.319\ g * \frac{32.2\ \frac{ft}{s}}{g} * 0.26\ s = 2.7\ \frac{ft}{s} \quad (3)$$

$$\Delta V_{max} = a * t_{max} = 0.319\ g * \frac{32.2\ \frac{ft}{s}}{g} * 0.33\ s = 3.4\ \frac{ft}{s} \quad (4)$$

Finally, the impact speed range was calculated using (5) and (6)

$$V_{impact,min} = V_{avg,min} - \frac{\Delta V_{max}}{2} = 63.0\ \frac{ft}{s} - \frac{3.4\ \frac{ft}{s}}{2} = 61.3\ \frac{ft}{s} = 41.8\ mph \quad (5)$$

$$V_{impact,max} = V_{avg,max} - \frac{\Delta V_{min}}{2} = 79.1\ \frac{ft}{s} - \frac{2.7\ \frac{ft}{s}}{2} = 77.7\ \frac{ft}{s} = 53.0\ mph \quad (6)$$

Appendix B

The coordinate system used for the rigid body kinematic calculations originates at the center of gravity of the bus. The positive-x direction is oriented towards the front of the bus, the positive-y direction is oriented towards the left side of the bus, and the positive-z direction is oriented upwards.

First, the delta-V vector at the center of gravity (ΔV_{cg}) was calculated using the pre-impact velocity (V_{pre}) and post-impact velocity (V_{post}) of the school bus determined from the PC-Crash simulation data of the collision.

$$\overrightarrow{V_{pre}} = |22\ mph\ i \quad 0\ mph\ j \quad 0\ mph\ k|$$

$$\overrightarrow{V_{post}} = |15.0\ mph\ i \quad 21.7\ mph\ j \quad -0.3\ mph\ k|$$

$$\overrightarrow{\Delta V_{cg}} = \overrightarrow{V_{post}} - \overrightarrow{V_{pre}} = [-7.0\ mph\ i \quad 21.7\ mph\ j \quad -0.3\ mph\ k]$$

Next, the change in rotational velocity ($\overrightarrow{\Delta\omega}$) was determined from the PC-Crash simulation data of the collision.

$$\overrightarrow{\Delta\omega} = \left[-1.20\ \frac{rad}{s}\ i \quad -0.06\ \frac{rad}{s}\ j \quad -3.25\ \frac{rad}{s}\ k\right]$$

Next, the distance vector from the cg ($\overrightarrow{r_{A/B}}$) to the seat position of the fatally injured was determined using a scaled schematic of the school bus.

$$\overrightarrow{r_{A/B}} = |-17.4\ ft\ i \quad 1.2\ ft\ j \quad 1.45\ ft\ k|$$

Finally, the delta-V vector at the position the fatally injured occupant was sitting was determined by inputting the above quantities into the rigid body kinematics equation

$$\overrightarrow{\Delta V_{occupant}} = \overrightarrow{\Delta V_{cg}} + \overrightarrow{\Delta\omega} \times \overrightarrow{r_{A/B}}$$

Appendix B (continued)

$$\overrightarrow{\Delta\omega} \times \overrightarrow{r_{A/B}} = \begin{vmatrix} i & j & k \\ -1.2\ \frac{rad}{s} & -0.06\ \frac{rad}{s} & -3.25\ \frac{rad}{s} \\ -17.4\ ft & 1.2\ ft & 1.45\ ft \end{vmatrix}$$

$$\overrightarrow{\Delta\omega} \times \overrightarrow{r_{A/B}} = \left[3.8\ \frac{ft}{s} i \quad 58.3\ \frac{ft}{s} j \quad -2.5\ \frac{ft}{s} k\right] = [2.6\ mph\ i \quad 39.8\ mph\ j \quad -1.7\ mph\ k]$$

$$\overrightarrow{\Delta V_{occupant}} = [-7.0\ mph\ i \quad 21.7\ mph\ j \quad -0.3\ mph\ k] + [2.6\ mph\ i \quad 39.8\ mph\ j \quad -1.7\ mph\ k]$$

$$\overrightarrow{\Delta V_{occupant}} = [-4.4\ mph\ i \quad 61.5\ mph\ j \quad -2.0\ mph\ k]$$

$$\left|\Delta V_{occupant}\right| = \sqrt{(-4.4\ mph)^2 + (61.5\ mph)^2 + (-2.0\ mph)^2} = 61.7\ mph$$

Forensic Engineering Analysis of a Shopping Mall Explosion

By Jerry R. Tindal, PE (NAFE 642M)

Abstract

On May 7, 2009 a catastrophic explosion occurred at a shopping mall located just outside of Washington, D.C. As a result of the explosion, several persons, including multiple firefighters, were injured, and a large portion of the mall was destroyed. This paper examines the cause of the explosion.

Keywords

Explosion, natural gas, underground pipe, distribution piping, gas main, utility clearances, underground electrical cables, gas leaks, NFPA 921, explosion investigation

Introduction

The section of the mall that sustained the primary explosion damage was located on the southern-most end of the mall and contained several tenants, including (moving from north to south) a sandwich shop, pregnancy center, two vacant spaces under renovation, pizza shop, and two specialty shops. **Figures 1, 2** and **3** depict the shopping mall and the referenced tenant spaces.

Figure 1
A Google earth image of the shopping mall. The section of the mall that sustained the most extensive explosion damage is circled.

Figure 2
A view from the front of the shopping mall of the tenant spaces that sustained the most extensive explosion damage.

Figure 3
A view from the rear of the shopping mall of the tenant spaces that sustained the most extensive explosion damage.

At approximately 10 a.m. on the date of the explosion, the owner of the pizza shop arrived and began preparing for the business day. The owner testified that at the time of his arrival there was no smell of gas in the restaurant, the oven and grill were operating normally, and there were no problems with the electrical power. Furthermore, there had been no gas or electrical problems with the tenant space since his original occupancy in January of 2005.

At approximately 11 a.m., the owner of the pizza shop opened to patrons for business as usual. Around 12 p.m., there was a sudden and complete loss of electrical power to the pizza shop, and the owner called and notified the electric utility of the outage. Utility company records indicated a power outage call was received at 12:08 p.m. Although no one in the pizza shop smelled gas at the time, the restaurant was evacuated due to the lights being out.

Jerry R. Tindal, PE, 922 Jeff Sharpe Road, Pelion, SC 29123; (803) 394-5671; jtindal@safe-labs.com

A short time after evacuating the restaurant, the owner re-entered to check on the conditions. The owner testified that he detected an odor of gas in the kitchen, though it was not strong initially. He verified that the kitchen equipment was off and called the gas company to report the odor of gas. Gas company records indicate a call reporting the gas odor around 12:27 p.m. A few minutes after calling in the report of a gas odor, the owner went to the back door of the restaurant and opened it. Outside he detected a strong smell of gas (stronger than inside), and observed an "eruption going on underground" as well as bubbling in a puddle of water collected on the asphalt surface.

Between 12:54 p.m. and 1 p.m., the fire department and the gas company arrived at the scene and began building evacuations and an investigation into the leaking gas. Around 1:02 p.m., the electric utility company arrived at the scene. At approximately 1:26 p.m., the building exploded. At the time of the explosion, several firefighters were near the front entrance of several of the tenant spaces in the building, and a gas utility worker was near the rear exit of the tenant spaces in the building. The explosion was captured by the dash camera of a fire truck parked in front of the building at the time. **Figures 4** through **9** depict captured images of the explosion from the dash cam video. The video was released and shown on multiple news outlets and can be easily located on Youtube.

Shopping Mall Construction and Utility Configuration

The shopping mall, which faced west, was constructed sometime in 1977 and incorporated both one- and two-story sections. The structure was built on slab with primarily hollow core concrete masonry unit (CMU) exterior walls and mixed wood-framed and steel-framed drywall sheathed interior walls. The roof assembly consisted of open-web steel bar joists supported on steel beams and columns. The roof was covered with board-insulated corrugated steel sheeting and a built-up roof system. The underside of the steel sheeting was insulated with fiberglass batt insulation. Drop ceilings were utilized in the finished tenant spaces.

Figure 4
Firefighters making entry seconds before the explosion.

Figure 5
Additional firefighters approaching the front entry just as the explosion occurs. Note the expanding fireball through the glass window panes.

Figure 6
Explosion as viewed from the front of the building. Fireball venting through the front windows. Two of the firefighters are circled.

Figure 7
Explosion as viewed from the front of the building. Note displacement of the roof and subsequent venting of the fireball.

Figure 8
Fireball continuing to vent through the displaced roof.

Figure 9
Fireball continuing to vent.

The underground electrical service lines to the identified tenant spaces of the mall were installed as part of the original construction of the building. A pad-mounted transformer was located approximately 52 feet east of the rear wall of the sandwich shop tenant space. Direct-buried service cables routed from the transformer provided power to the meter bases located on the rear walls of the tenant spaces. In July of 1980, the utility company had severed service at the ground level to the two most southern-involved tenant spaces and provided service routed from a separate transformer.

The pizza shop was the only tenant space involved in the explosion that utilized natural gas. A 2-inch polyethylene (plastic) underground pipe distribution main was located approximately 9 feet from (and parallel to) the rear wall of the mall area near the restaurant. A ¾-inch plastic service line was connected to the 2-inch plastic main and routed to the gas meter installed on the south exterior wall, near the southeast corner of the restaurant. Asphalt covered the entire exterior rear area of the building, including up to the rear wall of the building. The distribution and service gas lines were installed in October of 1989 and were operating at a pressure of approximately 50 psig at the time of the explosion.

Fuel Source

The fuel source for the explosion was determined to be natural gas originating from multiple failures in the 2-inch plastic underground gas distribution main. Gas utility company personnel, utilizing combustible gas indicators, entered the front of the pizza shop and conducted measurements from the front of the restaurant to the rear. At the rear of the restaurant, they detected natural gas migrating into the structure along the rear CMU wall and through the electrical and plumbing penetrations. Evidence of natural gas was also directly observed by the owner of the pizza shop, fire department personnel, and gas utility employees; it was observed bubbling up through a puddle of water accumulated in a cracked area of the asphalt surface behind the restaurant prior to the occurrence of the explosion. The puddle was located directly above the gas distribution main.

The natural gas flowed from leaks in the main, through the ground, and beneath the asphalt into the building via the electrical and plumbing conduits as well as through the hollow core CMU walls and openings/penetrations in the walls. The gas accumulated in the building until it was ignited, at which point the explosion occurred. **Figures 10** through **13** depict some of the construction features of the building, which facilitated gas migration into the structure.

Figure 10
The asphalt surface behind the mall extends all the way to the exterior CMU wall of the structure.

Figure 11
The hollow core CMU exterior walls extend into the ground well below the asphalt surface.

Figure 12
Penetrations through the CMU walls and the concrete slab in the rear of the building included electrical and plumbing.

Figure 13
Electrical conduit penetrations through the asphalt and into electrical panels that were located inside the building.

It is well known that gas leaking from an underground pipe failure, such as in this case, will migrate through the soil and into buildings, creating an explosion hazard[1,2]. The National Fire Protection Association (NFPA) 921 *Guide for Fire and Explosion Investigations* states[1]:

> ***10.9.9.1.1*** *It is common for fuel gases that have leaked from underground piping systems to migrate underground (sometimes for great distances), enter structures, and create flammable atmospheres. Both lighter-than-air and heavier-than-air fuel gases can migrate through soil; follow the exterior of underground lines; and seep into sewer lines, underground electrical or telephone conduits, drain tiles, or even directly through basement and foundation walls, none of which are as gastight as water or gas lines.*
>
> ***10.9.9.1.2*** *Such gases also tend to migrate upward, permeating the soil and dissipating harmlessly into the atmosphere. Whether the path of migration is lateral or upward is largely a matter of which path provides the least resistance to the travel of the fugitive gas, the depth at which the leak exists, the depth of any lateral buried lines that the gas might follow, and the nature of the surface of the ground. If the surface of the ground is obstructed by rain, snow, frozen earth, or paving, the gases may be forced to travel laterally. It is not uncommon for a long-existing leak to have been dissipating harmlessly into the air until the surface of the ground changes, such as by the installation of new paving or by heavy rains or freezing, and then be forced to migrate laterally and enter a structure, fueling a fire or explosion.*

The asphalt ground covering inhibited vertical dissipation of the gas and facilitated lateral travel of the gas toward and into the building.

Source of Ignition

The source of ignition of the fugitive gas that accumulated in the building was not conclusively determined. However, immediately prior to the explosion, flames were first observed originating near an electrical meter base on the rear of the building, which then rapidly propagated upward toward the soffit/eaves of the building.

Gas Main Failure

The underground distribution gas main leak point was excavated by natural gas utility company employees and their forensic engineering expert during the nighttime hours on the date of the explosion. The excavation work was not layered and was very poorly documented. The excavation pit was subsequently covered with plate steel, and the scene was secured.

A joint inspection of the scene and the excavated pit area was performed at a later date with all parties of interest. Examination of the excavated area indicated that the 2-inch plastic gas main converged on and crossed in between multiple direct buried electrical power cables in the area behind the pizza shop. Measured clearances between the plastic gas main and the remains of the electrical power cables within the excavated pit in the general area of the crossover were as little as 3 inches. Several feet of the electrical cables in the area of the crossover had been destroyed by an electrical arcing event that preceded the explosion. The faulted power cables with subsequent gas line damage were consistent with the loss of electrical power followed by a gas smell shortly before the explosion. The power cables were installed in 1977, and the extensive heat produced from the catastrophic electrical faulting of several feet of the cables resulted in multiple burned, charred, and melted holes in the plastic gas main. Although the cause of the power cable failure was undetermined due to the extent of damage, such cable failures (as will be discussed later) are engineering-foreseeable events. **Figures 14** through **19** indicate the excavated area of where the gas pipe main leaked.

Figure 14
A view of the excavated area immediately behind the pizza shop.

Figure 15
A close-up view of the excavated area. The 2-inch plastic gas main is approximately 9 feet from the rear exterior wall of the building.

Figure 16
The gas line converged on and crossed in between a nest of multiple electrical power cables. The power cable remains were located on both sides of the gas main.
The cable remains are circled.

Figure 17
Most of the remains of the destroyed electrical cables were removed before the joint exam by employees of the gas company. Clearances to the remaining cable sections were approximately 3 inches.

Figure 18
The faulting cables had charred and burned holes through the plastic gas main, allowing gas to escape.
Note the stub of a destroyed section of power cable (circled) adjacent to the burned section of gas line.

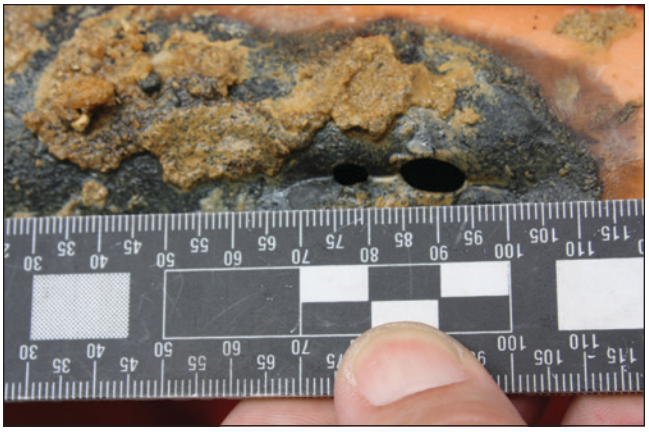

Figure 19
A close-up view of some of the holes charred, melted, and burned in the plastic gas main. The pipe was heavily charred, melted, and burned around the circumference with multiple holes.

Underground Power Cable Failure and Clearance Requirements

The failure of an underground electrical power cable is an engineering-foreseeable event. The power cables at the time of the failure were more than 30 years old, and the electrical forensic engineer investigating on behalf of the plaintiff testified that the cables were subject to failure at that point in time. In addition, during discovery, the electrical power utility company stated:

> *It is well known in the industry that such cables fail, despite reasonable care in their manufacture, installation and use, and that with appropriate distance between underground facilities such failures will ordinarily not damage other utilities or cause customer damage.*

The National Electric Safety Code (NESC)[3] establishes minimum clearance requirements between direct buried cables and other underground structures (including fuel lines) for the purpose of protecting each system from the effects of the other. Such clearance requirements are established because of the foreseeable failure of electrical cables with subsequent arcing and production of heat.

The National Fire Protection Association (NFPA) *Fire Protection Handbook, 16th Edition*[4] provides some insight into the purposes of the NESC, stating the following [underlined emphasis added]:

> *Introduction*
> *Since its first edition exactly 90 years ago, the Fire Protection Handbook has endeavored to fulfill the needs of the fire protection community for a single-source handbook on the state of the art in fire protection and fire prevention practices.*
>
> *Electrical Systems and Appliances, Section 8 Chapter 2*:
>
> *....All standards governing electric equipment include requirements to prevent fires caused by arcing and overheating, and to prevent accidental contact, which may cause an electric shock.... [page 8-7]*
>
> *...National Electric Safety Code (ANSI Standard C2)*
>
> *As interest increased in electrical safety in the U.S., a need arose for a code to cover the practices of public utilities and others when installing and maintaining overhead and underground electric supply and communication lines. Accordingly, a National Electric Safety Code was completed in 1916. Currently this code is published by the Institute of Electrical and Electronic Engineers (IEEE). [Page 8-13]*

Over 10 years before the shopping mall explosion incident happened, a similar natural gas explosion event occurred in South Riding, Va. A plastic underground gas line was damaged by heat produced from electrical arcing from a faulting underground electrical line. Gas leaked from the damaged gas line and into a newly constructed home. Tragically, however, this explosion incident resulted in the fatality of a young mother, serious injuries to the father, and minor injuries to two children. The Natural Transportation Safety Board (NTSB) *Pipeline Accident Report: Natural Gas Explosion and Fire at South Riding Virginia,* July 7, 1998[5] states [underlined emphasis added]:

> *…The Safety Board therefore concludes that had the gas and electrical service lines involved in this accident been adequately separated, the heat from the arcing electrical conductor failure would probably not have damaged the gas service line, and the accident would not have occurred…*
>
> *...Since the National Electric Safety Code already addresses the separation issue for electrical facilities, the Safety Board believes that electrical industry associations and the U.S. Department of Agriculture's Rural Utilities Service should inform their member utilities of the circumstances of this accident and of the need to ensure that underground electrical facilities are installed and maintained with separation between plastic gas pipelines in accordance with the National Electrical Safety Code.*

The 1984 Edition of the NESC was the current edition of that standard published at the time the natural gas lines were installed in proximity to the electrical power cables behind the pizza shop at the shopping mall. The NESC Handbook, 1984 Edition, *Development and Application of the American National Standard National Electrical Safety Code Grounding Rules, General Rules, and Parts 1, 2, and 3,*[6] states the following [underlined emphasis added]:

Section 35. Direct Buried Cable (This section was developed in the 1973 Edition…)

350. General
(This rule was added in the 1973 Edition)
…The rules of this section detail the arrangement and installation conditions required for safe installations. These rules are essentially an expanded version of those included in Section 32.

351. Location and Routing
…The discussions of the rules in Section 32 apply to the similar or identical requirements in Rule 351. Because direct buried cables lack the protection of a conduit, they need additional care in installation in order to provide the same level of safety and reliability at an economical cost…

352. Clearances From Other Underground Structures (sewers, water lines, fuel lines, building foundations, steam lines, other supply or communication conductors not in random separation, etc.)
(This rule was developed in the 1973 Edition…)

Special care is required in locating direct buried cables near other facilities. These rules are intended to provide (1) adequate room for maintenance of all facilities and (2) appropriate protection for each system from the effects of the other.

The discussions in Section 32 of the NESC Handbook (referenced in Section 351 above) provide additional insight into reasons for clearance and protection measures. The clearance and protection requirements include foreseeable electrical cable failures and the impact on adjacent underground systems. Section 32 of the NESC Handbook states in part [underlined emphasis added]:

320B. Clearances From Other Underground Installations (This rule was developed in the 1973 Edition…)

…Conduits should be located as far as practical from other underground structures, especially from water mains and gas mains….the greater the distance between such systems, the less the chances of damage….

To arrest the action of an electric-power arc, and to prevent it from affecting communication cables, a barrier wall of concrete not less than three inches thick, or equivalent protection, should be placed between ducts carrying supply conductors and adjacent ducts carrying communication conductors…

…When a supply cable fails, the arc may communicate the trouble to other cables…

The clearance requirement stipulated in the NESC between underground gas lines and underground electrical cables is a minimum of 12 inches. Had the gas utility company contacted the electric utility at the time they were installing the gas line, the electric utility would likely have stipulated a 12-inch clearance be maintained between the two utilities.

Underground Plastic Gas Line Protection

The 12-inch clearance requirement was not limited to electrical industry standards and practices. It is also well known and established in gas industry standards and practices for the purposes of protecting the piping from damage, including damage resulting from heat sources.

The potential for damage to underground plastic gas piping due to heat exposure is well recognized in the gas industry. Natural gas distribution main systems are commonly engineered to incorporate polyethylene plastic pipe (an appropriate material) to transport natural gas. Polyethylene pipe has a relatively low melting temperature and is therefore highly susceptible to damage from potential heat sources. The pipe installed was identified as Polyethylene (PE) 2406, Dupont Aldyl A and was marked as compliant with ASTM D2513, which is entitled *Standard Specification for Thermoplastic Gas Pressure Pipe, Tubing and Fittings.* NFPA 921 Table 6.2.8.2 "Approximate Melting Temperatures of Common Materials" indicates a melting temperature of 251ºF to 275ºF for polyethylene. NFPA 921 section 6.2.8.4 states that *"Thermoplastics soften and melt over a range of relatively low temperatures, from around 75°C (167°F) to near 400°C (750°F)."*

ASTM D2513[7] references ASTM D2774 *Standard Recommended Practice for Underground Installation of Thermoplastic Pressure Piping.* As far back as the 1973 Edition of ASTM D2774[8] (and subsequent editions), the standard cautions installers with the following [underlined emphasis added]:

6. Installation Precautions

6.2 Care should be taken to protect the pipe from excessive heat or harmful chemicals…

The Code of Federal Regulations (CFR) that provides the minimum installation requirements for gas distribution mains recognizes the need to provide proper clearances to protect plastic gas mains from damage and particularly plastic lines from any heat source. 49 CFR 192.325 (c)[9] states [underlined emphasis added]:

192.325 Underground clearance

(b) Each main must be installed with enough clearance from any other underground structure to allow proper maintenance and to protect against damage that might result from proximity to other structures.

(c) In addition to meeting the requirements of paragraph (a) or (b) of this section, each plastic transmission line or main must be installed with sufficient clearance, or must be insulated, from any source of heat so as to prevent the heat from impairing the serviceability of the pipe.

The Federal Register[10] provides insight into the intent of the provisions of 49 CFR 192.325 cited above [underlined emphasis added]:

In response to a great many comments pointing out the difficulties that distribution companies would have attaining the proposed 12 inches of clearance, the clearance requirements for mains are now couched in performance type language. This will allow these operators flexibility to attain the desired objectives of proper maintenance and protection from external damage…

The proposed prescriptive clearance requirement in 49 CFR 192.325 for gas mains was 12 inches; however, it was reworded into performance-type language to allow operator flexibility (different means and methods) for achieving the same equivalent desired objectives of the provision. The objective provisions include not only achieving maintenance of the piping but also clearly and distinctly achieving the proper protection of the piping from external damage.

The American Society of Mechanical Engineers (ASME) developed the *ASME Guide for Gas Transmission and Distribution Piping Systems,*[11] which provides clarity and direction in the application of 49 CFR 192. The intent of the ASME guide document as it relates to Section 192.325 provides the following [underlined emphasis added]:

Page viii
The basic objective of the Guide is to provide assistance to the operator in complying with the Minimum Federal Safety Standards by providing "how to" information related to the Standards.

Page viii
The guide material present in this Guide includes information and some of the acceptable methods to assist the operator in complying with the Minimum Federal Safety Standards. The recommendations contained in the Guide are based on sound engineering principles, developed by a committee balanced in accordance with accepted committee procedures, and must be applied by the use of sound and competent engineering judgment…

Page 107:
1. Clearance
Sufficient clearance should be maintained between mains and other underground structures to:

(a) Permit installation and operation of maintenance and emergency control devices (such as leak clamps, pressure control fittings and pinching equipment).

(b) Permit installation of service laterals to both mains and to other underground structures that might be required.

(c) Provide heat damage protection from other underground facilities such as steam or electric power lines, particularly where plastic piping is installed in common trenches with such sources of heat.

Guide Material Appendix G-13, pages 299 and 300

Considerations to Minimize Damage By Outside Forces

1 Introduction

This Guide Material Appendix is intended as an aid in minimizing the possibility of damage to underground gas piping facilities by outside forces.

5 Other

Consideration should be given to the following:

(d) Where a plastic pipeline is installed in a common trench with electric underground lines, the need for additional clearance to prevent damage to the gas line from heating or a fault in the power line.

A primary objective of 49 CFR 192.325 is to provide protection of gas lines (particularly highlighting plastic gas lines) from heat damage from heat sources, including faulting electric power lines. Faulting electrical power lines are a known foreseeable source of heat, as indicated in the ASME guide document. As previously stated, the proposed prescriptive means of accomplishing this goal for the protection of mains was to provide a clearance of 12 inches between the main and the other underground structures, which is consistent with the 1973 National Electric Safety Code and subsequent editions of that standard.

The ANSI/ASME B31.8-1986 code *Gas Transmission and Distribution Piping Systems* [12] also highlights a design intent to protect plastic gas lines from sources of heat including power lines. The referenced code provides the following [underlined emphasis added]:

Page xiii

…The Code sets forth engineering requirements deemed necessary for safe design and construction of pressure piping….

Page 1

802 Scope and Intent

802.11 This Code covers the design, fabrication, installation, inspection, testing and safety aspects of operation and maintenance of gas transmission and distribution systems, including gas pipelines….gas mains, and service lines up to the outlet of the customer's meter set assembly…

Page 45

842.38 Clearance Between Mains and Other Underground Structures. Plastic piping shall conform to the applicable provisions of 841.142. Sufficient clearance shall be maintained between the plastic piping and steam, hot water, or power lines and other sources of heat to prevent operating temperatures in excess of the limitations of 842.32 (b) or 842.33(b).

Finally, the American Gas Association (AGA), which is made up of the gas utility industry as a whole, published *GEOP: Gas engineering and operating practices, Vol. III, Distribution book D-2, Mains and services – Operating considerations* [13], which provides [underlined emphasis added]:

Page xiii

Preface

Mains and Services – Operating Considerations is one of 12 books that will constitute the six-volume A.G.A. Gas Engineering and Operating Practices series addressing various technical aspects of gas supply, transmission, distribution, measurement, utilization, and related technical services. Series contributors were selected for their subject knowledge from 22 A.G.A. Operating Section committees, as well as from industry consultants, suppliers, and other specialist. Authors for Mains and Services – Operating Considerations came from the Distribution Construction and Maintenance, Distribution Design and Development, Laboratory and Chemical Services, and Plastic Materials Committees…

Page 1

Scope

The intent of this book is to provide engineers, technicians, managers, accountants, and other gas industry personnel – particularly those newly introduced from other operating areas to construction, operation, and maintenance of gas mains and services. The areas addressed provide fundamental knowledge, from construction planning through the various phases of maintenance and operations…

Pages 77 to 79

Installation of Plastic Pipe

The following is a listing of service pipe installation practices as set forth in the various plastic pipe codes. A summary of Minimum Federal Safety Standards from Part 192, which deal with

or influence plastic piping, is found in the A.G.A. Plastic Pipe Manual for Gas Services…

Maintain when possible 12 inches (0.3 metre) of clearance from other underground facilities, such as telephone cables, foreign pipelines, manholes and utility poles…when 12-inch clearance cannot be attained, the service should be cased or shielded with rock shield, plastic pipe of larger diameter, or sewer tile. Some companies use a heat shield (rock shield, ceramic pipe, etc.) if proper spacing cannot be attained around electric cables.

The gas utility industry literature clearly recognizes that 12 inches clearance provides appropriate thermal protection of plastic gas piping relative to other underground structures, including electric cables, and when such clearance cannot be obtained proper shielding should be provided. As previously noted, this is consistent with the design goal intent of 49 CFR 192.325 for gas mains.

Engineering Hazard Analysis

Sound engineering design and construction practices follow available authoritative engineering guides, standards, and literature to appropriately address hazards related to a particular design issue.

A hazard is a condition in which harm or damage could occur. The hazard in this case was locating a plastic gas main in close proximity to an underground electrical power cable that could foreseeably fail, generate substantial heat, and compromise the plastic gas main.

Risk is typically defined in terms of the severity of an event combined with the probability of an occurrence. Should the plastic main become compromised by the heat generated during an electrical cable failure, natural gas would be released beneath the asphalt and likely migrate into the building creating conditions favorable for a catastrophic explosion. Such an explosion could destroy the building and cause severe injuries or death. The risk of not providing proper clearances between plastic gas mains and electrical cables is therefore unacceptable.

Cause of the Explosion

NFPA 921 defines the cause of a fire or an explosion as "*the circumstances, conditions, or agencies that brought about or resulted in the fire or explosion incident, damage to property resulting from the fire or explosion incident, or bodily injury or loss of life resulting from the fire or explosion incident*."

Natural gas has a very low ignition energy requirement and subsequently can be ignited from most *normally* present ignition sources located within buildings. If there is an explosive concentration of fugitive natural gas in a building, it is very difficult to avoid contact with *normally* present ignition sources. Subsequently, the potential for a catastrophic explosion is substantial. Therefore, the prevention of natural gas leaks (*fugitive* gases) into structures is more feasible than the elimination of normally present potential sources of ignition. The fugitive natural gas is what is *out of place*, generally not the ignition source; and, as a result, it is the presence of accumulated fugitive natural gas that leads to the explosion. The cause of the explosion in this case is therefore the circumstance that resulted in leakage from the plastic gas main.

There were in existence at the time the gas utility company installed the gas main, authoritative engineering guides, standards, and other industry literature that addressed the hazards associated with locating plastic gas piping in proximity to electrical power cables and the proper means of protecting the pipe in such circumstances. Based on a review of the referenced engineering guides, standards, and other industry literature, it is most probable that 12 inches of clearance would have prevented the damage to the plastic gas line during the arcing event of the failed electrical cable. Therefore, the gas leak — and subsequently the explosion — would have been prevented.

The gas utility company knew — or should have known — of the hazard associated with installing the underground plastic pipe main in close proximity to direct buried electrical power cables. The gas utility company was in the business of engineering, installing, operating, and maintaining gas distribution systems. Specifically, the gas utility company took on the task of installing a plastic gas main in close proximity to an existing direct-buried electrical power line, and subsequently knew (or should have known) the associated hazards and proper means of protecting the gas line in such an installation.

An understanding of the hazards represented by other underground structures (e.g., electrical cables) that the gas utility company was installing its gas mains in close proximity to would be necessary on the part of

the gas utility company in order to know how to properly address and protect against such hazards and to comply with 49 CFR 192.325.

Sound engineering practices involve researching and evaluating the appropriate authoritative standards and industry literature provisions related to locating underground plastic gas piping in proximity to other underground structures, including direct-buried electrical power cables. Furthermore, sound engineering practices would involve contacting the owner/installer of adjacent utilities to determine what safe clearances were required from their structures. According to the electric utility company, that clearance would have been a minimum of 12 inches at the time the gas utility performed its installation.

The gas utility company's failure to comply with the provisions of 49 CRF 192.325 and follow sound engineering practices and industry standards caused the explosion.

References

1. NFPA 921-2014. Guide for fire and explosion investigations. Quincy, MA; National Fire Protection Association.

2. Kennedy P, Kennedy J. Explosion investigation and analysis: Kennedy on explosions. Chicago, IL: Investigations Institute; 1990.

3. ANSI/IEEE C2-1984. National Electric Safety Code. Piscataway, NJ: Institute of Electrical and Electronics Engineers, Inc.

4. National Fire Protection Association. Fire protection handbook, 16th edition. Quincy, MA: The National Fire Protection Association; 1986.

5. Pipeline accident report: natural gas explosion and fire at South Riding, Virginia. Washington, DC: National Transportation Safety Board; July 7, 1998 *(*adopted 2001).

6. Clapp A (ed). NESC Handbook: Development and application of the American National Standard National Electrical Safety Code grounding rules, general rules, and parts 1, 2, and 3. Piscataway, NJ: The Institute of Electrical and Electronics Engineers; 1984.

7. ASTM D 2513-87. Standard Specification for Polyethylene (PE) Gas Pressure Pipe, Tubing, and Fittings. West Conshohocken, PA: ASTM International.

8. ASTM D2774-1973. Standard practice for underground installation of thermoplastic pressure piping. West Conshohocken, PA: ASTM International.

9. United States Department of Transportation. Code of Federal Regulations (CFR) Title 49 Transportation Part 192 Transportation of Natural and Other Gas by Pipeline: Minimum Federal Safety Standards. Washington DC: United States Government Printing Office; October 1, 1988.

10. Federal Register, Volume 35, No. 161, Page 13254. Washington DC: United States Department of Transportation; August 19, 1970.

11. American Society of Mechanical Engineers. ASME Guide for gas transmission and distribution piping systems. New York, NY: American Society of Mechanical Engineers; 1986.

12. ANSI/ASME B31.8-1986. Gas transmission and distribution piping systems. New York, NY: American Society of Mechanical Engineers.

13. American Gas Association. GEOP: Gas engineering and operating practices, Vol. III, Distribution book D-2, Mains and services – Operating considerations. Arlington, VA: American Gas Association; 1986.

Forensic Considerations Regarding Traction and Tribometry of Bathing Surfaces

By John Leffler, PE (NAFE 709S) and Mark Blanchette, PhD

Abstract

In 1974, the federal Consumer Product Safety Commission (CPSC) funded a study of injury patterns involving bathing surfaces. The study found the majority of injuries were due to slips and falls. The data from the CPSC-driven tribometry research was used to develop (with the cooperation of bathing surface manufacturers) a standardized test specification and minimum traction threshold. The standard that resulted in 1979, ASTM F462, was a positive step forward — but over 36 years the shortcomings of this long-obsolete standard have become increasingly evident. Nevertheless, F462 remains the sole codified standard for bathing surface traction in the United States. This paper will discuss the limitations of F462, the use (and misuse) of the standard in claims resolution and litigation, the efforts to modernize F462, and some considerations for investigating bathing surface incidents.

Keywords

Premises liability, bathing, bathtub, pedestrian, slip resistance, tribometer, traction, barefoot

Author's Note

Following completion of this paper, ASTM F462 was formally withdrawn by ASTM, though it continues to be used in the absence of a replacement.

Introduction

A forensic case involved a man who allegedly slipped and fell in a hotel bathtub in May of 2013. This plaintiff's expert conducted testing of the bathtub in accordance with ASTM F462, *Standard Consumer Safety Specification for Slip Resistant Bathing Surfaces,* and asserted that the bathtub did not meet the requirements of that standard[1]. The specifics of this case and the countering of that expert's assertions provided context for the following analysis of F462.

Efforts have been considered for years regarding the replacement of F462. Recent methodologies have provided new options for modernizing F462, but one of the complicating issues is that bathtub traction is federally regulated.

Summary of the Initial Timing of ASTM F462 and Related Standards

- ASTM F462-1979 was first released in May 1979. It has been reapproved without change repeatedly since then — most recently in 2007.
- The September 1979 revision of ANSI/ASME A112.19.1, *American National Standard for Enameled Cast Iron Plumbing Fixtures,* referenced F462[2]. This ASME standard, and its subsequent revisions, are referenced, in turn, by the U.S. government (e.g., 24 CFR 3280.604 for Manufactured Housing).
- The 1984 revision (released in July 1985) of ANSI/ASME A112.19.4, *American National Standard for Porcelain Enameled Formed Steel Plumbing Fixtures,* referenced F462[3]. This ASME standard is also referenced by the U.S. government.

Federal Foundations of ASTM F462

In late 1973, ASTM's newly founded F15.03 Subcommittee on Safety Standards for Bathtubs and Shower Structures began contacting plumbing product manufacturers at the direction of the also recently formed CPSC toward an effort to address bathing surface safety through standards[4]. Federal funding also went in 1974 to Abt Associates for a survey and analysis of National Electronic Injury Surveillance System (NEISS) bathroom incident data, which included slip incident data involving both textured and untextured bathing surfaces as well as incidents wherein the

John Leffler, PE, 1730 Mt. Vernon Road, Suite H, Atlanta, GA 30338, (770) 390-0980, jleffler@forcon.com;
Mark Blanchette, PhD, 26440 La Alameda, Suite 350, Mission Viejo, CA 92691, markblanchette@sempersci.com

surface had soaps or oils on the surface[5]. This survey did not involve any evaluation of human traction *requirements*, nor traction measurement of incident-involved bathtubs. The findings of the Abt Associates report listed as stated goals that "every tub and shower stall will be provided with a standing surface which is slip resistant," and that "realistic test methods are badly needed." The means of facilitating this were to include an analysis of the "parameters of movement associated with accident sequences" and a focus on accurately simulating the wet bare foot and the bathtub conditions (e.g., soapy) present in bathtub slip events.

With CPSC support, the National Bureau of Standards worked with F15.03 committee to create what became the F462 standard. As a minimum traction threshold value (for bathing surfaces) was to be established, it was necessary to choose a tribometer, a testfoot material, and a liquid contaminant.

The three final candidates for the tribometer were the Horizontal Pull Slipmeter (HPS), the British Pendulum, and the then-new NBS-Brungraber Mark I tribometer[4]. The Mark I was chosen due to its combination of portability and ability to be calibrated across its measurement range. It had been designed by civil engineering professor Robert Brungraber, PhD, PE, in 1975, with funding from the National Bureau of Standards (NBS, now the National Institute of Standards and Technology or NIST) — hence the name "NBS-Brungraber Mark I." At one time, the manufacturing drawings were reportedly available through NBS, as it was a publicly funded design. The tribometer was one of the first readily portable tribometers (i.e., suitable for field use) on the market in the United States.

The selection of the liquid contaminant was a lengthy process[6]. Considerations included whether to use a soap or detergent, what concentration to use, and whether the prepared soap solution would be stable over time[7]. It was discussed whether to prescribe a single formulation, but the eventual choice was any soap compliant with federal specification P-S-624G or ASTM D799 (withdrawn in 2000).

The Abt Associates report had called for finding a testfoot material that would simulate the skin of the bare foot. But several explored options (including a shredded leather/rubber composite, the tanned skin of unborn calves, and neoprene foams) did not prove useful, due to their measurement performance or limitations in reliable sourcing[7]. Eventually, Dow Corning's silicone rubber Silastic 382 was chosen[4].

As mentioned, a goal within the Abt Associates report was to analyze the "parameters of movement associated with accident sequences," yet the eventually chosen traction threshold value was not based on actual human slip research. The value was chosen based on *comparative* traction measurements of 50 different bathing surfaces (i.e., bathtub A versus bathtub B, not bathtub A versus human traction requirements) provided by various manufacturers in 1976 — and tested with a single Mark I tribometer. The 50 tested surfaces included both porcelain-coated and plastic/composite products. The threshold – a static coefficient of friction (SCOF) value of 0.04 – was chosen simply to exclude those bathing surfaces on the market that had no slip-resistance traction/texture features at all[4].

Analysis of the Technical Foundations of F462

In ASTM F462, the traction level of the bathtub is to remain at or above 0.04 for the life of the manufacturer's guarantee. Since the 0.04 SCOF minimum traction threshold requirement in F462 has no correlation to actual reliably determined human traction research, from a forensic investigation standpoint, testing to F462 does not tangibly address the actual safety provided to humans by the available traction of a bathing surface.

Given that one of the key goals of the comparative bathing surface testing was to eliminate non-textured surfaces, it is ironic that the F462 requirements have not prevented some bathtub manufacturers from making reportedly compliant bathtubs that have no apparent slip-resistance texture features (see **Figure 1**).

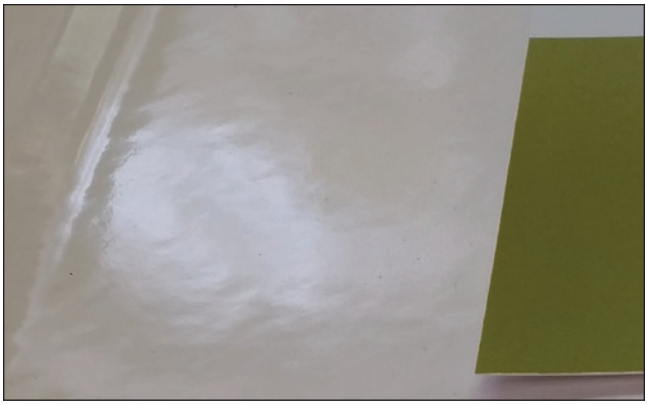

Figure 1
A new commercial "F462 compliant" porcelain enamel bathing surface with no visible texture features.

Analysis of Competence of ASTM F462 — Tribometer

ASTM F462 specifies the use of only one tribometer. Dr. Brungraber's company (Slip-Test) manufactured the Mark I tribometer until about 1992; Dr. Brungraber retired in 2010, and neither parts nor service have been available for the Mark I since 2010*.

The Mark I's test measurement performance is susceptible to the device's internal friction; the design utilizes two sets of parallel stainless steel shafts upon which components slide (see **Figure 2**). As such, this design is sensitive to manufacturing dimensional tolerances and manufacturing consistency — yet the manufacturing drawings for the Mark I (which date from 1975) were created without a thorough tolerance analysis or the application of Geometric Dimensioning and Tolerancing (GD&T)[8]. The effect of unit-to-unit variability sources can be studied across a population of tribometer units, but there is no evidence this was done in the development of the Mark I. Further, to the authors' knowledge, there has never been a published reproducibility study conducted with the Mark I, though the need for one was highlighted back in 1977 in NBS 953[9].

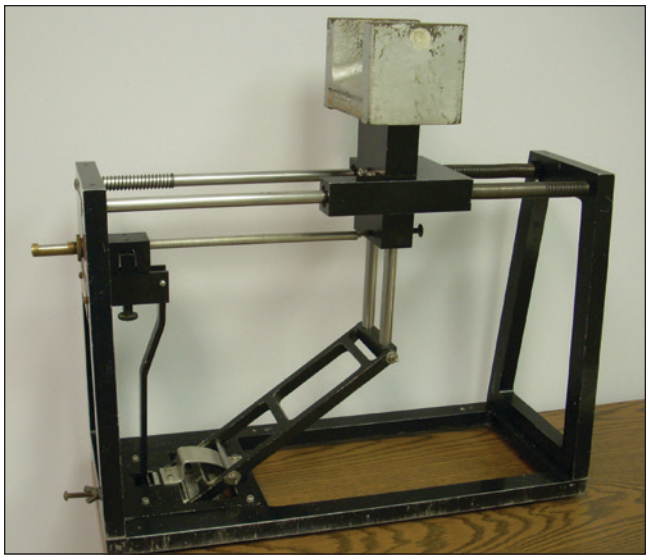

Figure 2
NBS-Brungraber Mark I tribometer.

Reproducibility/repeatability analysis, conducted using an *interlaboratory study* (ILS, aka "round robin" study) shows the statistical differences between measurements obtained by different operators using different units of the same test device on the same test samples[10]. Such testing should capture variability introduced by differences in as-manufactured tribometer part dimensions, internal friction, operator technique, and operator interpretations of the test method. Reproducibility/repeatability statistics provide critical information as to whether measurements made with a test device bear a reliable relationship to either: 1) a standardized threshold value (e.g., 0.04 SCOF); or 2) measurements made by others.

Reproducibility/repeatability data are frequently referred to as the *precision* of a methodology. ASTM's *Form and Style for ASTM Standards* guideline (also known as the "Blue Book") currently require that a precision statement be included in any ASTM standard test method within the first five years following initial publication, and test methods that do not achieve this are withdrawn[11]. At a minimum, the net effect is that a Mark I operator cannot know how his or her measurements relate to the measurements obtained in the 1976 comparative bathing surface study, or how his or her measurements relate to those of other operators. In a typical litigation setting, if an expert witness's analysis methodology cannot be duplicated by others, the expert witness may be subjected to a *Daubert* (or similar) challenge[12].

Neither F462 nor Slip-Test prescribed any particular maintenance or manufacturer calibration requirements for the Mark I tribometer, and no manufacturer has offered maintenance services for the Mark I in more than five years. As such, the comparative functional condition of all the 22- to 39-year-old Mark I tribometers in existence is uncertain. While F462 specifies the use of only the Mark I, there are forensic investigators who will use an alternative (non-Mark I) tribometer on a bathing surface and reference F462 — often without competent expert opposition. But such a methodology is technically indefensible (quoting from Powers et al):

> "The fact that the measurement of friction is a function of both the material being tested and the measuring system itself explains why several studies have shown that different devices yield different COF measurements for the same surface[13]."

Considering this in a forensic context, there is no reason to expect that measurements made on a bathing surface with a tribometer other than a Mark I would be comparable to those of a Mark I — and, as such, the measurements would be irrelevant to F462.

Another key issue with F462 testing is the SCOF value of 0.04 (specified as the minimum threshold). On

* See author John Leffler's disclosure following the conclusions section.

a level surface, the Mark I doesn't actually function at a measurement value of 0.00, so the operator must offset the starting position of the device to a measurement of about 0.01 - 0.02. This is the effective "zero" traction for the device. Therefore, the F462 "passing" measurement of 0.04 represents a value just barely beyond this effective "zero" point (i.e., the lower limit of the tribometer's measurement capability) on a measurement scale that goes to 1.00. In other words, the "passing" value is 2% higher than an unmeasurable value.

Over the years, some of these issues have been brought up in negative votes against ASTM's periodic re-approval ballots for F462. The standard is widely criticized and is a regular candidate for withdrawal, but it is the only standard for bathing surface traction. On this topic, *Haney v. Marriott International, Inc.* may be of interest to the reader[14]. The CPSC has requested that the standard remain in place until a replacement is published. The complexities and costs of creating a new "competent" F462 (which will be discussed later in this paper) are perhaps the primary reason why it remains unchanged.

Forensic Case Inspection of Subject Hotel Bathtub

An inspection revealed a porcelain enamel-coated metal bathtub shown in **Figure 3**. According to the hotel manager (who had been at the property since 1986), the bathtub was likely original to the building's 1975-76 construction. The brand, model, and manufacturer's warranty information for the bathtub were unknown; destructive removal of the bathtub would not necessarily have provided this information.

Figure 3
Incident-involved bathtub.

A pattern of the bathtub manufacturer's slip-resistance traction features was visible across the bottom surface of the bathtub (see **Figure 4**). If the subject bathtub were to be subject to the requirements of modern standard ASME A112.19.1M, the traction features would be required to come within certain distances of the sides of the bathtub — the subject bathtub conformed to these modern dimensional requirements.

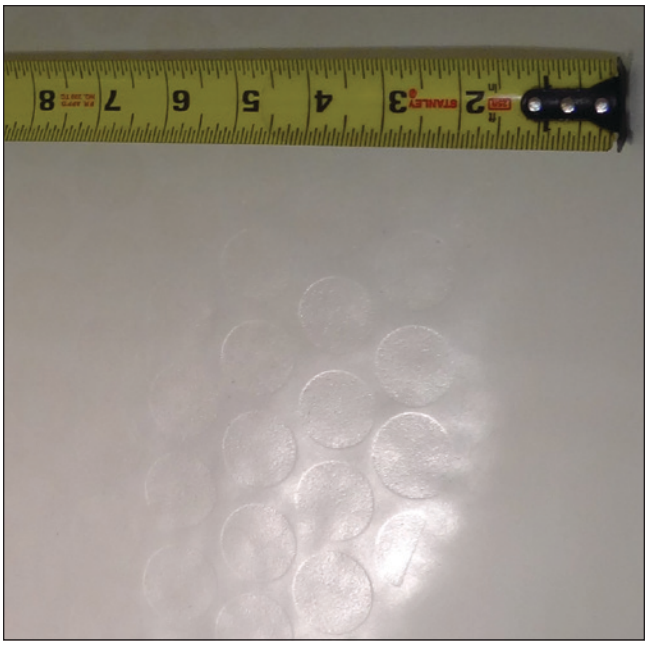

Figure 4
Slip-resistant features along bottom of subject bathtub.

Analysis: Applicability of Standards to Subject Bathtub

Assuming the manager was correct that the subject bathtub dated from 1975 or 1976, ASTM F462 was still being developed. As such, there were no applicable slip resistance requirements. There were no requirements for bathing surface traction until September 15, 1979 when F462 compliance was first required by reference in ASME A112.19.1M-1979.

If the subject bathtub was manufactured after September 15, 1979, depending upon its construction, it may have been required by the ASME A112 standards to meet ASTM F462. ASTM F462 states in section 5.3 that "the slip resistance of the bathing surface shall remain at or above the level required by this specification during the life of the manufacturer's guarantee." It is highly unlikely that the subject bathtub, which was (based on the manager's testimony) at least 29 years old, was still under the manufacturer warranty in 2013. Further, the ASME A112 standards focus on new plumbing fixtures (e.g., bathtubs), and there was no discussion of warranties, guarantees, or durability of slip-resistance traction features.

Summary of Forensic Considerations in the Context of Subject Incident

- As a prefacing note, this paper discusses extrinsic factors of the subject forensic case. There were intrinsic considerations as well, as the plaintiff had potentially contributory medical conditions. However, intrinsic issues are not the focus of this paper.

- If the bathtub was original to the hotel construction, F462 was not yet adopted at that time, and there were no standard requirements in place for bathtub traction.

- If the bathtub was subject to ASTM F462 at the time of manufacture, that standard does not require any particular level of slip resistance beyond the period of the manufacturer warranty. It was reasonable to conclude that the decades-old subject bathtub was out of warranty, so F462 would not apply.

- The ASME A112 standards do not add any bathtub slip resistance durability requirements beyond what is specified in F462. It was reasonable to conclude that the subject bathtub was out of warranty, and thus would not violate those standards.

- The plaintiff's expert's results from his Mark I testing cannot be reliably correlated to the F462 traction threshold requirements — he did not use the Mark I utilized in the F462 research, and there is no reproducibility analysis describing the effects on measurement results of different operators using different Mark I tribometers on the same surface. Because of this, his methodology also was not reasonably reproducible by other parties — making it a candidate for a *Daubert* or other reliability challenge.

- Even if F462 was applicable to the subject bathtub, test results for the subject bathtub would not assist the triers of fact with reliable information regarding the safety of the bathtub floor surface due to the issues with the technical foundations of the standard.

- Given the described issues with ASTM F462, the adequacy of an in-use bathtub's traction typically gets down to the question of reasonable notice:

  - If a property holder has not (in the reasonable conducting of business) been made aware of a pattern of bathtub slips that cannot be linked to bathtub-traction-unrelated issues (e.g., claimant intoxication, persistent and atypical bathing lubricants, rough child play, or claimant intrinsic medical issues), then arguably they do not have reasonable notice of a bathtub hazard. In the context of another matter, see *Billings v. Starwood Realty et al* [15].

    - The subject hotel had four reported bathtub falls between January 2008 and May 2012. Of those four, two had contributing factors (one person was a toddler, and the other was reaching outside the bathtub for a towel). This arguably does not comprise a significant pattern, given the thousands of guests that stayed at this hotel every month.

  - Bathtub manufacturers do not publish recommendations (or, more importantly, methods) for property holders to periodically analyze the traction of their bathtubs. In the absence of such recommendations, the property holder does not have actionable reasonable notice provided by the manufacturer that the installed bathtubs may (over time) lose their slip-resistance characteristics to the point of becoming hazardous.

  - If a property holder does not have the opportunity to visually observe (through reasonable practices of inspection) that the slip-resistance traction features of a bathtub floor surface have obviously worn out, then arguably they do not have reasonable notice of a bathtub hazard. Complicating this further, not all "F462-compliant" bathtubs have observable slip-resistance traction features. Lastly, there is no objective method established in industry to reliably verify that a bathtub's traction features have indeed "worn out."

    - The subject bathtub had visible slip-resistance traction features across its bottom surface to within the perimeter edge requirements of modern ASME standards.

  - In the event that property holders decide they want to increase the traction of their bathtubs,

there are a variety of options (sandblasting, chemical etchants, "sticky" coatings, appliques, rubber mats), all of which are advertised as competent by their manufacturers. Yet the foregoing discussion points out that there is little relevant science behind the codified traction of *new* bathtubs, and the science behind the traction of aftermarket refurbishing treatments (for which there are no standards) may not be objective. An understanding of such details is likely beyond the expertise of the average property holder.

Future Opportunities for Bathing Surface Safety Standards

It is reasonable to conclude that public safety would be better served by a more competent traction standard for bathing surfaces (i.e., a standard with a reliance on human slip research). As mentioned, such a standard would be complex and costly to develop — which is perhaps why it has not happened to date. Nevertheless, recent methodologies may provide useful barefoot-testing-based foundations for a competent replacement of ASTM F462, subject to consensus approval. Elements to consider with this human slip testing may include:

- Intrinsic elements:
  - Selection of the desired gait parameters to be modeled (e.g., velocity, straight walking versus step-over, changing direction, stride length versus step-over height).
  - Definition of what comprises a "slip" (e.g., foot velocity, slip distance) in this context.
  - Management of slip expectation in test subjects.
  - Test subject population characteristics (e.g., age, sex, mass, height, disabilities, number of subjects).
  - Barefoot sole conditioning (e.g., dry versus wet skin).
  - Accommodating differences between test subjects' barefoot skin friction due to factors such as callouses and the depth and orientation of dermal ridges.
- Extrinsic elements:
  - Different bathing surfaces to be represented (e.g., porcelain enamel, mosaic tile, gelcoat/fiberglass, vacuum-formed).
  - Geometry of test surfaces (planar versus the slight concavity of a bathtub).
  - Differences in friction mechanisms (e.g., fine roughness of textured porcelain enamel versus molded dimples on vacuum-formed plastic surfaces).
  - Patterns and geometry of traction features (e.g., geometry and distribution of "medallions" of texture on otherwise untextured enamel; geometry and distribution of molded dimples on plastic surfaces).
  - Contaminant supply to the test surface (e.g., static or flowing liquid, use of soap or detergent, concentrations).
  - Whether to record forceplate data, slip events (slip/near-slip/no-slip), or both.
  - Agreement on an objective and standardized way to uniquely characterize, describe, and refer to the different surface materials and traction features.

Consistent with ASTM F2508 and DIN 51130, one key goal of any proposed human slip research should be to produce a suite of progressively slippery standardized reference surfaces that can be made available in duplicate [16, 17]. These surfaces can be used by bathing surface manufacturers for comparison to production surfaces and by tribometry researchers to verify whether a particular tribometer can rank and differentiate the suite of surfaces in the same order the humans did. With reference surfaces, rather than having a minimum traction *threshold value* based on one tribometer (like with ASTM F462), a future standard could be based on the tribometer-specific traction value measured on a minimum-traction *threshold surface* (i.e., a reference bathing surface that provides the traction needed to deter human slips in testing). With such a threshold surface, different tribometers (properly qualified) could be used for testing, regardless of what measurement scale they utilize or what value they measure

on that threshold surface. Simply stated, this approach again allows for the establishment of a relative traction threshold value that is tribometer specific, and, in turn, would allow for the testing of bathing surfaces by tribometers that do not have ILS data. This is a critical concept in interpreting tribometer measurements and slip risk, as without the reproducibility/repeatability data from an ILS to rely on, an individual tribometer's traction measurements are not directly comparable to measurements from other units of the same model (i.e., Mark I to Mark I).

As it takes specialized production equipment to make bathing surfaces, existing bathing surface manufacturers would be the most obvious source for standardized reference surfaces. There would need to be agreement among them as to how to standardize both terminology and manufacturing processes for reference surface traction features — given expected concerns regarding trade secrets. Based on recent human slip research, it is possible that the minimum traction threshold will be raised above that of ASTM F462, potentially requiring different surfacing methods than are currently in common use [18]. Participation by the manufacturers would be advisable as well from the standpoint of gaining consensus approval for F462's replacement.

Recent Human Subject Research Relevant to Bathing Surface Traction

Bathing surface gait kinematics are markedly different than those of normal walking[20]. Shorter steps are taken, step-over thresholds are higher, and the bather is barefoot. The presence of wet or soapy surfaces (and past experience) may alert the bather to the need for caution [19,20]. Barefoot pedestrian testing is relatively rare in the literature. German standard DIN 51097 and research by Sariisik were both based on barefoot testing, though this testing was conducted on ramps [21,22]. Others have pointed out that the gait dynamics of walking on ramps are different than walking on a level surface [23]. As such, gait dynamics on ramps would be different from walking in or out of a (level) bathtub.

The friction mechanisms of bare feet (on wet surfaces) are significantly different from those of footwear. The components of footwear that influence underfoot traction include the outsole tread design, tread groove width, depth and orientation, outsole material and hardness, micro- and macroscopic outsole roughness, and heel contour. Characteristics of the human foot that affect the traction at the foot-floor interface include the dermal ridges of the skin on the heel (comparable to fingerprints), skin thickness, fatpad thickness and deformity, skin hardness, contour of the calcaneus, and skin conditions such as callouses. Moreover, these barefoot characteristics will vary between people, and potentially influence slip events during human subject testing and the development of a traction threshold.

Human slip research by Powers et al was useful in identifying a suite of progressively slippery reference surfaces for level walking (see ASTM F2508) — a concept (discussed above) that could aid in establishing reliable methodologies for improving bathing surface safety[13,16]. Another study that is perhaps more on point (as a conceptual foundation for F462 replacement research) is by Siegmund et al., in which test subjects stepped into and out of a bathtub that had been fitted with forceplates in the foot contact areas[18]. The forceplates were used to measure utilized COF during various combinations of bathtub entry and exit motions (and associated kinematics), with a flow of liquid contaminant within the bathtub.

Considerations for Tribometry of Bathing Surfaces

There has been much debate, from a tribometry standpoint, as to the appropriate test foot material (if any exists) to be used for the assessment of bathing surface traction. Medoff, Besser, and Marpet have reported on creating silicone rubber tribometer testfeet from human heel casts (to obtain realistic friction ridges), and they suggest that such testfeet would need a minimum of three layers to represent the skin, the underlying fat pad, and the calcaneous [24]. The challenges of creating a somewhat biofidelic "barefoot" tribometer testfoot are significant — most "skin tribometry" studies have not focused on bare feet.

Other work by Besser and Marpet has focused on dropping the guided bare foot of a seated human test subject onto a sloped test surface, and then repeating the test at progressively increasing surface slopes until the foot slips [25]. The tangent angle of the surface slope then corresponds to the slip resistance value of the surface.

Work by Blanchette and Brault in the preliminary stages (unpublished data) attempts to compare the COF of the ASTM F2508 adjunct reference surfaces as measured by several tribometer testfoot materials and cadaver heel pads.

Conclusions

- For the forensic case discussed, there was no evidence that ASTM F462 applied to the subject bathtub, nor that testing to F462 would have reliably informed the triers of fact.

- Given the issues with F462, some bathtub fall cases may instead rely on analysis of "reasonable notice" of a hazard — to the property holder and to the bather.

- Due to the issues with ASTM F462, both public safety and the field of forensic analysis are poorly served by the standard. It needs to be replaced as soon as practically possible.

- Replacing ASTM F462 would be expensive, time consuming, requiring of many disparate contributors, requiring of new human slip research, and requiring of government support.

Disclosures

In addition to employment as a forensic engineer, John Leffler is lead engineering consultant to tribometer manufacturer Slip-Test, Inc., a corporation formed in 2010 based upon the intellectual property and business inventory purchased from Dr. Robert Brungraber's original Slip-Test company, upon Dr. Brungraber's retirement. With that purchase, this author also received Dr. Brungraber's files, his former Mark I tribometer, and a small stock of Mark I parts, yet due to issues discussed in this paper, the tribometer was promptly sold in "as is" condition — there was no foreseeable use for it. Further, due to the Mark I's issues, no attempt has been made to offer servicing or parts for Mark I tribometers — as such work could not be warranted as reliable.

Mark Blanchette is the F13.40 Research Subcommittee Chair in the ASTM F13 Pedestrian/Walkway Safety & Footwear Technical Committee.

References

1. ASTM F462-1979r2007. Standard consumer safety specification for slip-resistant bathing facilities. West Conshohocken, PA; ASTM International.

2. ASME A112.19.1M-1979. Enameled cast iron plumbing fixtures. New York, NY; American Society of Mechanical Engineers.

3. ASME A112.19.4M-1984. Enameled formed steel plumbing fixtures. New York, NY; American Society of Mechanical Engineers.

4. Brungraber RJ, Adler SC. Technical support for a slip-resistance standard. In: Anderson C, Senne J editors. Walkway surfaces: measurement of slip resistance, ASTM STP 649. Philadelphia; American Society for Testing and Materials: 1978.

5. Stone RF et al. A systematic program to reduce the incidence and severity of bathtub and shower area injuries. Cambridge MA; Abt Associates Inc.: 1975.

6. Armstrong PL, Lansing SG. Slip-resistance testing: deriving guidance from the National Electronic Injury Surveillance System (NEISS). In: Anderson C, Senne J editors. Walkway surfaces: measurement of slip resistance, ASTM STP 649. Philadelphia; American Society for Testing and Materials: 1978.

7. From correspondence and documentation within the files of Robert Brungraber, PhD, PE.

8. ASME Y14.5-2009. Dimensioning and tolerancing. New York, NY; American Society of Mechanical Engineers.

9. Brungraber R. A new portable tester for the evaluation of the slip-resistance of walkway surfaces. NBS Technical Note 953. Washington DC; National Bureau of Standards: 1977.

10. ASTM E691-2011. Standard practice for conducting an interlaboratory study to determine the precision of a test method. West Conshohocken, PA; ASTM International.

11. Form and style for ASTM standards. West Conshohocken, PA; ASTM International: 2013.

12. Daubert v. Merrell Dow Pharmaceuticals, Inc., 509 U.S. 579 (1993)

13. Powers CM, Blanchette MG, Brault JR, Flynn J, Siegmund GP. Validation of walkway tribometers: establishing a reference standard. J. Forensic Sci. 2010;55(2):366-370.

14. Haney v. Marriott International, Inc., U.S. Dist. LEXIS 74872 (2007) at *15.

15. Billings v. Starwood Realty, CMBS, I, LLC et al, 2006 U.S. Dist. LEXIS 65182.

16. ASTM F2508-2013. Standard practice for validation, calibration, and certification of walkway tribometers using reference surfaces. West Conshohocken, PA; ASTM International.

17. DIN 51130-2014. Testing of floor coverings – determination of the anti-slip property – workrooms and fields of activities with slip danger - walking method - ramp test. Berlin; Deutsches Institut für Normung.

18. Siegmund GP, Flynn J, Mang DW, Chimich DD, Gardiner JC. Utilized friction when entering and exiting a dry and wet bathtub. Gait & Posture. 2010;31:473-478.

19. Cham R, Redfern MS. Changes in gait when anticipating slippery floors. Gait and Posture. 2002;15:159-171.

20. Heiden TL, Sanderson DJ, Inglis JT, Siegmund GP. Adaptations to normal human gait on potentially slippery surfaces: The effects of awareness and prior slip experience. Gait & Posture. 2006;24.

21. DIN 51097-1992. Testing of floor coverings; determination of the anti-slip properties; wet-loaded barefoot areas; walking method; ramp test. Berlin; Deutsches Institut für Normung.

22. Sariisik A. Safety analysis of slipping barefoot on marble covered wet areas. Safety Science. 2009;47.

23. Redfern MS, DiPasquale J. Biomechanics of descending ramps. Gait and Posture. 1997;6:119-125.

24. Medoff H, Besser M, Marpet M. Progress in the characterization of barefoot pedestrian friction. Proceedings of the American Academy of Forensic Sciences; Volume XVIII: February 2012.

25. Besser M, Marpet M, Medoff H. Barefoot-pedestrian tribometry: In-vivo method of measurement of available friction between the human heel and the walkway. Industrial Health. 2008;46.

Preliminary Analysis of Roadway Accident Rates for Deaf and Hard-of-Hearing Drivers — Forensic Engineering Application

By Martin E. Gordon, PE (NAFE 699S) and Justin J. Pearson

Abstract

According to the World Health Organization, there are more than 360 million people worldwide with hearing loss. The National Highway Traffic Safety Administration (NHTSA) has reported that close to 30% of the United States population 65 years or older has significant hearing loss. The objective of this paper was to determine if deaf and hard-of-hearing drivers are more likely to be involved in motor vehicle accidents than hearing drivers. Data was extracted from the National Automotive Sampling System (NASS) and motor vehicle accident records from the Rochester Institute of Technology (RIT) and National Technical Institute for the Deaf (NTID) campuses. The results of the NASS data analysis indicate that deaf and hard-of-hearing drivers are one and a half to nine times as likely to be seriously injured or killed in a motor vehicle accident. Motor vehicle accident records from RIT and NTID suggest that deaf and hard-of-hearing drivers are approximately three times as likely to be involved in a motor vehicle accident as hearing individuals. Forensic engineers may be able to use this data to assist in forensic engineering analysis in cases where deaf or hard-of-hearing drivers are involved.

Keywords

Forensic engineering, traffic crash reconstruction, deaf drivers, hard-of-hearing drivers, accident rates

Introduction

The World Health Organization estimates that there are more than 360 million people worldwide with hearing loss, but there is no research entity dedicated to the study of road safety as it relates to deaf and hard-of-hearing (D/HH) locally, nationally or internationally. In fact, very little has been done worldwide to study deaf and hard-of-hearing drivers [1]. In the United States, as indicated in **Figure 1**, close to 30% of the population 65 years or older has significant hearing loss. A study commissioned by the National Highway Traffic Safety Administration (NHTSA) in 2005 recognized that very few studies of D/HH drivers have been conducted, and these studies had inconclusive results. The study points out that there is no evidence that warrants driving restrictions for the D/HH. In fact, the Americans with Disabilities Act of 1990 (ADA) and the Rehabilitation Act of 1973 (Rehabilitation Act) normally prohibit states from using risk assessment to prevent people with disabilities from driving. Instead, special driving tests are given to individuals to determine if they are a threat to public safety [2].

Currently, D/HH persons are able to obtain drivers licenses in all 50 states. However, in the 1920s, at least four states would not issue driving licenses to the D/HH[3]. The licensing requirements for the D/HH in New York State simply require a restriction indicating "hearing-aid" or "full-view mirror" [4].

By using the National Accident Sampling System (NASS)[5] and data from accidents occurring on the campus of the Rochester Institute of Technology (which includes the National Technical Institute for the Deaf), a potentially significant link between deafness and rates of injury, death, and accident involvement was discovered. This paper presents the *preliminary* findings from data mining these two sources. It is hoped that the paper will lead to a better understanding of what can be done when performing forensic engineering analysis of traffic accidents involving the D/HH. Additionally, it is hoped that further research may point to technologies that may be used to decrease driving risks for the D/HH and improve highway safety for all roadway users.

Martin E. Gordon, PE, Rochester Institute of Technology, 78 Lomb Memorial Drive, Rochester, NY 14623, (716) 913-2912, megite@rit.edu

Age Group	% of Population that is Deaf
3-17 years	1.8
18-34 years	3.4
35-44 years	6.3
45-54 years	10.3
55-64 years	15.4
65 years and older	29.1
Average for all ages	**8.6**

Figure 1
Deafness by age[2].

Data Mining

Two sources were used for data mining — the 2013 NASS GES database and a campus motor vehicle accident database between 2011 and 2015 for the Rochester Institute of Technology (RIT), which contains the National Technical Institute for the Deaf (NTID) on its suburban campus.

The 2013 NASS GES database was searched for a driver impairment type "deaf." For accidents sampled by NASS between 2008 and 2013, there were 36 cases involving a driver that had a "deaf" impairment. It is suspected that there are many more cases involving D/HH operators that do not show up with a "deaf" impairment flag. NASS administrators do not explain under what conditions "deaf" will be listed as impairment. If involved drivers were killed or seriously injured, it is not known how an investigator would know the hearing status of the operator.

The database from RIT and NTID was constructed to allow investigators an easy way to indicate whether a driver was hearing or deaf. The total campus population is around 17,000 students, of which approximately 5% to 6% are D/HH. The database included partial information from 384 accidents with complete information for only 319 of these accidents. D/HH drivers accounted for 49 of these accidents while hearing drivers were involved with 335 accidents. Only accidents with complete information (319 total) were used for statistical analyses. The accidents were of various severities, with most falling into the "minor" classification — not unexpected given a maximum campus speed limit of 35 mph and the many campus parking lots.

Data Analysis

NASS GES Data Source

Utilizing accident records for drivers from 2008-2013, the Rao-Scott Chi-Square test for association rejects the hypothesis of no association between hearing/deaf status and severity of injury with 0.02% significance (that is, 0.02% chance of observing data at least as extreme as found in the GES if there was no relation between deafness and injury severity).

This indicates that there is a relation between deafness and injury severity. Specifically, the probability of sustaining injuries of particular severities differs for deaf and hearing drivers. A visual overview of the injury distributions by impairment suggests that deaf drivers are more likely to experience injury in an accident, as can be seen in **Figure 2**.

Distinguishing only between drivers that did or did not experience definite injury — regardless of accident severity — a 95% odds ratio shows that hearing drivers are at least 1.4702 times (and at most 9.901 times) as likely to be uninjured in an accident as a deaf driver. This is the same as saying that deaf drivers are at least 0.101 and at most 0.6802 times as likely to be uninjured in an accident as hearing drivers. These general conclusions highlight the need for more research, since factors such as restraint usage, frontal impacts vs. rollovers, ejected vs. contained, could not be considered because of an insufficient quantity of deaf driver data sets containing these factors.

Data includes belted and unbelted drivers — future data mining may try to separate these groups to isolate deafness as a cause of higher injury rates. The authors are unaware whether hearing drivers or deaf drivers have different rates of seatbelt use. Data for hearing drivers came from the same source as for D/HH drivers, namely the NHTSA GES records. Driver impairment (such as "deaf" or "hard-of-hearing" and "none") was recorded, so it was possible to distinguish between groups for analysis — given the caveats discussed in the previous section.

Cases where injury status was unknown — and cases where the driver had died prior to the accident — were removed as unsuitable. Also disregarded for both hearing and D/HH drivers were cases where injury proved fatal, as none of the D/HH records collected were of fatal accidents. "Possibly injured" was treated as "uninjured" because it was not a definitive

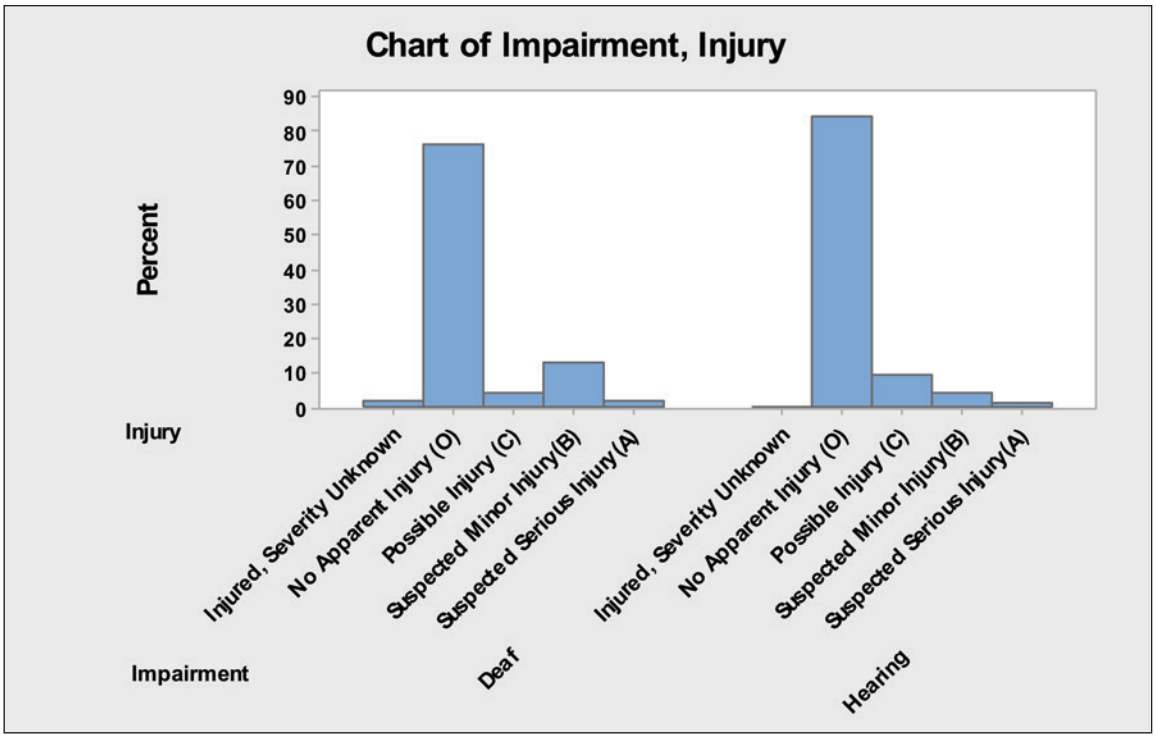

Figure 2
Injury percent by deaf or hearing.

injury (and, given the nature of the inquiry, it would be better to conservatively underestimate likelihood of injury than risk overstating it). All other categories were treated as "injured," since the GES records use the KABCO injury scale, which classifies suspected injuries as definite injuries of unknown severity — not very helpful for distinguishing severity of injury, but sufficient to determine that the driver was injured. The NHTSA GES does include police-reported injuries in its records on the person or persons involved with the accident (the "person" dataset). From the *Analytics User Manual 1988-2014*:[5]

> *Person – (1988-current): This data file contains information describing all persons involved in the crash including motorists (i.e., drivers and passengers of in-transport motor vehicles) and non-motorists (e.g., pedestrians and pedal cyclists). It provides information such as age, sex, and vehicle occupant restraint use and injury severity.*

It should be noted that NHTSA changed how it tracked just about every factor multiple times over the period examined. Each year's data was reformatted to a common 2013 scheme.

The GES records provided weights to represent a national sample for each year, and analysis was done on the weighted data. This project had data covering 2000 to 2013, but only the data from 2008 to 2013 was used in this initial study.

RIT/NTID Data Source

The preliminary campus data gives yearly information on the deaf and hearing student populations as well as counts of the on-campus motor vehicle accidents for both. This can be used to compare accident rates between deaf and hearing students.

Performing the Breslow-Day test for interaction between the year and the relation between deafness and accidents, the authors find that the p-value is greater than 0.05. Therefore, the authors fail to reject the hypothesis of no interaction. As a result, the accident data over the years 2011 to 2015 was simply pooled. A contingency table that compares accident frequency by deaf and hearing population can be found in **Figure 3**. The "accident" column represents people that were involved in an accident. The "no accident" column was calculated by subtracting the "accident" column from the total population. A contingency table that compares accident percent for the same populations is shown in **Figure 4**.

The Pearson Chi-Square test for association has a p-value less than 0.05, so the authors reject the null

Population Group	Accident	No Accident	Total
Deaf	34	2,577	2,611
Hearing	285	47,159	47,444
13 Total	*319*	*49,736*	*50,055*

Figure 3
Frequency of accident by population.

Population Group	Accident	No Accident
Deaf	1.3%	98.7%
Hearing	0.6%	99.4%

Figure 4
Percent of accidents by population.

hypothesis of no association and conclude that deafness is related to likelihood of being in an accident.

Figure 5 presents an odds ratio and relative risk for deaf drivers compared to their hearing peers. Looking at the 95% confidence interval for the odds ratio, the authors see that the odds of being in an accident on campus are at least 1.5265 and at most 3.1224 times greater for deaf drivers than for hearing drivers.

Statistic	Value	95% Confidence Low Limit	95% Confidence High Limit
Odds Ratio	2.1832	1.5265	3.1224
Relative Risk	2.1677	1.5224	3.0867

Figure 5
Odds ratio and relative risk — deaf vs. hearing drivers.

Application to Forensic Engineering

Almost any person who has contact with the deaf or hard-of-hearing community has a story related to a deaf driver — usually one that involves an accident or near-accident. In the primary authors' experience, most stories involve a driver using sign language to communicate with passengers while operating a motor vehicle. Many of these stories provide anecdotal evidence that would suggest that deaf drivers are more likely to be involved in motor vehicle accidents. Obviously, anecdotal stories and evidence are of limited value in a forensic engineering analysis. It is because of this lack of hard evidence that this initial quantitative analysis of accident data involving deaf and hard-of-hearing drivers was undertaken. Prior to this study, no study (to the authors' knowledge) had been done to quantitatively assess whether deaf and hard-of-hearing drivers are indeed at a greater risk for accidents than their hearing driver peers.

Forensic engineers should determine whether a deaf or hard-of-hearing person was an operator of one of the involved vehicles in any motor vehicle accident. If a motor vehicle accident is determined to involve a deaf or hard-of-hearing driver, a forensic engineer might want to investigate whether there were passengers in the vehicle along with the deaf driver. The reason for this is the fact that signing requires the use of at least one hand and a portion of the visual attention of the driver. Although not proven at this point, a person may draw a parallel between signing while driving and texting while driving. It is hoped that future data mining and research will determine whether this similarity is in fact true.

One of the major issues involved in a study of this type is the fact that the deaf and hard-of-hearing community is very protective of their driving rights. As mentioned earlier, it was not too long ago that there were states that prohibited deaf drivers from obtaining a driver's license. The suggestion that the deaf community as a whole is subpar in the operation of motor vehicles goes counter to the notion that a deaf and hard-of-hearing person is just as capable a driver as any hearing person. In fact, during multiple casual discussions with deaf individuals regarding driving, there were many instances in which deaf individuals claimed that they were better drivers than their hearing counterparts because of their alleged superiority in visual awareness[6]. While this may be true, it can be argued that part of that superior visual awareness is being used up while one is communicating using sign language.

Future Work

Any ethical engineer has a duty to warn if a significant hazard is discovered in the line of his or her engineering work. It is partially with this in mind that this paper was developed for the forensic engineering community. Furthermore, if an engineer possesses adequate resources, the engineer could begin exploring a solution to the hazard or strive to better understand the hazard. For the hazard exposed in this paper, an engineer might explore technologies that could mitigate the hazard. For example, potentially useful accident-avoidance

technologies may be currently available in many new automobiles that could prove useful in reducing the risk to deaf drivers[7].

In addition, it is hoped that by further analyzing the data, a better understanding can be created regarding why it is that deaf drivers are more likely to be in a motor vehicle accident and more likely to be killed or injured in that accident. The issue comparing signing while driving to texting while driving is one example of an area where more research needs to be done. Further research also needs to be completed on a more representative dataset that expands beyond the reaches of the RIT/NTID campus. Only in this way could a direct link between deafness and a higher likelihood for involvement in a motor vehicle accident be proven or disproven for society at large.

Finally, the issues exposed in this paper are not yet well understood. Is it the fact of being deaf or hard-of-hearing that creates an increased risk, or is it the use of a visual sign language that causes an increased risk? Or, perhaps the danger is created through a multitude of unknown mechanisms. Perhaps studies could be performed using driving simulators or closed driving courses to evaluate numerous hypotheses.

Conclusion

Statistical analysis of certain data shows that deaf and hard-of-hearing drivers on the campus of RIT/NTID are 1.5 to 3.1 times more likely to be involved in a campus motor vehicle accident. Statistical analysis of certain national data shows that a hearing driver is approximately 1.5 to 10 times more likely to remain uninjured in an accident as compared to a deaf or hard-of-hearing driver. It is recognized that the data sets did not completely address D/HH drivers in a robust manner, and further data mining may lead to differing results. There may be some similarity between signing while driving and texting while driving. Forensic engineers should attempt to determine whether the involved drivers in a motor vehicle accident were deaf or hard-of-hearing.

References

1. Hersh M, Ohene-Djan J, Naqvi S. Investigating road safety issues and deaf people in the United Kingdom: An empirical study and recommendations for good practice. Journal of Prevention & Intervention in the Community 2010; 38(4):290-305.

2. Dobbs B. Medical Conditions and Driving: A Review of the Scientific Literature (1960 - 2000), United States Department of Transportation National Highway Traffic Safety Administration, Washington DC 2005. p 154.

3. The Right to Drive. Gallaudet University <https://my.gallaudet.edu/bbcswebdav/institution/Deaf%20Eyes%20Exhibit/community-09driveright.htm>. Accessed 2015 December 23, 2015.

4. NYS DMV License Restrictions. New York State Department of Motor Vehicles <http://dmv.ny.gov/driver-license/license-restrictions-medical-conditions>. Accessed 2015 December 23, 2015.

5. National Automotive Sampling System. National Center for Statistics and Analysis. National Highway Traffic Safety Administration. Washington DC: United States Department of Transportation; 2014.

6. Based on casual interviews with deaf drivers conducted by the primary author at RIT/NTID in 2015.

7. Cicchino JB, McCartt AT. Experiences of model year 2011 Dodge and Jeep owners with collision avoidance and related technologies. Traffic Injury Prevention 2015;16(3):298-303.

Forensic Engineering Analysis of a Sequence of Power Infrastructure Failures Atop an Office Building

By Mauricio Cueva-Eguiguren, PE (NAFE 776S)

Abstract

A series of equipment failures occurred in a high-rise office building in Puerto Rico. The top 18th floor was occupied by the infrastructure systems of the building to include heating, air conditioning, electrical and plumbing systems, and two 1,500kVA emergency generators that provided power for the entire building when the utility power was not available. The first failure occurred within a 3,000kVA, 13.8kV/480-277VAC stepdown power transformer on a Sunday night — a day after the annual maintenance of the electrical equipment took place. The failure of this transformer resulted in the operation of the two emergency generators — last maintained a month earlier. The second failure occurred in one of the two control panels associated with the fuel day tanks for the emergency generators due to power disturbances (harmonics) in the electrical distribution system in the building. This resulted in an overflow of fuel oil in one of the day tanks (615 gallons) and the spill of approximately 1,000 gallons of fuel oil on the 18th floor and lower floors (including the cellar).

Keywords

Forensic engineering, transformer, generator, harmonics, controls, distribution

Definitions

Real power in an electric circuit is the rate of flow of energy past a given point of the circuit. In a simple alternating current (AC) circuit (consisting of a source and a linear load), both the current and voltage are sinusoidal. If the load is purely resistive, the two quantities reverse their polarity at the same time. The units of real power are measured in watts.

Reactive power in a simple AC circuit is when energy storage elements, such as inductors and capacitors, may result in periodic reversals of the direction of energy flow. The portion of power due to stored energy, which returns to the source in each cycle, is known as reactive power. The units of reactive power are measured in VARs.

Power factor of an AC electrical power system is defined as the ratio of the real power flowing to the load to the reactive power in the circuit. Power factor is measured as a percentage.

Fundamental frequency, often referred to simply as the fundamental, is defined as the lowest frequency of a periodic waverform. In a simple AC circuit, such as the electrical power system in the United States, this is 60 Hertz (cycles per second).

Power quality determines the fitness of electric power for use with consumer devices. Synchronization of the voltage frequency and phase allows electrical systems to function in their intended manner without significant loss of performance or life. The term is used to describe electric power that drives an electrical load and the load's ability to function properly. Without the proper power, an electrical device (or load) may malfunction, fail prematurely, or not operate at all.

Harmonic voltages and currents in an electric power system are a result of non-linear electric loads. Harmonic frequencies in the power grid are a frequent cause of power quality problems. Harmonics in power systems can result in increased heating in the equipment and conductors, misfiring in variable-speed drives, and torque pulsations in motors. Reduction of harmonics is considered desirable. Harmonics are AC voltages and currents with frequencies that are integer multiples of the fundamental frequency. On a 60-Hz system, this could include 2nd order harmonics (120 Hz), 3rd order

Mauricio Cueva-Eguiguren, PE, 21 North Main Street, Ste 210, Port Chester, NY 10573; (914) 690-2745; mce@acticonengineering.com

harmonics (180 Hz), 4th order harmonics (240 Hz), and so on. Normally, only odd-order harmonics (3rd, 5th, 7th, 9th) occur on a 3-phase power system.

Current harmonics: In a normal alternating current power system, the current varies sinusoidally at a specific frequency, usually 60 Hz in the United States. When a linear electrical load is connected to the system, it draws a sinusoidal current at the same frequency as the voltage (though usually not in phase with the voltage). Current harmonics are caused by non-linear loads. When a non-linear load, such as a capacitor or an inductor (motor), is connected to the system, it draws a current that is not necessarily sinusoidal.

Voltage harmonics are mostly caused by current harmonics. The voltage provided by the voltage source will be distorted by current harmonics due to source impedance. If the source impedance of the voltage source is small, current harmonics will cause only small voltage harmonics.

Introduction

A high-rise office building located in the business district of San Juan, Puerto Rico was in operation for several years at the time of the event. The first 17 floors were occupied by private institutions, and the 18th floor was dedicated for the infrastructure systems of the building to include heating, air conditioning, electrical, and plumbing systems. In addition, two 1,500kVA emergency generators (A and B emergency generators) were located on the 18th floor, providing electrical power for the entire building when utility power was not available.

The annual electrical maintenance of the electrical equipment was part of the building's preventive maintenance program[1,2,3], and it occurred Saturday, February 9, 2008. The electrical maintenance required a complete shutdown of the electrical power system, including shutting down the operation of the two emergency generators. The electrical maintenance that took place included infrared surveys of the electrical distribution system, which took approximately 8 hours. Around 4 p.m., the electrical maintenance was completed — at which time the utility power was restored to the building.

A security guard reported that the two 1,500kVA emergency generators began to operate on Sunday, February 10, 2008 around 10 a.m. At the time, the security guard (under the direction of the building engineer) contacted the local utility to inquire if a power outage in the business district had occurred. When the security guard learned that a power outage had not occurred, he advised the building engineer, who returned to the building to ensure all electrical systems in the building were operating properly.

When the building engineer arrived at the building, he noticed that the emergency generators were still operating; however, he was not alarmed because the generators were capable of providing the necessary electrical power for the building. However, upon further investigation with the utility personnel, they discovered that the 3,000kVA, 13.2kV-480/277 VAC stepdown transformer in the building had failed. This was why the emergency generators had operated since Sunday around 10 a.m.

On February 11, 2008 the building engineer made the necessary arrangements for the evaluation of the 13.2kV-480/277 VAC stepdown transformer failure and to obtain a replacement unit. In addition, he called the maintenance company for the emergency generators to verify that the units would be able to operate continuously for the next few days, which was confirmed by the maintenance company.

A security guard noticed an overflow in the fuel day tanks on the 18th floor on February 12, 2008 at approximately 1 a.m., and he immediately called the building engineer. When the building engineer and his assistant arrived at the building, they discovered a malfunction of the "A" fuel day tank control panel, since all the lights in the control panel were illuminated. The malfunction was determined by the fact that the low- and high-level alarm lights were illuminated, which could not occur under normal conditions. They immediately isolated the fuel line from the "A" fuel day tank using the manual valves and began to recover the spilled fuel from the surroundings.

As a result of the malfunction of the "A" fuel day tank control panel, the building engineer contacted the maintenance company for the emergency generator and requested that it investigate the failure and repair this unit. When personnel from the maintenance company arrived, they confirmed the malfunction of the "A" fuel day tank control panel and proceeded to replace the failed unit as well as the "B" fuel day tank control panel as requested by the building engineer.

The failure of the "A" day tank control panel resulted in the spill of approximately 1,000 gallons on the 18th floor and lower floors, including the cellar. Based on this, the building was vacated for approximately four months until the decontamination and repairs took place.

As a result of the equipment failures and fuel oil spill, the building owner filed a claim with his insurance carrier for damages. The claim was denied because the damages were considered unrelated events. Furthermore, the fuel spill claim was denied because it involved hazardous materials (fuel oil) that were not covered by the policy. Based on this, the insurance carrier advised the building owner to file a single claim for the transformer failure.

In light of the above, the building owner engaged a forensic engineer to investigate the equipment failures and fuel oil spill as well as to determine if these events were related.

Methodology

In order to investigate the sequence of electrical equipment failures that led to approximately 1,000 gallons of fuel oil spill in the building, each equipment failure was investigated separately — starting with the transformer failure.

a. Transformer Failure

The transformer in the building was used to reduce the utility power from 13.2kV to 480/277VAC for use in the building. This transformer is a three-phase 3,000kVA, 13.2kV-480/277 VAC stepdown transformer manufactured in May 2003 (see **Figure 1**). This transformer has five taps on the primary side (13.2kV). Cooling for the electrical room was through a dedicated ventilation system, which brought outside air into the room exhausting to the outside. The electrical room did not have humidity control.

A site inspection was conducted on May 22, 2008 in order to investigate the transformer failure. The site inspection revealed several short circuits in the transformer windings, as shown on **Figures 2** through **6**. In addition, the manufacturer's drawings, operation and maintenance manuals were reviewed in order to determine if the installation of the transformer complied with the manufacturer's recommendations[4].

- The maintenance of the electrical equipment in the building took place on February 9, 2008 starting at 10 a.m. At that time, the transformer was de-energized, thus allowing it to cool down for approximately 6 hours.

- Although these transformers typically were supplied with cabinet space electric heaters, the one supplied for this building was not. Cabinet space electric heaters are required when transformers are installed in environments subject to high humidity levels.

- The transformer instruction manual provided the following guidelines:

  a. Transformers that operate in high humidity environments must be dried for an appreciable time period.

  b. Under severe environment conditions and extended shutdown periods, transformers should be inspected for visible signs of moisture before re-energizing. Where humidity is encountered, the transformers must be dried as specified in their instruction manual[4].

  c. Moisture is detrimental to most insulation systems. As such, transformers that have been exposed for long periods of high humidity when moisture is visible on insulation surfaces must be dried before being energized.

  d. The process of drying is accomplished by the application of hot air, radiant heat, or internal heat in order for the hot air to rise through the windings.

  e. Insulation resistance tests, which are used on liquid-filled transformers, are of little value on dry-type transformers, such as the one in this case. The nature of insulation used in dry-type transformers is such that the megger and power factor readings are not reliable and may be misleading.

- The transformer was placed back in service at approximately 4 p.m. upon completion of the maintenance on February 9, 2008.

- A moisture inspection of the transformer was not performed prior to placing it back in service.

- The National Climate Data Center (NCDC) reported that 0.04 inches of water precipitation occurred in San Juan, Puerto Rico on February 9, 2008 with an average temperature for the day of 77 degrees Fahrenheit, signifying the presence of elevated humidity.

- Evidence of multiple short circuits was visible in the center and right sides of the primary windings of the transformer.

- A previous transformer failure occurred on a similar transformer in 2002 following an extended shutdown similar to the 2008 shutdown. An investigation following the 2002 transformer failure revealed high levels of moisture in the transformer windings.

b. Fuel Oil Control Panel Failure

The "A" and "B" emergency generators were located on the mezzanine of the 18th floor with the corresponding fuel day tanks. Since the "A" and "B" fuel day tanks do not hold sufficient fuel for the emergency generators to operate for extended periods of time, these fuel day tanks are supplied with fuel from two 5,000-gallon fuel tanks located in the cellar. The fuel from these two tanks is supplied through two 15.6 gpm fuel pumps; only one pump is required for the "A" and "B" fuel day tanks to be refilled, with the second pump as backup (see **Figures 7** through **10**).

The "A" and "B" control panels were mounted on top of the day tanks, and they control the operation of the 15.6 gpm fuel pumps through the local control panel located in the cellar. When a low level signal from the fuel day tanks is received, the day tank control panels send the signal to the 15.6 gpm fuel pump local control panel. The local fuel pump control panel provides a permissive signal to the 15.6 gpm fuel pump to start supplying fuel to the fuel day tanks. Once the fuel day tank levels are satisfied, then the low level signal from the "A" and "B" fuel day tank control panels is removed, and the fuel pump stops pumping fuel to the day tanks.

The "A" and "B" fuel day tanks include low- and high-level switches, which provided a signal to their respective control panels. In addition, the day tanks included a rupture basin signal that also went to the "A" and "B" fuel day tank control panels. These control

Figure 1
Transformer 13.2kV – 480/277V.

Figure 2
Transformer short circuit #1.

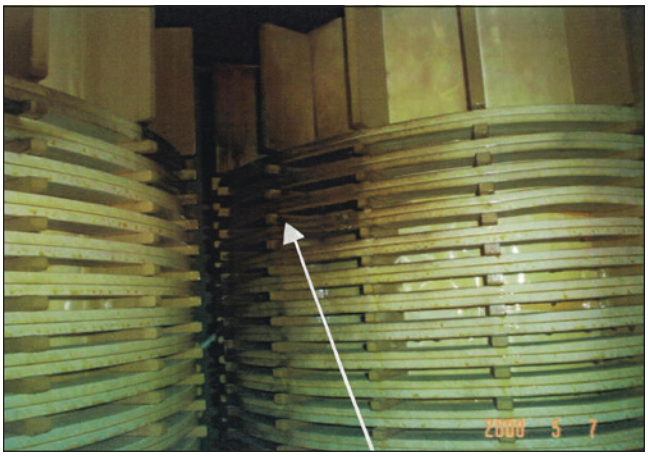

Figure 3
Transformer short circuit #2.

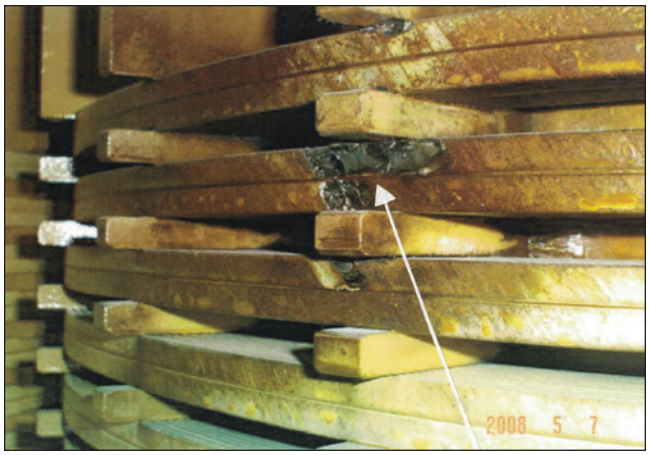

Figure 4
Transformer short circuit #1 close-up.

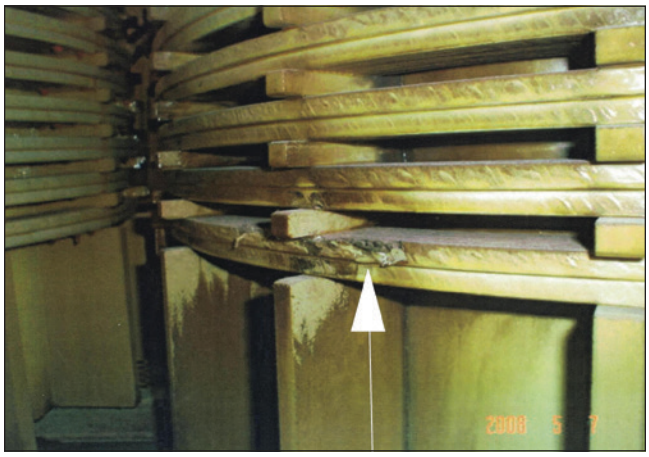

Figure 5
Transformer short circuit #2 close-up.

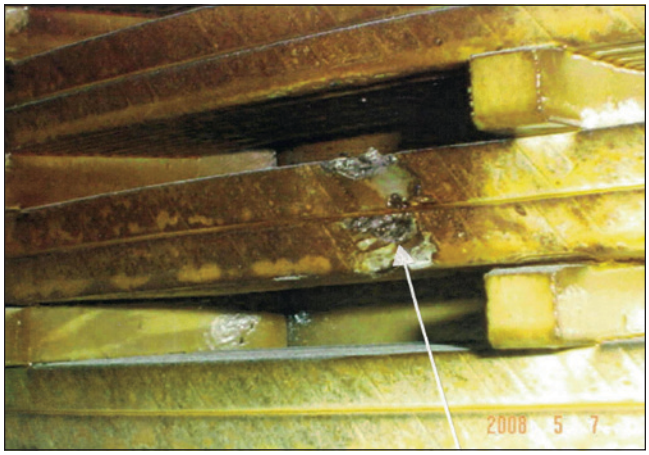

Figure 6
Transformer short circuit #3 close-up.

panels used the signals to process the information within these panels (see **Figures 11** and **12**). A signal was sent from these control panels to the emergency generator control panels located in the emergency generator room and to a remote alarm panel located in the lobby of the building.

The "A" and "B" fuel day tanks had a containment basin, which held approximately 615 gallons. The containment basin was designed to hold the fuel from these day tanks in the event that there was a rupture in either tank. In addition, this containment basin had a level switch, which provided a local audible alarm on the 18th floor in the event of either fuel day tank rupture.

In order to determine the cause and origin for the fuel day tank control panel "A" failure, a test protocol was developed to test both control panels. The tests were performed at a local laboratory in San Juan, Puerto Rico. The tests included internal and external visual inspections of the panels to determine if there were any visual indications of defects or failures in control panel A.

Following the visual inspections of both control panels, functional tests were performed on both units to verify their operation. The control panel operation tests involved simulating various levels of fuel in the tank, starting with empty to full level and then full to empty. The fuel tank levels were gradually changed to verify the following panel indications: empty, 10%, 25%, 50%, 75%, 85%, 90%, 95%, and full conditions. One functional test was performed in control panel "B" and two functional tests on control panel "A" in order to verify repeatability.

Figure 7
Fuel day tank "A" with control panel.

Figure 8
Fuel day tank "A" with control panel.

Figure 11
Fuel day tank "A" control panel (front view).

Figure 9
Fuel day tank "A" and catch basin.

Figure 12
Day tank "A" control panel (rear view).

Figure 10
Fuel day tank "A" catch basin.

The results of the visual and functional tests for both control panels showed that they operated properly. It was concluded that the control panel "A" malfunction was a time-specific malfunction that took place on or about February 12, 2008 and not a long-term effect.

c. Power Disturbances and Harmonics

In addition to testing the fuel day tank control panels, power quality monitoring tests were performed on the electrical distribution system in the building with the aid of a local electrical contractor. The power quality monitoring included the incoming 13.2kV electrical power service from the utility, the 480 VAC emergency generator power, and the 120/208 VAC electrical power panel RP2-17, which provided power to the fuel day tank control panels.

The results of the visual and functional tests for the electrical power service from the utility, emergency generator, and power panel RP2-17 revealed a high level of harmonics that exceeded the industry standard levels. The harmonic levels recorded for power panel RP2-17 greatly exceeded the recommended industry standard levels. The results were as follows:

120 VAC POWER PANEL RP2-17			
	Phase A	***Phase B***	***Phase C***
Voltage Harmonics (total)	5.25%	5.3%	5.4%
Current Harmonics (total)	65%	39.5%	8.5%

EMERGENCY GENERATOR			
	Phase A	***Phase B***	***Phase C***
Voltage (THD)	6.22%	6.44%	6.01%
Current (THD)	11.20%	11.77%	11.39%

ELECTRICAL PANEL RP2-17			
	Phase A	***Phase B***	***Phase C***
Voltage (THD)	5.25%	5.30%	5.40%
Current (THD)	65.00%	39.50%	8.50%

Table 1
Voltage and current total harmonic distortion (THD) content (percentage).

In accordance with Institute of Electronics & Electrical Engineers (IEEE) Standard 141, 1993 revision, *Recommended Practice for Power Distribution for Industrial Plants*[5], the recommended maximum harmonic content for operating electronic equipment in industrial facilities is less than 5% for total harmonics with a maximum individual harmonics content of 3%. As shown in **Table 1**, the total harmonic current content for power panel RP2-17 is more than 21 times higher than the recommended value in this standard.

In addition, IEEE Standard 141, Paragraph No. 9.2 – Importance of Understanding Effects of Harmonics, states the following[3]:

"In addition to these new non-sinusoidal loads, more power factor improvement capacitors are being applied in industrial systems and in electric utility transmission and distribution systems for both voltage control and release of system capacity. With the addition of each new capacitor bank, the system's resonant frequency is lowered (see 9.6). With the resonant frequency lowered, the systems become more susceptible to natural resonance with non-sinusoidal loads. With the lowering of the system resonance, power systems are now becoming more and more impacted by the flow of the characteristic harmonic currents produced by these loads.

Harmonic currents flowing in power circuits can induce harmonic voltages and/or currents in adjacent signal circuits. The present-day use of microprocessors for control of processes and power systems results in equipment using low-level signals that are subject to noise or interference from outside sources."

The effect of harmonics in the current and voltage waveforms shown in **Figure 13** were very similar to the results obtained from the power quality monitoring tests in the electrical distribution system in the building, which are shown in **Figures 14** and **15**.

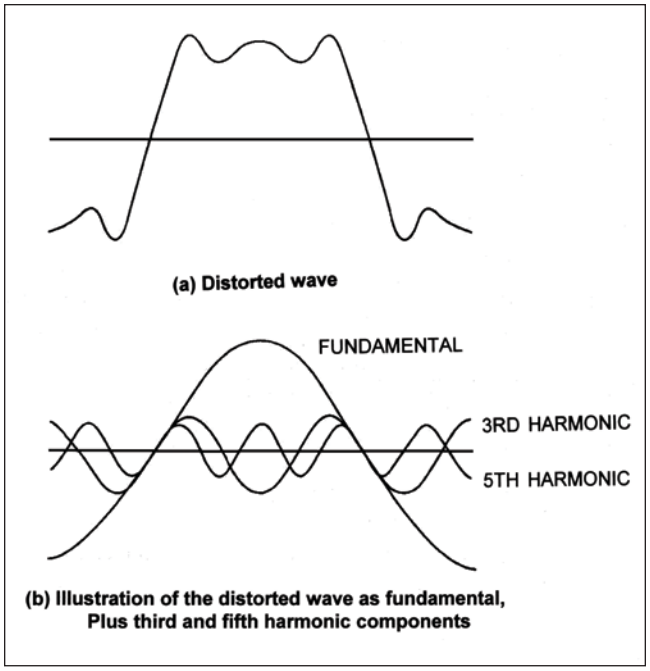

Figure 13
Voltage or current waveforms with harmonic distortions. Upper waveform illustrates with total voltage or current waveform. Lower waveform illustrates the fundamental (60 Hz waveform) and the 2nd & 3rd harmonic waveforms.

Furthermore, IEEE Standard 141, Paragraph No. 9.8.2.5 - Electronic Equipment[3] states the following:

"Power electronic equipment is susceptible to misoperation caused by harmonic distortion. This equipment often is dependent on accurate determination of voltage zero crossings or other aspects of the voltage waveshape. Harmonic distortion can result in a shifting of the voltage zero crossing or the point at which one phase-to-phase voltage becomes greater than another phase-to-phase voltage. These are both critical points for many types of electronic circuit controls, and misoperation can result from these shifts.

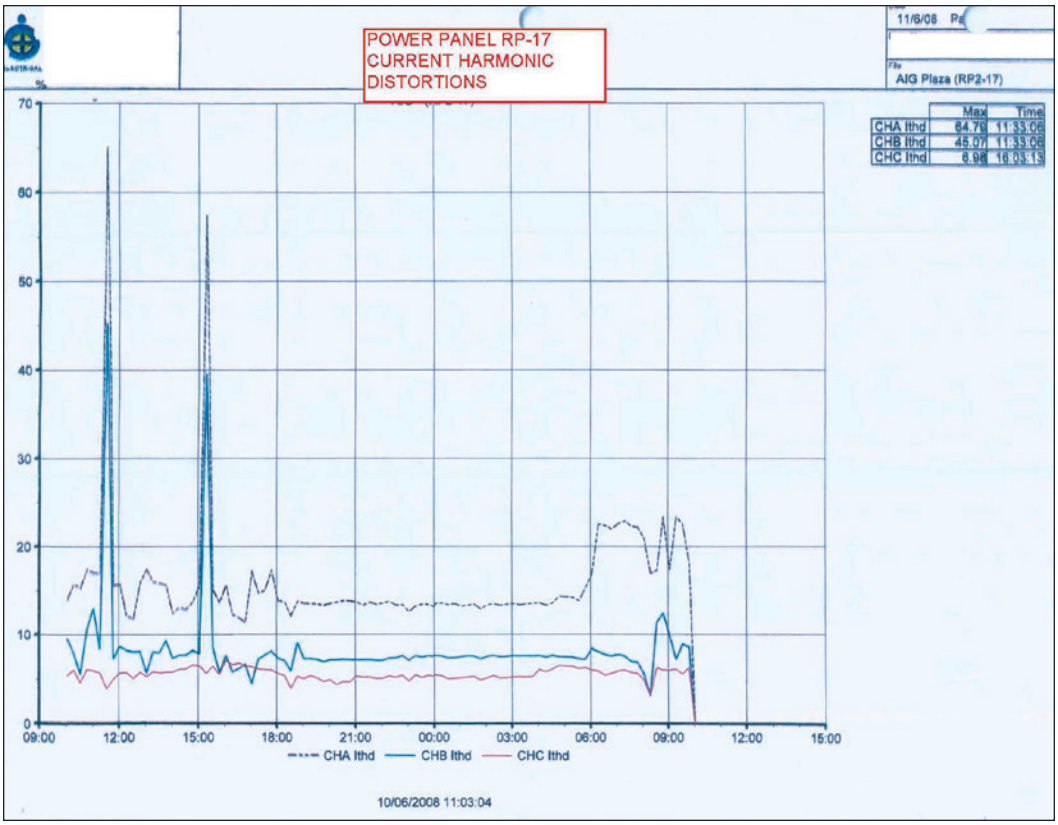

Figure 14
Power panel RP2-17 – current harmonic distortions.

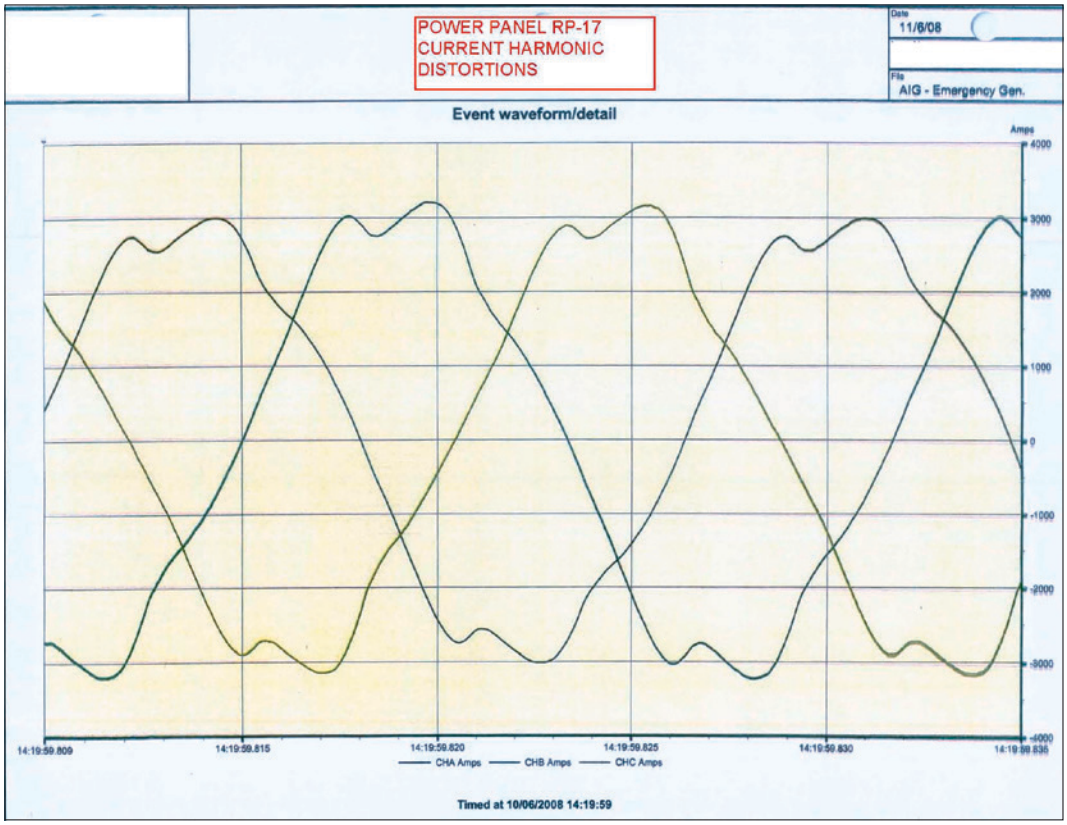

Figure 15
Power panel RP2-17 – sine wave current and voltage harmonic distortions.

Other types of electronic equipment can be affected by transmission of AC supply harmonics through the equipment power supply or by magnetic coupling of harmonics into equipment components. Computers and allied equipment, such as programmable controllers, frequently require AC sources that have not more than 5% harmonic voltage distortion factor, with the largest single harmonic being no more than 3% of the fundamental voltage. Higher levels of harmonics result in erratic, sometimes subtle, malfunctions of the equipment, which can, in some cases, have serious consequences. Instruments can be affected similarly, giving erroneous data or otherwise performing unpredictably. Perhaps the most serious of these are malfunctions of medical instruments."

In addition, industry standard IEEE 241, 1990 revision, Paragraph No. 3.12.3 - Harmonic Producing Equipment[2], states the following:

"Capacitors do not generate harmonics. However, the reduced reactance of the capacitor to the higher frequencies may cause excessive harmonic current in the circuit containing the capacitors. In cases of resonance, this current may be very large and may overheat the capacitors. In addition, the high currents may induce interference with communication, signal, and control circuits."

Based on the above, it is evident when the 3,000kVA, 13.2kV-480/277 VAC stepdown transformer failed, the two emergency generators operated in order to provide electrical power to the building. When the emergency generators operated, the fuel day tank control panels "A" and "B" operated with distorted voltage and current waverforms supplied by Panel RP2-17. The distorted voltage and current waveforms were most likely due to the current and voltages harmonics created by the capacitor banks, which were installed in 2002 (see **Figures 14** and **15**). The distorted voltage and current waveforms have adverse effects in communications and electronic equipment, such as the fuel day tank control panels "A" and "B" as stated in industry standards IEEE 141[3] IEEE 241[2] and IEEE 519[5]. The adverse effects include misoperations of electronic equipment, as was the case with the fuel day tank control panel "A" on February 11, 2008.

The building personnel responded to the fuel overflow event when notified by the security guard, and proceeded to control and collect the fuel overflow in the building. The building engineer stated that the fuel day tank control panel "A" had clearly malfunctioned as manifested by the fact that the low- and high-level alarm lights were both illuminated at the same time. Illumination of the low- and high-level alarm lights could not have happened unless the control panel "A" malfunctioned. The building engineer further stated that the fuel overflow was due to the malfunction and consequent failure of control panel "A" to properly control the fuel flow from the main tanks in the cellar to the day tank "A" located on the 18th floor.

Conclusion

The forensic engineer concluded that the fuel oil spill atop of the high-rise office building was a single event, resulting from a sequence of failures starting with the transformer failure that provided the electrical power to the building. The transformer failure was the result of energizing it without following the manufacturer's recommendations to inspect and remove the humidity in the windings after being de-energized for a period of time in a high humidity environment. As a result of the transformer failure, the emergency generators in the building operated for approximately 37 hours when one of the day tank fuel control panels malfunctioned due to a high level of harmonic content on the electrical distribution system in the building[5,6,7]. The day tank fuel control panel malfunction resulted in the fuel oil spill as described.

References

1. IEEE 493-1990. Recommended practice of reliable industrial and commercial power systems. Piscataway, NJ; Institute of Electrical and Electronics Engineers.

2. IEEE 241-1990. Recommended practice for electric power systems in commercial buildings. Piscataway, NJ; Institute of Electrical and Electronics Engineers.

3. IEEE 141-1993. Recommended practice for electric power distribution for industrial plants. Piscataway, NJ; Institute of Electrical and Electronics Engineers.

4. IEEE C57.12.91-1995. Test code for dry-type distribution and power transformers. Piscataway, NJ; Institute of Electrical and Electronics Engineers.

5. IEEE 519-1992. Recommended practices and requirements for harmonic control in electrical power systems. Piscataway, NJ; Institute of Electrical and Electronics Engineers.

6. ANSI C34.2-1968. Recommended practices and requirements for semiconductor power rectifiers. Washington, D.C.; American National Standards Institute.

7. IEEE 399-1990. Recommended practice for industrial and commercial power system analysis. Piscataway, NJ; Institute of Electrical and Electronics Engineers.

Forensic Engineering Investigation of PVC Piping Failure in a Multistory Condominium Building

By John Certuse, PE (NAFE 708F)

Abstract

Polyvinyl chloride (PVC) piping systems in larger commercial buildings are subjected to greater stresses due to normal building movement when segment length, diameter, and schedule are increased in comparison to smaller residential installations. The likelihood for increased stresses in these system installations must be recognized and accommodated for in the initial piping system design. Performance aspects, such as thermal expansion and building settling, must be considered as well as piping configurations and hanger support placement. This paper addresses the investigation methodology used to identify the causes of chronic building construction defects that resulted in water and mold damage to a recently renovated multistory condominium building.

Keywords

Plumbing, piping thermal expansion, PVC, hanger, framing, shrinkage

Background

The property discussed is a four-story wood frame condominium building containing 30 luxury residences of approximately 1,600 to 2,200 square feet. Construction of the building (**Figure 1**) began in 2005 and was completed in the summer of 2008. The property was occupied continuously since that time. The building site was a former marble/granite quarry site with minimal soils in need of removal with the initial construction on a solid granite base. The building was also built on property with a downward slope at the back of the building, resulting in a partial below-grade driveway and parking garage with the building's foundation on top of and fastened to bedrock.

Figure 1
Property as seen.

Above the partially below grade-level parking garage were four floors of wood frame construction as well as a wood-framed roof truss system. Since the building was in northern New England, it was outfitted with a metal roof, which is popular in areas of heavy snow accumulations. The 18,000-square-foot building was configured with two main buildings abutting each other, with a footprint of approximately 9,000 square feet each.

Leaks, Mold, and Suspected Causes

In the fall/winter of 2013-2014, seven years after construction was completed, four pairs of horizontally adjacent and vertically aligned (see **Figure 2**) condominium units were found to be damaged by long-term exposure to moisture and subsequent mold growth.

As seen in **Figure 3**, water leakage was initially thought to be caused by a leaking roof boot seal around vent piping, due to the manner in which the boot was damaged. The boot was damaged in a manner consistent with heavy snow load deflecting the roof sheathing and distorting the rubber seal and aluminum flange. It was later determined that this was not possible, however, due to the steel roof construction and strength of the roof truss system. Another explanation was sought.

John Certuse, PE, 15 Extension St., Attleboro, MA 02703; (508) 226-8800; john@iseengineering.com

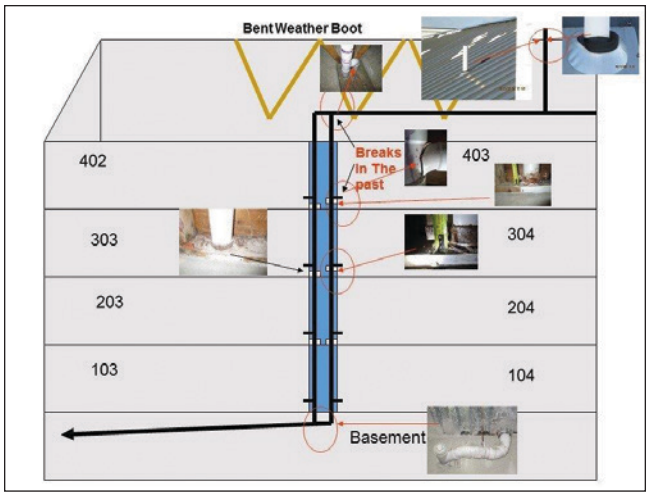

Figure 2
Diagram of building piping system.

Figure 3
Damaged roof vent boot.

Figure 4
Vent piping entering attic space.

Below the attic, as seen in **Figure 4**, the two piping waste stacks serving both buildings passed vertically through a common wall between both building units and intersected in the attic space.

Origin of Water Leakage Identified

After the initially suspected origin of leakage from the roof boot seal of the vent piping was discounted, further investigation identified that water was found in a common piping chase way behind the abutting condominium units' kitchen cabinets. At the time of the author's involvement in this investigation, four of the condominium units were sealed off and undergoing restoration for water and mold damage (**Figure 5**).

Piping Fastening System Description

The waste stack vent piping system functioned as a discharge system for sewage, gray and wastewater; it also vented through the attic and roof. The system piping was configured within the building to extend vertically from the basement/garage level sewage connection to the roof vent through a commonly shared chase way as seen in **Figure 5**. The system was supported at each floor penetration with standard riser clamps within the common piping chase way space (**Figure 6**). No provision for expansion or contraction was incorporated into the design or construction of the system — by either the engineer who designed the system or the mechanical contractors who built it.

Figure 5
Kitchen walls removed, exposing piping.

Kitchen wastewater was connected to the 4-inch main drain waste line by way of horizontal 2-inch PVC piping sections that passed through (and were restrained within) holes in framing members, significantly limiting vertical movement. (**Figure 7**).

Examination of Existing Piping and Repair History

During the investigation, it was revealed that in previous years broken piping fittings were found in the 2-inch piping connection between the stack riser and each unit's kitchen sink drain. The plumbing contractor, who was reportedly the same contractor who installed the system,

repaired the damaged fittings and pipe. Further inquiry by forensic engineering investigators found that these reported pipe damages were in three additional condominium units, and a recent pipe break in another unit was found during mold remediation by contractors.

Figure 6
Vent stack pipe resting on riser clamp.

Figure 7
Horizontal piping restrained within framing.

Figure 8
Provided photo of cracked "tee" fitting at riser.

Although photograph documentation was not provided from the earlier pipe breaks from past years, the most recent event's damaged fitting was photographed by the condominium management staff and provided to investigators (**Figure 8**).

As a result of the past repairs to the three units' fractured piping, the manner in which that piping had originally been installed could not be documented.

Although past piping repairs had already been performed, examination of the piping chase way and vent stack piping revealed that the piping was not resting on the riser clamps designed to secure a pipe against vertical downward movement and that the riser clamps were actually suspended off of the sill plates (**Figure 9**).

Figure 9
Riser clamp suspended above sill plate due to framing settling and pipe expansion on third floor of building.

The installation method of this piping being constrained (see **Figure 10)** without accommodation for expansion, contraction, or building movement — combined with reports of where past plumbing repairs were located (and how they failed) — led to the author's opinion that a plumbing system design defect was the cause of the piping failures and building damage.

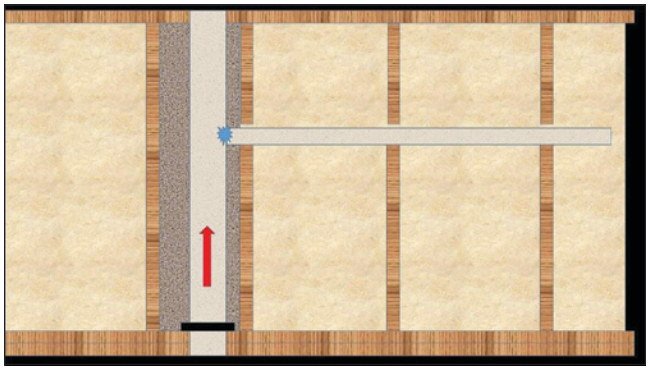

Figure 10
Diagram of piping connection to vent riser.

Conditions Leading to Pipe Failure

Thermal Expansion of PVC and Other Piping Materials

In comparison to other materials used in the manufacturing of piping, PVC (polyvinyl chloride), as well as other plastic piping materials, has a large thermal expansion coefficient, as referenced in the *Mechanical Engineers Reference Manual.*

MATERIAL	EXPANSION COEFFICIENT (10^{-6} in/in °F)
Aluminum	10
Carbon steel	6.5
Cast iron	5.9
Copper	9.3
Stainless steel	9.9
ABS acrylonitrile butadiene styrene	35.0
HDPE high density polyethylene	67.0
PE polyethylene	83.0
CPVC chlorinated polyvinyl chloride	44.0
PVC polyvinyl chloride	28.0

When the piping was initially installed, an estimated ambient temperature of 70 degrees Fahrenheit was assumed. It is possible that due to cooking, dishwasher heating, and hot water consumption activities, discharge temperatures into the waste piping could reach as high as 120 degrees Fahrenheit in accordance with the *International Plumbing Code.* Additionally, the piping in the attic during summer months would also be subjected to higher heat loads. Based upon this, the estimated thermal expansion of the piping is calculated as follows (ref *Mechanical Engineering Reference Manual*):

Dl = Lo α (T1-To)

Dl – Change in length
Lo – Original length
α – Coefficient of linear expansion PVC (.000028 *in/in°F*)
T1 – Final temperature degrees Fahrenheit (heat load applied)
To – Initial temperature degrees Fahrenheit (at installation)

The piping system has an estimated 70 cumulative feet from the main sewage line connection to the midpoint height within the attic space. With a ΔT of 50 degrees Fahrenheit, the expansion of the piping due to elevated temperature is calculated to be 1.18 inches.

Construction Framing Shrinkage

New lumber has higher moisture content than lumber that has been part of the building system over a period of time. As such, dimension reductions due to loss of moisture shrinkage should be expected. According to the American Society of Plumbing Engineers (ASPE) *Plumbing Engineering Design Handbook,* Volume 2:

Protection from Damage/Wood Shrinkage: *Provide slip joints and clearance for pipe when wood shrinks. Approximately ⅝ inch (16 millimeter) per floor is adequate for typical frame constructions, based on 0.4 percent shrinkage perpendicular to wood grain. Shrinkage along the grain usually does not exceed 0.2 percent.*

Based upon the ASPE guidelines regarding the amount of shrinkage of wood framing members, ⅝ of an inch per floor would equate to 2.5 inches of "settling" or shrinkage from the initial vertical height of the building.

Considering the movement of the piping off of the sill plate due to wood framing shrinking (2.5 inches) in addition to the vertical movement of the piping due to thermal expansion (1.18 inches), the total sum of these distances of 3.68 inches supports a conclusion that the vertical piping stack was not supported by the building framing and was not acting in unison with the building structure as one coordinated "system."

Piping Failure Analysis

Due to thermal expansion of the piping, as well as shrinkage of the four stories of the wood framing of this structure, the vertical riser vent stack was not being supported by the riser clamps fastened to the piping at the sill plate locations at each floor penetration. Wood framing shrinkage also added to the distance between the riser clamps and sill plates.

These conditions, in addition to the constraints on the horizontal kitchen waste lines, caused the weight of the estimated 200+ feet of vertical stack piping (and any internal liquid) to be imparted to these 2-inch horizontal pipes. As seen in **Figure 8**, this condition resulted in cracking of the "T" fittings connecting these 2-inch

waste lines to the vertical 4-inch riser within the chase way due to excessive weight and stress overload.

Additionally, the base of the stack systems, which were supported by a steel Milford hanger, was also deflected in a downward direction due to this one pipe support securing a major portion of the weight of the piping system (**Figure 11**).

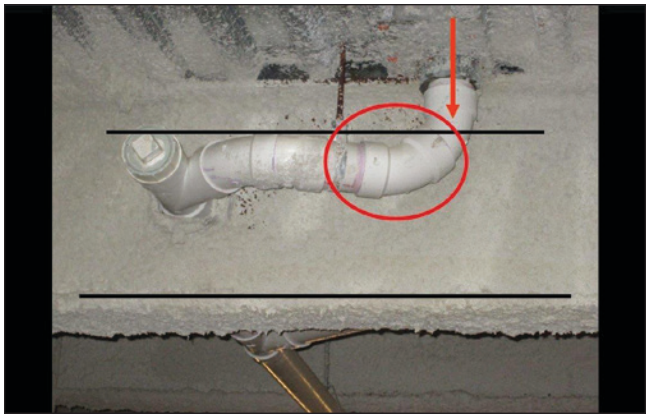

Figure 11
Basement vent stack out of plumb due to excessive weight.

Manufacturer and Code Direction

The following manufacturer and Code guidelines address piping design issues regarding thermal expansion, wood framing shrinkage (in relation to piping support), as well as the need for and installation of expansion joints.

American Society of Plumbing Engineers – *Plumbing Engineering Design Handbook* 2nd Edition Volume 4:

Expansion Joints: *It is recommended that expansion joints be located in an accessible space to allow maintenance or replacement. The guides allow axial movement…An expansion joint should be installed every 30 feet according to the manufacturer's recommendations.*

Drain, Waste and Vent Piping: *Expansion and contraction usually do not present a problem in DWV installations in one- and two-family dwellings due to the short lengths of piping involved. It does create problems in high-rise buildings where long stacks are installed.*

2003 *International Plumbing Code* Section 308.8 – Expansion Joint Fittings:

Expansion joint fittings shall be used only when necessary to provide for expansion and contraction of the pipes. Expansion joint fittings shall be of the typical material suitable for the use with the type of piping of which such fittings are installed.

The manufacturer's pipe design guide (2003 edition) states: "Engineers, designers and installers should use resources such as the *American Society of Plumbing Engineering Design Handbook.*" This design guide also states: "For vertical stacks in multistory applications compensation for expansion, contraction, or building settling is often accommodated by the use of offsets or expansion joints."

Conclusion

In smaller residential structures where pipe sizes and lengths are relatively small, the effects of pipe thermal expansion and building movement are not as severe. In comparison, care must be exercised by piping designers and installers to recognize the characteristics of piping material behavior and building structural movement in larger buildings. The effects of thermal expansion of PVC piping will be greater in the longer piping lengths used in larger commercial building construction and must be accommodated for. The same can be said for stresses imparted into piping in wood frame construction due to wood dimensional shrinkage caused by a loss of moisture over time.

Expansion joints and thermal expansion loops must be incorporated into the initial piping system design with care given as to the placement of these vital components — with forethought into issues such as the accessibility for maintenance and inspection. The configuration of piping must also be considered so as to avoid stresses caused by thermal expansion and building settling.

Engineers, architects, and contractors should communicate and not "operate in a vacuum," allowing issues that extend across engineering disciplines and manufacturers' recommendations to be addressed in the initial stages of the system design, long before construction begins or retroactive repairs and redesign modifications become necessary.

Bibligoraphy

Ellis R, Smith T, et al. Plumbing engineering design handbook, Vol 2. Rosemont, IL: American Society of Plumbing Engineers; 2010.

Ellis R, Smith T, et al. Plumbing engineering design handbook, Vol 4. Rosemont, IL: American Society of Plumbing Engineers; 2012.

International plumbing code. Country Club Hills, IL: International Code Council; 2003.

Lindeburgh M. Mechanical engineering reference manual, 10th edition. Belmont, CA: Professional Publications Inc.; 1997.

Forensic Engineering Analysis of Failed UTV Roll Cages

By Olof H. Jacobson, MS, PE (NAFE 496F), Stephen A. Batzer, PhD, PE (NAFE 677M), Mark H. Kittel, PE (NAFE 757M), Jesse A. Grantham, PhD, PE (NAFE 597S), Guy J. Barbera, PE (NAFE 732M), and Allen Molitoris, PE (NAFE 464C)

Abstract

Two cases were analyzed that involved pitchover/rollover accidents of the same model side by side utility terrain vehicle (UTV). In each case, the UTV ran over a bump on a dirt road and pitched over. The roll cages collapsed, and the drivers suffered significant injuries. Both roll cages collapsed in a similar manner. The design and failure modes of the roll cage structure were analyzed. Engineering analysis included dynamic analysis, laboratory testing, vehicle dynamic testing, finite element analysis, and a review of fundamental mechanical engineering design concepts. Roll cage design and applicable standards were evaluated. Reasonable alternative designs were identified and analyzed.

Keywords

Roll cage, ROPS, rollover, pitchover, design, testing

Vehicle Description

The subject UTV is a four-wheeled, side-by-side vehicle that is equipped with two bucket seats, a steering wheel, and pedals that are similar to automobile controls. The vehicle is equipped with a tubular steel roll cage and three-point automotive-style seat belts.

This UTV is an off-road vehicle with a short wheel base (76 inches), a narrow track width (48 inches), and a high center of gravity. The vehicle has correspondingly low yaw, pitch and roll moments of inertia, resulting in a higher probability of rollovers. The UTV was capable of speeds in excess of 65 mph and had a suspension configured for sporting use. The UTV's roll cage is a tubular steel structure that is bolted to the vehicle frame at four points. The geometry of the roll cage is based on open-sided rectangular shapes with no diagonal bracing. The B-pillars consist of dual tubes that are bent into Z-shapes.

The longitudinal roll cage side header tubes between the A and B pillars include a bolted connection on each side. An optional plastic roof was installed on top of the roll cage in one case. An undamaged exemplar roll cage is seen in **Figure 1**.

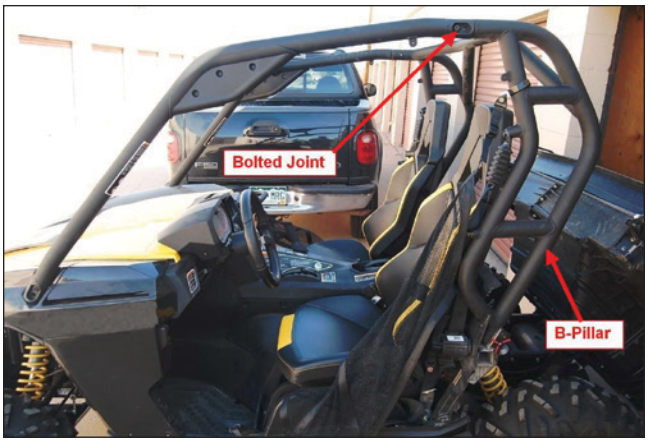

Figure 1
Undamaged exemplar UTV roll cage.

Case A Description

The UTV was descending a 7 percent grade on a two-track dirt forest service road. A water bar (a transverse mound of dirt that diverts water from the road) formed a bump across the road. Engineering analysis indicates the UTV was traveling 29 to 34 mph when it crossed the water bar. After crossing the water bar, the UTV pitched forward and rolled one time longitudinally (end-over-end). The UTV then landed on its wheels and swerved right before rolling over laterally 1¼ times and coming to rest on the driver's side.

Olof H. Jacobson, MS, PE, 10822 W. Toller Drive, Suite 150, Littleton, CO 80127; (303) 948-9515; oj@jacobsonforensic.com

The roll cage collapsed at the B-pillars, and the two bolted connections in the side header tubes failed during the first roof-to-ground contact. The vertical occupant space was reduced by more than 13 inches. The plastic roof separated from the roll cage near the end of the rollover motion.

The driver, who was using the seat belt, was partially ejected. His head struck the ground, resulting in a paralyzing spinal cord injury. His left arm and leg were pinned under the driver's side at rest, resulting in additional injuries.

Scene Geometry: The accident occurred on a two-track dirt road that is 7 feet wide. Sagebrush borders the road on both sides. The road slopes downward at a grade of 7 percent.

The road is relatively straight, approaching the water bar, and it curves slightly to the right downhill from the water bar. With respect to the plane of the road, the peak of the bump was approximately 1 foot high, and the entire bump was 8.4 feet long. A plan view of the accident scene is shown in **Figure 2**. Photographs of the accident site are shown in **Figures 3** and **4**.

UTV Motion: When the UTV crossed the water bar, the rear axle kicked up, and the UTV pitched forward in an end-over-end motion. The right front tire and bumper dug into the dirt and sagebrush to the left of the road 63 feet downhill from the water bar. The UTV continued its forward pitchover rotation, and the vehicle struck the ground on its roof with the rear end facing downhill. The UTV completed one full revolution in the forward pitchover direction and landed on

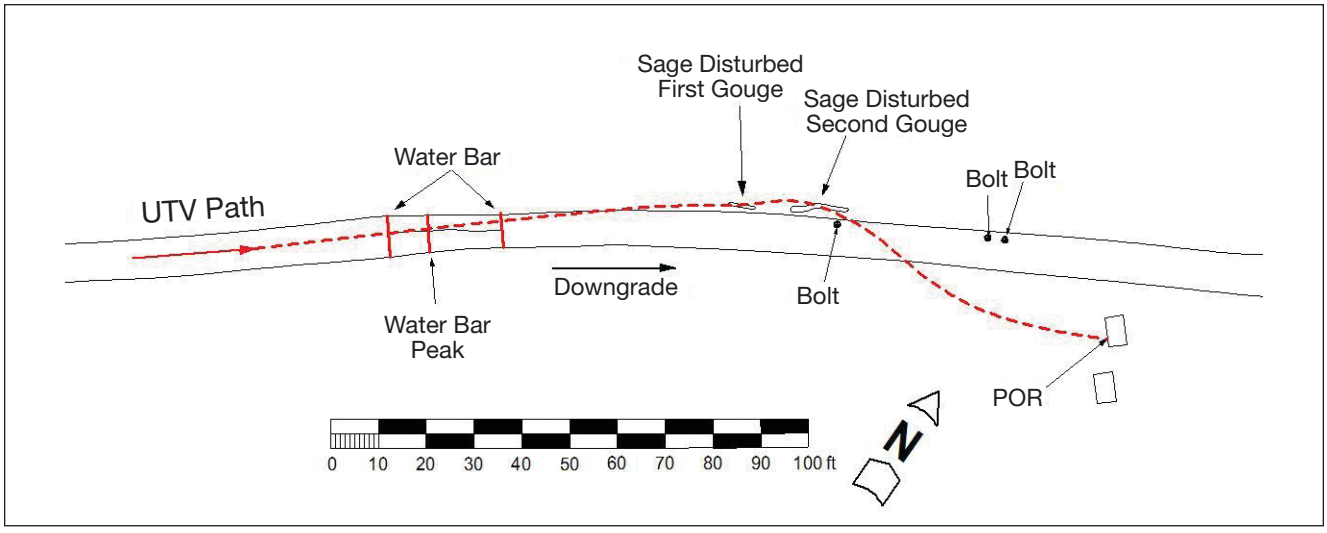

Figure 2
Case A: Scale drawing of accident scene.

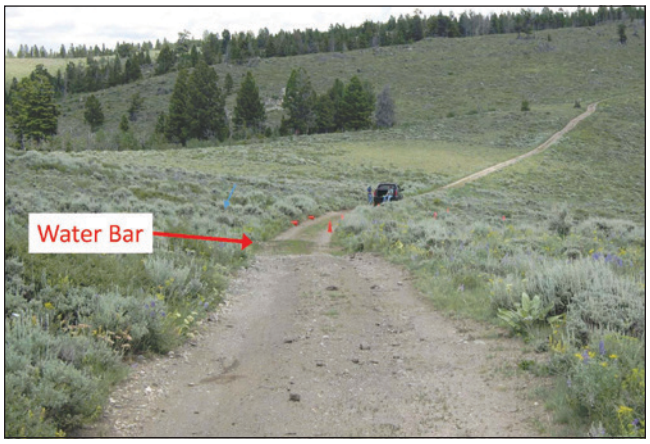

Figure 3
View of accident location, looking downhill in direction of UTV travel.

Figure 4
Side view of water bar. UTV traveled from right to left.

its wheels in a slightly clockwise orientation (i.e., rotated to face slightly toward the right). The UTV then swerved to the right and rolled over laterally with the driver's side leading. The vehicle rolled over laterally 1¼ times before coming to rest on the driver's side. The sequence of the rollover motion is shown in **Figures 5** through **7**.

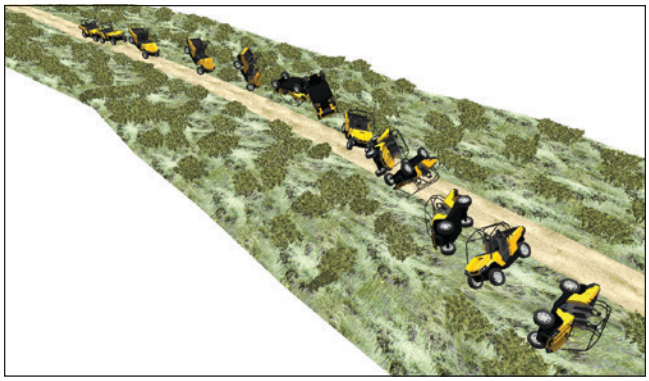

Figure 5
Case A: Overall vehicle motion.

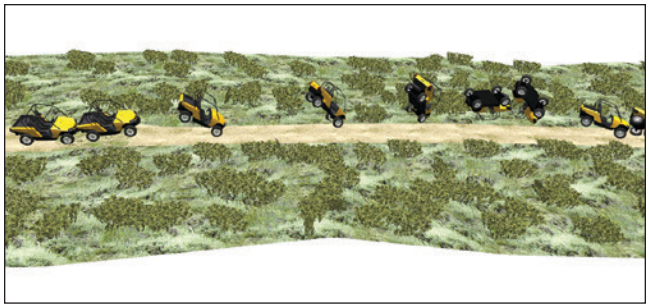

Figure 6
Case A: Initial pitchover motion.

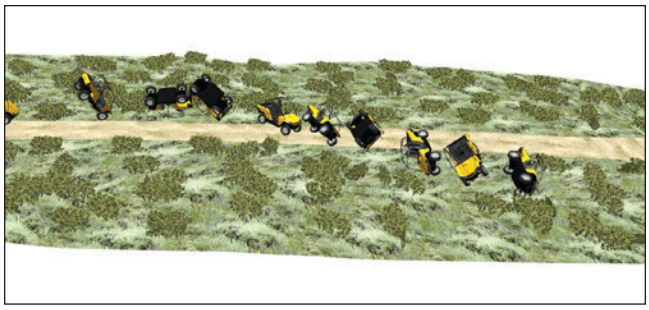

Figure 7
Case A: Final lateral rollover motion.

UTV Damage: The right front corner of the front bumper was scraped and deformed rearward. The right front wheel was folded under with the bottom of the wheel pushed inboard, including associated buckling of the lower suspension A-arm. This evidence indicates that the right front wheel rolled along the ground with the vehicle in a nose down attitude until the front bumper dug in as the vehicle continued to pitch forward onto the roll cage. Given the short wheelbase, the center of gravity of the UTV was not significantly higher during this nose down ground contact when compared to its initial height. The center of gravity did not subsequently fall a significant distance between the time the front end struck the ground and the time when the roll cage struck the ground. Analysis of the UTV geometry, the UTV damage, and geometry of the scrape marks on the ground indicates that the center of gravity did not fall a significant distance above the ground during the initial pitchover when the roll cage collapsed.

The plastic roof exhibited heavy scrapes in the longitudinal direction from rear to front, indicating that the UTV initially landed on its roof while traveling with the rear end leading (following a nose-down pitchover). A second set of lateral scrapes was present on the roof from right to left, indicating that the vehicle subsequently landed on its roof one time while rolling over laterally in a counterclockwise direction (from the driver's perspective) with the driver's side leading. The lateral scrapes were overlaid on top of the longitudinal scrapes, indicating that the lateral rollover occurred after the forward pitchover.

The roll cage collapsed at both B-pillars above the driver's head. The lateral roll cage cross member behind the driver's head buckled downward into a V-shape, and the B-pillars were deformed inward. The bolted connections in both side header tubes separated, and the bolts were found sheared in the bolt holes. Three of the four fractured bolt heads were found in the roadway. The fracture surfaces showed that the bolts failed in shear.

The permanent downward deformation of the roll cage above the driver's head measured 13 inches. The maximum dynamic deformation during the rollover was likely in excess of 13 inches. Roll cage damage is seen in **Figures 8** through **11**.

As described above, the UTV's center of gravity did not gain significant height above the ground during the initial forward pitchover. When the roof struck the ground, the roll cages collapsed and deformed but did not fully compress down to the body of the UTV. It is reasonable to conclude that increased roll cage strength would have reduced the exposure to occupant injuries. In the opinion of the authors, even a moderate increase in roll cage strength would have prevented the collapse of the roll cage.

Figure 8
Case A: Side view of roll cage damage.
Front half of roll cage has been temporarily placed on the vehicle. (The A-pillars were cut at the front frame attachment points after the accident by rescue personnel.)

Figure 9
Case A: Rear view of roll cage damage.

Figure 10
Case A: Failed bolted connection in side header tube.

Figure 11
Case A: Failed bolted connection in side header tube.

Case B Description

The accident occurred on an off-highway vehicle (OHV) trail that is developed and maintained for recreational vehicle use by the U.S. Forest Service. The UTV driver was in the lead of a group of off-road vehicles on a perimeter trail in an area with relatively smooth and level terrain. The driver and his passenger were both wearing helmets and seat belts.

The driver reported that he was traveling approximately 43 to 46 mph as he approached a low spot in the trail. He did not brake or accelerate as he entered the low spot. As the UTV came up the rise on the far side of the depression, the rear end of the vehicle unexpectedly kicked up vertically. The UTV pitched forward with the nose down, and it tumbled end-over-end.

The UTV passenger reported that the driver had accelerated up to approximately 40 mph, and his speed was consistent on the approach to the depression. Witnesses indicated that the UTV was traveling at a reasonable speed for the terrain, and they were surprised that the UTV pitched over.

Scene Geometry: The trail is relatively flat throughout the rollover path. A shallow dip is present at a small drainage channel that enters the trail from the left. The entry to the dip descends very gradually over a distance of 25 to 30 feet. The profile transitions to a slight rise, leaving the low spot over a distance of 10 to 12 feet, with the final 7 feet at a 14 percent upgrade. Photos of the site are seen in **Figures 12** and **13**.

UTV Motion: Engineering analysis indicates that the UTV was traveling at a maximum of 43 miles per hour as it traversed the slight depression in the trail. As the UTV came up the rise on the far side of the depression, the rear end of the vehicle kicked up vertically, and the UTV pitched forward with the nose down, tumbling end-over-end. The UTV completed two full rotations in the forward pitch direction (end-over-end) and came to rest on the driver's side. The UTV traveled 157 feet from the top of the dip to the point of rest.

UTV Damage: One corner of the front bumper was deformed rearward. The roll cage collapsed at the B-pillars above the driver's head, and the bolted connections in the side header tubes failed in shear. The front half of the roll cage collapsed downward at the bolted connections, and the bolts attaching the front of the roll cage to the frame had also failed in shear. The

Figure 12
Case B: Accident site.

Figure 13
Case B: Accident site.

deformed roll cage is seen in **Figures 14** and **15**. Note the similarity to the deformation pattern in Case A seen in **Figures 8** and **9**. The bolted connections failed in the same manner as in Case A.

Longitudinal scrape marks at the tops of the A-pillars and B-pillars indicate that the UTV was on its roof while pitching forward and tumbled end-over-end two times. The absence of scrape marks on the side header tubes between the A-pillars and B-pillars indicates that the bolted connections failed during the first pitchover, allowing the front section of the roll cage to deform downward during the first ground contact.

The permanent downward deformation of the roll cage at the B-pillars measured 2¾ inches on the driver's side and ½ inch on the passenger's side. The downward deformation of the header tubes of the forward portion of the roll cage (at the failed bolted connections) measured 10 inches on the driver's side and 6¼ inches on the passenger's side. The A-pillars were deformed downward 7 inches on the driver's side and 8 inches on the passenger's side. The maximum dynamic deformation during the pitchover was in excess of these static measurements.

The driver's head contacted the ground, but the passenger's head did not, as was evidenced by the scrapes on the driver's helmet and the absence of scrapes on the passenger's helmet. The driver sustained injury from the head contact, and his hands were injured due to impingement between the ground and the upper portion of the steering wheel during the pitchover. As the front portion of the roll cage collapsed, the top of the steering wheel protruded above the plane of the roll cage. The passenger was not injured.

When the rear end of the UTV unexpectedly kicked upward after coming off the bump, the UTV initially traveled on its front wheels for some distance prior to the front end tripping and beginning the pitchover. After the first full revolution of the pitchover motion, the vehicle landed on its wheels as it continued pitching forward. Since the vehicle would lose very little speed during the wheel contact with the ground, the calculated speed of 43 mph is a maximum — the actual speed could have been lower.

The level of B-pillar roll cage deformation in Case B suggests that when the roof struck the ground, the forces of contact were marginally greater than the

Figure 14
Case B. Side view of failed roll cage.

Figure 15
Case B. Rear view of failed roll cage.

strength of the roll cage. In the opinion of the authors, even a moderate increase in roll cage strength would have prevented the collapse of the roll cage. Such an increase in strength would include durable fastening of the front roll cage to the rear roll cage at the bolted header joints; the failure of these joints contributed to the driver's hand injuries.

The absence of injury to the passenger further indicates that increased roll cage strength would have reduced the exposure to occupant injuries.

History and Development of UTV Market

UTVs are a relatively new class of personal recreational vehicles that have evolved as a hybrid of two different products: low power utility vehicles and four-wheel all-terrain vehicles (ATVs).

Low power work site vehicles, often referred to as "mules," are four-wheel vehicles with low horsepower engines and low top-speed capabilities. These vehicles are typically used around farms, ranches, and work sites to haul tools/supplies and to transport personnel. Utility vehicles were initially manufactured in the late 1970s as work vehicles for hauling light loads and traversing mild terrain. Design features of traditional utility vehicles included relatively low power engines and limited suspension travel, or no suspension in some cases, which kept the operation of the vehicle to relatively low speeds due to uncomfortable ride quality and poor handling on rough terrain.

UTVs also evolved out of the four-wheel ATV product lines. These vehicles are technologically sophisticated, high-speed machines where the rider sits atop the vehicle, much like a motorcycle rider. The ATV is a "rider-active" vehicle where the rider's body position is an important part of maintaining vehicle control. When an ATV rolls over or pitches over, the rider is ejected.

In contrast to ATVs, the driver of a UTV is seated inside the vehicle. The driver is restrained with a seat belt and inside a roll cage. The driver cannot move his body to affect vehicle stability, and he or she should remain within the protective space of the roll cage during a rollover. The UTV is not "rider-active," meaning that the operator does not actively affect the vehicle's handling through body positioning, as is done on an ATV or motorcycle.

Since the occupants of a UTV are seated similar to an automobile, the opportunity exists to protect the driver with a properly designed occupant protection system, consisting of the seat belt, the seat, and the roll cage. With the occupant seated, safety considerations require that the UTV employ appropriate means of protecting the operator in the event of a crash or if the vehicle overturns.

The subject UTV is visually similar to a "mule" work vehicle, but it has been upgraded with a sophisticated, high-powered engine and sophisticated suspension to combine the cargo hauling and two-passenger capability of a traditional utility vehicle with the speed and off-road capability of an ATV.

The subject UTV employs a roll cage that is visually similar to the rollover protection system (ROPS) devices found on lower-speed work vehicles. However, in contrast to the engineering and technical sophistication of the rest of the vehicle, the roll cage portion of the occupant protection system is not comparable to the balance of the UTV. The roll cage on the subject UTV is not safe for the capabilities of the machine, and it is not safe for its foreseeable use. The subject UTV roll cage was defectively designed as it did not provide its intended function of reliable intrusion resistance. The roll cage should have been designed for the foreseeable use of the UTV, including the potential for rollovers and pitchovers. The roll cage should be adequate to protect the occupants during the foreseeable event of a rollover or pitchover.

Roll Cage Design

The roll cage consists of a tubular steel cage bolted to the UTV frame at four points. The geometry of the roll cage is based on open-sided shapes, which are approximately rectangular with no diagonal bracing. The B-pillars consist of dual Z-shaped tubes. The side header tubes include a bolted connection on each side. The roll cage is fabricated from steel tubing with a nominal outside diameter of 2 inches, a wall thickness of 0.131 inches, and a yield strength of 71,000 psi.

During the accident sequences investigated, both B-pillars collapsed and both bolted connections failed during the initial pitchovers. In Case A, the lateral cross member above the driver's head also buckled, allowing the B-pillars to deform inward. Three fundamental engineering deficiencies were identified in the subject roll cage:

- Z-shaped B-pillars
- Rectangular, open-sided truss geometry without diagonal bracing
- Single-shear bolted connections in the side header tubes

Failure of the subject roll cage in relatively low-speed rollover events is foreseeable, given the fundamental engineering deficiencies in the roll cage design. Details of the deficiencies are as follows:

1. **Z-shaped B-pillars:** From an engineering perspective, the Z-shaped B-pillars are an obvious potential failure point. Bends in a load-bearing column create a weak point where buckling will occur. This type of bent structure is normally avoided in engineering design. The use of straight vertical columns instead of the "dog leg" B-pillars would increase the strength of the B-pillars significantly.

   Testing of the subject roll cage resulted in a B-pillar buckling failure under a vertical load of 16,510 pounds (see testing section below). Analysis shows that the use of vertical columns with the same steel tubes would increase the buckling failure load to approximately 88,600 pounds, a more than five-fold increase over the original design. The use of straight vertical columns in place of the Z-shaped B-pillars would not change the cost of the roll cage. The use of straight vertical columns is economically feasible, technically feasible, and an obvious design choice to a mechanical engineer. Details of adapting the straight columns to the existing frame geometry could be overcome with proper engineering analysis. Fundamental engineering design principles should have been incorporated into the entire UTV design from the conceptual stage.

2. **Roll Cage Geometry:** The geometry of the roll cage is based on open-sided shapes, which are approximately rectangular with no diagonal bracing. A properly designed roll cage should be based on triangular trusses. Rectangular trusses can deform into parallelograms with relatively little resistance to deformation. Rectangular trusses are inherently much less rigid than triangular trusses. This concept is demonstrated graphically in **Figure 16**.

Fundamental mechanical engineering design practice and numerous roll cage design standards require triangular trusses. This is accomplished with diagonal bracing. Diagonal braces can be included in a four-point mount design, or they can be added by utilizing six mounting points to the frame. Diagonal bracing is standard in roll cages designed for off-road racing vehicles where the probability of rollover is higher than in passenger cars. Longitudinal and lateral diagonal bracing should have been included in the UTV roll cage design. Fundamental engineering design principles should have been incorporated into the entire UTV design from the conceptual stage.

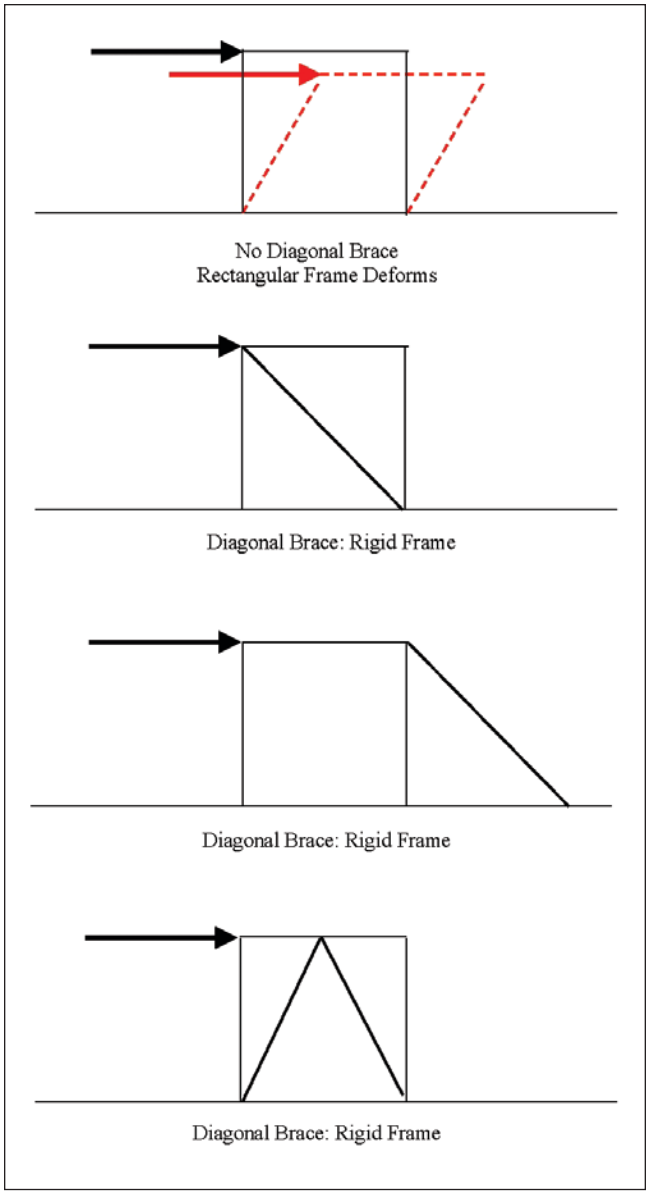

Figure 16
Schematic diagram of rectangular truss deformation vs. triangular truss stiffness.

3. **Bolted Connections:** In the two cases, both bolted connections in the side header tubes failed during the pitchovers. Engineering shows that the bolted connections would fail under a vertical load of approximately 1,200 pounds. The steel tubes without bolted joints would have supported a vertical load of approximately 3,500 pounds. This use of bolted connections weakened the longitudinal members of the roll cage by a factor of nearly three. (See **Appendix A**.)

   The bolted joints in the roll cage were loaded transversely, and the bolts failed in single shear. This is a fundamental design weakness. Bolts are typically loaded in tension, but if they must be loaded in shear, they should be loaded in double-shear. In addition, the cross-sectional area of the bolts should be sufficient to support the expected loads such that the strength of the bolted joints is consistent with the overall strength of the roll cage.

   If tube joints are necessary, the tubes could be joined by using one of several standard methods. For example, a reduced diameter tube end inserted inside a full diameter tube end locked together with through bolts would not load the bolt in shear, and the joint could be as strong as the base steel tubing. Other alternate designs include engineered products such as the Camburg Tube Clamp seen in **Figure 17**. In this design, if properly oriented, bending moments and resultant shear forces would be transferred through interlocking features and not through the bolts.

The use of vertical columns, diagonal bracing, and properly designed joints as described above would have prevented the collapse of the subject roll cages. These design concepts are economically feasible and technically feasible. These design concepts are widely known and accepted in mechanical engineering design and roll cage design.

Roll Cage Testing

An exemplar roll cage was tested in a laboratory setting. The cage was bolted to a steel base plate, and a downward vertical load was applied across the lateral member at the B-pillars. As the cage was deformed vertically, load and displacement data was recorded until the vertical force peaked and then began to decline, indicating that the stress had exceeded the yield strength of the steel tubing. The roll cage failed due to buckling in the bends in the Z-shaped B-pillars.

The test setup is shown in **Figure 18,** and the load displacement data is shown in **Figure 19**. The B-pillars buckled at a vertical load of 16,510 pounds.

Figured 17
Camburg tube clamp
(http://camburg.com/fabrication-parts/billet-tube-clamps/)

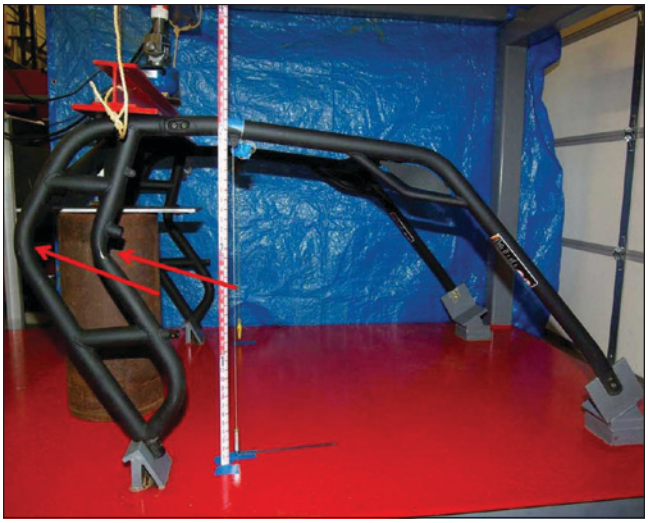

Figure 18
Laboratory testing of an exemplar roll cage.
Z-shaped B-pillars buckled at bends (arrows).

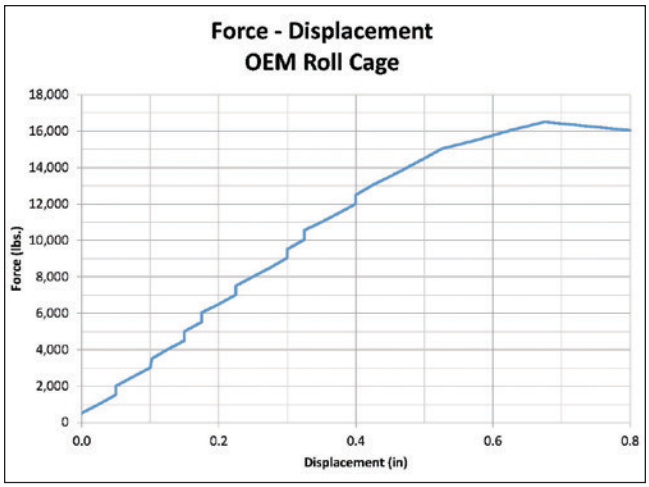

Figure 19
Load/displacement data from test shown in Figure 18.
Peak force was 16,510 pounds.

Engineering Analysis – B-pillar Column Buckling

Engineering analysis shows that replacing the Z-shaped B-pillars with straight columns would have significantly increased the strength of the roll cage. The following simple modifications would have increased the buckling strength of the B-pillars as follows:

B-pillar design	Tube Diameter (inches)	Wall Thickness (inches)	Buckling Load (pounds)	Increase
Subject, Z-shaped tube	2.00	0.131	16,510	Baseline
Straight, original tube (see Figure 23)	2.00	0.131	88,600	540%
Straight, larger diameter tube	2.25	0.131	105,400	640%
Straight, thicker wall tube	2.00	0.250	155,000	940%
Straight, larger/thicker tube	2.25	0.250	187,800	1,140%

This data demonstrates that simple modifications to the roll cage design would have significantly increased the strength of the roll cage. It should be noted that in the test, the B-pillars were loaded evenly, and the load was purely vertical. This represents an ideal loading condition to be used as a baseline for further analysis and does not represent the actual loads applied to the roll cages during the subject pitchover events. Fundamental engineering design principles should have been incorporated into the entire UTV design from the conceptual stage.

Finite Element Analysis of Additional Reasonable Alternative Designs

Additional reasonable alternate roll cage designs were evaluated with finite element analysis (FEA). The physical testing described above was used to validate a finite element model of the roll cage.

The FEA analysis was performed with LS-Dyna version 971 software. A Lagrangian mesh formulation was used to simulate the deflection of the roll cage under quasi-static loading. The roll cage was loaded in the vertical direction at a rate of 100 mm/s through a simulated platen at the top of the B-pillar. Automatic surface-to-surface contact was enforced at the platen-to-roll-cage contact and bolt-to-bolt-hole interaction. Static and dynamic coefficients of friction used were 0.1 and 0.07, respectively. Runs were made with a symmetric half-section with the center point of the front and rear header fixed to prevent Z-axis (lateral) motion, X-axis rotation and Y-axis rotation. This was done to promote computational efficiency. The force results of the half-model were doubled to give the total force resistance of the full FEA model.

A graphical output from the FEA model is shown in **Figure 20**. The FEA model predicted a failure load of 17,200 pounds with a deflection of 0.5 inches compared to the laboratory test results of 16,500 pounds with a deflection of 0.675 inches. The FEA model had a somewhat stiffer initial response as shown by the steeper curve. Peak loading was about 4% greater than the measured physical peak cage load, and peak deformation of the model occurred with ~0.2 inch less deformation compared to the physically tested roll cage. The general shape and resulting peak load are very similar. **Figure 21** shows the data from the physical test and the output of the FEA model. Overall, the testing provided a reasonable validation of the FEA model.

The validated FEA model was then used to analyze various roll cage alternative designs. The FEA analysis shows that replacing one of the Z-shaped B-pillars on each side with a straight column would change the failure mode of the roll cage. With a vertical column, the B-pillar does not buckle. In this design, the B-pillar rotates rearward about its base, and the angle at the A-pillar opens up. Three additional conceptual alternatives are discussed below.

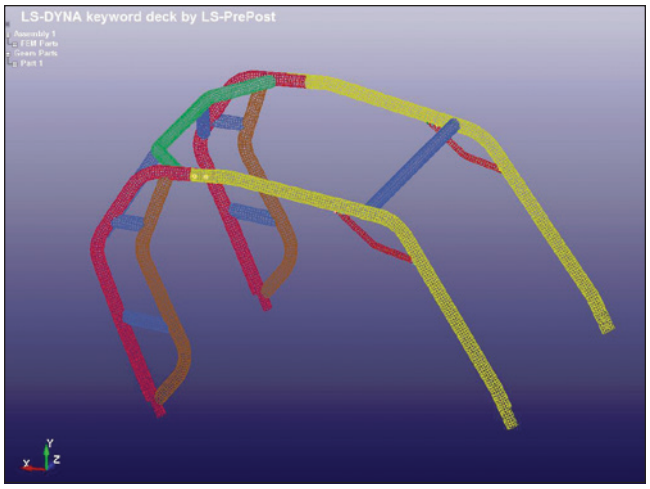

Figure 20
LS-DYNA graphical output of roll cage model.

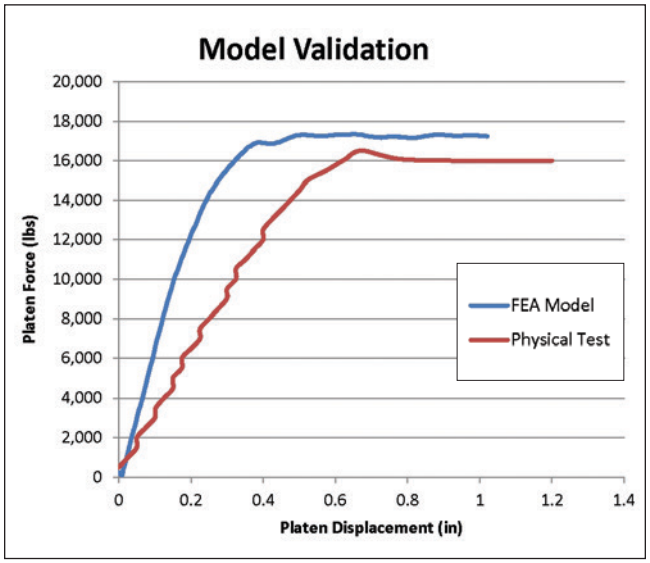

Figure 21
Validation of FEA model vs. laboratory test.

Conceptual Alternative 1

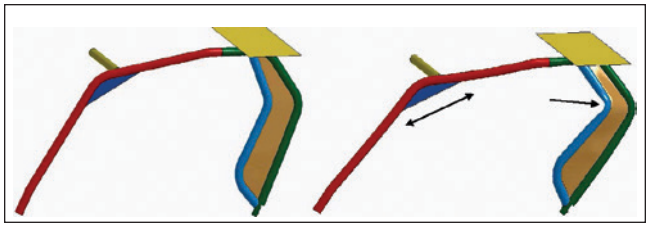

Figure 22
Graphic of conceptual alternative 1. Conceptual design shown in left panel. Resulting deformation shown in right panel.

Figure 22 shows the first alternative concept, which uses a 0.090-inch (2.3 mm)-thick steel web to fill in the area between the two B-pillar uprights in order to transfer shear loading between the uprights. As such, this concept deletes the two horizontal connecting tubes. The rear-most cage to chassis attachment points are identical to the baseline model. The model is shown in the unloaded and heavily loaded states with 4 inches of deformation. Note the maximum distortion at the top bend of the rear cage forward upright. Also, note the straightening of the A-pillar / roof rail segment and minor rotation about the rear mount. The peak load of conceptual Alternative 1 measures 21,600 pounds at 0.5 inches of platen movement.

Conceptual Alternative 2

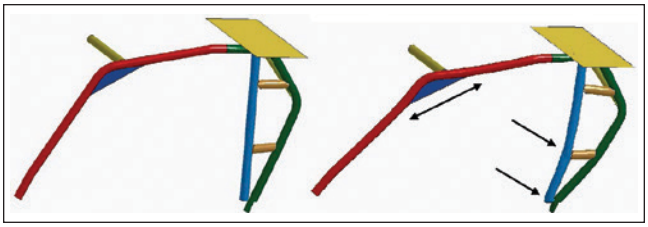

Figure 23
Graphic of conceptual alternative 2. Conceptual design shown in left panel. Resulting deformation shown in right panel. Z-shaped tube has been replaced by a straight vertical tube (see blue member).

Figure 23 shows the second alternative concept that uses a vertical tubular member in place of the original Z-shaped tube, eliminating the bends in the column. The bottom of the tube has been modeled as a fixed connection to the chassis. Thus, the fixation of the rear cage to the vehicle chassis has been strengthened by replacing the two fixed rear chassis connections with four fixed connections. This design concept is shown below in the unloaded and heavily loaded states with 4 inches of vertical deformation. The rear upright is not grossly distorted; the B-pillars rotated rearward about the mount with plastic deformation. The A-pillar / roof rail intersection straightened. The peak load of conceptual Alternative 2 measures 37,900 pounds at 2.0 inches of platen movement.

Conceptual Alternative 3

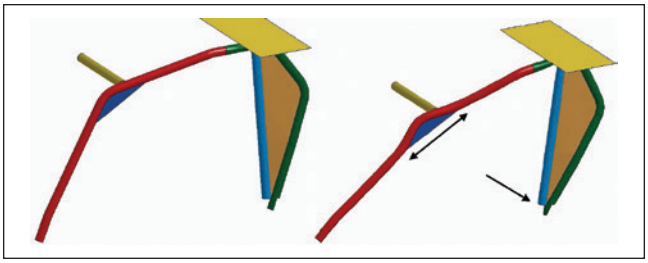

Figure 24
Graphic of conceptual alternative 3. Conceptual design shown in left panel. Resulting deformation shown in right panel.

Figure 24 shows the third alternative concept, which is a combination of concepts 1 and 2. The design

is shown in the unloaded and heavily loaded states with 4 inches of vertical deformation. Since the vertical upright is attached to the rear upright with the web, the bottom of the forward vertical tube is not fixed to the mount and can rotate with deformation. This is identical to the frame attachment of the baseline model. When this model is loaded, the rear uprights do not buckle. Instead, they rotate rearward about the rear cage mounts, and the A-pillar / roof rail segment straightens. The peak load of conceptual Alternative 3 measures 47,500 pounds at 3.0 inches of platen movement.

Summary of FEA Analysis of Conceptual Alternative Designs:

Conceptual Design	Buckling Load (pounds)	Increase
Subject	17,200	Baseline
Conceptual Alternative 1	21,600	126%
Conceptual Alternative 2	37,900	216%
Conceptual Alternative 3	47,500	276%

Vehicle Dynamics: Dynamic Testing of Pitchover Tendencies

Exemplar UTVs from various manufacturers were tested in an off-road environment to evaluate dynamic performance. Testing was conducted in an OHV riding area with both man-made and natural terrain features. The exemplar vehicles were driven over a variety of terrain and obstacles to gain an understanding of performance and handling characteristics. On certain obstacles, the subject UTV had a tendency to kick the rear of the vehicle up, resulting in a nose-down pitch instability after the vehicle became airborne. The obstacle that produced the rear kick-up tendency was a step-up style jump, approximately 12-18 inches tall, with a short approach ramp that was negotiated at a speed of approximately 34 mph.

Operating a competitor's UTV on the same feature and at the same speed as the subject UTV confirmed that the both vehicles had the rear kick-up tendency. Both UTVs had adjustable springs and shock absorbers. Utilizing the full range of compression and rebound damping adjustments, along with the spring preload adjustments, resulted in no appreciable improvement in the rear kick-up tendency or in the pitch instability. The only improvement noted was when the front and rear springs were swapped on the subject UTV (installing the stiffer rear springs in the front and the softer front springs in the rear). In this configuration, the rear kick-up tendency was decreased but was still present.

The rear kick-up tendency was likely due to the geometry of the vehicles and is a characteristic that is likely inherent in most, if not all, UTVs. As such, it is readily foreseeable that a rear kick-up event could be encountered during typical operation of the subject UTV. Considering the high-performance capability of the UTV, it is foreseeable that an unintentional rear kick-up event with pitch instability could occur during normal use at speeds either higher than the tested 34 mph, or on a bump feature that caused more severe pitching, even at lower speeds. It is foreseeable that a UTV operated at reasonable speeds could experience a rear kick-up event severe enough to cause the vehicle to unexpectedly pitch nose-down, resulting in an end-over-end tumble during normal operation.

The UTV is intended to be operated off-road over uneven terrain. The UTV has the capability to operate over such terrain at high speeds, which makes overturn events such as the subject cases foreseeable to a design engineer. For these reasons, the UTV design is unsafe without a robust roll cage that can withstand the kind of over-turn events that could foreseeably occur. In contrast, it may not be foreseeable to a typical consumer that the UTV may pitch over forward in "normal" use, and it is not foreseeable that the roll cage is likely to fail in even a low-speed rollover or pitchover event.

UTV Design and Roll Cage Requirements

The subject UTV is an off-road vehicle with a short wheel base, a narrow track width and a high center of gravity. The low yaw, pitch and roll moments of inertia indicate that a UTV is much more prone to instability, pitchovers, and rollovers than a highway passenger vehicle. A UTV is intended for off road use exclusively where it is foreseeable that bumps and uneven surfaces will be encountered.

Testing shows that due to the dynamic characteristics of the UTV and its intended off-road use, it is or should be foreseeable to the designer that the UTV will roll over or pitch over, potentially at high speed. Dynamic testing shows that after running over certain bumps, it is foreseeable that the UTV may pitch nose down and land with the front end down.

When a hazard such as the propensity to roll over or pitch over exists in a vehicle design, the best design choice is to modify the design to remove the hazard. If this is not feasible, a secondary method to protect occupants is to provide a guard to prevent or reduce the probability of injury. The least effective approach is to utilize warnings and operator training.

Given that it may not be possible to prevent pitchovers and rollovers, the UTV roll cage should have been designed for the foreseeable use of the product. The roll cage should have been designed and tested to withstand the foreseeable rollovers and pitchovers of the UTV. A properly designed roll cage would have guarded against the danger resulting from the inherent propensity to pitch over and roll over. Fundamental engineering design principles should have been incorporated into the entire UTV design from the conceptual stage.

The roll cage is an important component of the overall occupant protection system. From a consumer's perspective, the UTV appears to be technologically sophisticated and robust. The roll cage conveys the impression of strength and safety. The cost of the subject UTV, which is similar to an automobile, suggests a level of sophistication and safety to the consumer. Although the roll cage conveys the impression of strength and safety to the consumer, it does not share the level of engineering and technical sophistication of the rest of the vehicle.

As mentioned, it may not be foreseeable to a typical consumer that the UTV may pitch over forward in "normal" use, and it is not foreseeable that the roll cage is likely to fail in even a low-speed rollover or pitchover event.

Standards

The manufacturer of the subject roll cage referred to portions of various automotive and agricultural standards, which, upon inspection, were not applicable to the subject UTV.

Agricultural and Automotive Standards

Standards are published for agricultural ROPS and automotive roof strength. These standards are not adequate for the intended and foreseeable use of UTVs.

The UTV is not an agricultural tractor. Tractors typically roll over at low speed and often experience only ¼ roll onto the side or rear. The agricultural standards require very low forces, on the order of 1.5 times the vehicle weight.

The UTV is not an automobile. Automobile rollovers are relatively rare events when compared to UTVs. Automobile pitchovers are even more unusual. The automotive standards involve relatively low forces, on the order of 1.5 to 3 times the vehicle weight.

It is likely that a foreseeable rollover or pitchover incident will expose the vehicle to forces well in excess of those expected in the minimal agricultural and automotive standards available. Standards are a minimum requirement. Designing the UTV roll cage to meet only the minimal requirements of agricultural and automotive standards was a defect in the design of the subject roll cage. Proper engineering design requires a roll cage strength that is adequate for the foreseeable uses of the UTV, including foreseeable misuse.

Roll Cage Standards for Off-Road Vehicles and Racing Applications

Numerous standards and recommended practices exist for the proper design of a roll cage. Typical roll cage design standards include requirements for two vertical hoops and diagonal bracing, both longitudinally and laterally. The subject UTV roll cage does not comply with these standards. Modifications to comply with these standards and practices could have been easily included with minimal cost. The roll cage standards describe proper methods for joining tubes where a joint is necessary, without improperly loading bolts in shear.

Review of the design concept and performance characteristics of the subject UTV suggest that it is more closely akin to a high-performance off-road go-cart or an off-road racing vehicle. Traditionally, vehicles with the power, speed, and terrain capability of the UTV were built for competition in off-road racing events and were required to employ a structurally sound roll cage. As such, the roll cage requirements from racing organizations would likely have been the most reasonable design guide for the UTV designers to follow. Basic features of conventional roll cage designs include straight vertical support structures, cross-bracing (triangular trusses), and six attachment points (three on each side) to the vehicle chassis. The purpose of these design features is to ensure adequate strength and stability of the safety structure for foreseeable crash events.

The design of the subject roll cage does not include the basic features of a conventional roll cage. The vertical support structures consist of bent columns, there is no lateral cross bracing, and there are only four attachment points of the cage to the chassis. The lack of basic roll cage features results in a structure that is easily deformable in low to moderate speed rollovers and offers inadequate protection for the performance capabilities of the vehicle.

It was technologically and economically feasible for a UTV in this market to be equipped with a properly designed roll cage in accordance with roll cage standards and sound engineering design practices.

Conclusions

- In both Case A and Case B, the subject UTVs were traveling at relatively low speed (29 to 34 mph and 43 mph or less, respectively).
- As each UTV traversed a relatively benign rise in terrain, the rear end of the UTV unexpectedly kicked up into the air, and the vehicle landed in a nose-down pitchover orientation.
- During the pitchover, the roof came into contact with the ground, and the roll cage collapsed.
- The roll cage collapsed during the initial roof contact, and it did not provide any useful occupant protection during the final rollover.
- During the pitchover, in both Case A and Case B, the driver's head contacted the ground due to the failure of the roll cage, resulting in injury. In Case B, the driver's hand was also injured due to crushing between the ground and the steering wheel.
- The roll cage was defective and unreasonably dangerous. Fundamental engineering concepts were ignored in the design of the roll cage, resulting in the roll cage failing during foreseeable pitchover and rollover events.
- It was technologically and economically feasible to design a roll cage that would have remained sufficiently intact to protect the occupants. Fundamental engineering design principles should have been incorporated into the entire UTV design from the conceptual stage.
- A properly designed roll cage would not have failed in the subject accidents. A properly designed roll cage would have prevented the driver's head contact with the roof and ground during the pitchover. In Case B, a properly designed roll cage would have also prevented the driver's hand injury.

APPENDIX A

Bolted Joint Stress Analysis

Bolt Geometry

Per Shigley SAE grade 8.8 bolt	$S_{ybolt} := 660\ \text{MPa} = 95.7\ \text{ksi}$
Per Machinery Handbook, 3/8 inch blt minor diameter	$\phi_{minor} := 8.344\ \text{mm} = 0.329\ \text{in}$
Cross sectional area	$A_{shear} := \frac{\pi}{4}\ \phi_{minor}^{\ 2} = 0.085\ \text{in}^2$

Beam Geometry

Length of beam from front to rear supports	$l := 37\ \text{in}$
Tubing Outer Diameter	$D := 2.025\ \text{in}$
Tubing Wall Thickness	$t_{wall} := \frac{1}{8}\ \text{in} = 0.125\ \text{in}$
Tubing Inner Diameter	$d := D - 2\ t_{wall} = 1.775\ \text{in}$
Second Moment of Area about Bending Axis (Shigley)	$I := \frac{\pi}{64}\ \left(D^4 - d^4\right) = 0.338\ \text{in}^4$
Distance from Load to Forward Support	$b := 28\ \text{in}$
Distance from Load to Rear Support	$a := l - b = 9.0\ \text{in}$
Spacing of bolts (from UTV inspection)	$s := 1.0\ \text{in}$

Failure load - tubing wihtout a bolted connection (Beam Bending)

Yield strength of tubing steel	$S_y := 71.121\ \text{ksi}$
Second Moment of Area about Bending Axis (Shigley)	$I = 0.338\ \text{in}^4$
Tubing Outer Diameter	$D = 2.025\ \text{in}$
Distance to Neutral Bending Axis	$c := \frac{D}{2} = 1.013\ \text{in}$
Length of the Beam	$l = 37.0\ \text{in}$
Distance from Load to Forward Support	$b = 28.0\ \text{in}$
Distance from Load to Rear Support	$a = 9.0\ \text{in}$
Bending Stress	$\sigma = \frac{M \cdot c}{I}$
Moment required to produce failure	$M_{tube} := \frac{S_y \cdot I}{c} = 23752.5\ \text{in} \cdot \text{lbf}$
Classical Bending Diagram (Shigley)	$M = \frac{F \cdot b \cdot x}{l}$
Force Required to Yield the Tubing	$F_{tubing} := \frac{M_{tube} \cdot l}{b \cdot a} = 3487.5\ \text{lbf}$

APPENDIX A (continued)

Bolted Joint Stress Analysis

Failure load at bolted connection - **moment** applied at center of the bolt pattern (Single Shear of 2 Bolts)

Yield Strength	$S_{ybolt} = 95.7$ ksi
Area over which bolt shearing would act	$A_{shear} = 0.085$ in^2
Force required to shear a single bolt	$F_{shear\_bolt} := \langle S_{ybolt} \rangle \ \langle A_{shear} \rangle = 8113.3$ lbf
Couple Distance between bolt heads	$s = 1.0$ in
Moment Required to Shear Bolt Heads	$M_{bolts} := \langle F_{shear\_bolt} \rangle \ s = 8113.3$ in·lbf
Length of the Beam	$l = 37.0$ in
Distance from Loading to Forward Support	$b = 28.0$ in
Distance from Loading to Rear Support	$a = 9.0$ in
Force Required to Shear Bolts due to Bending	$F_{bolt} := \frac{M_{bolts} \cdot l}{b \cdot a} = 1191.2$ lbf

Bibliography

ANSI/AMT B11.TR3-2000. Risk assessment and risk reduction — a guide to estimate, evaluate and reduce risks associated with machine tools. McLean, VA; Association for Manufacturing Technology.

Batzer S. et al. Dynamic roof crush intrusion in inverted drop testing. 19th International Safety Conference on the Enhanced Safety of Vehicles. Paper No. 05-0146. Washington DC; 2005.

Gibson-Harris S. Would a warning have prevented the accident? Journal of the National Academy of Forensic Engineers. 1986;3(2): 51-56.

Hall G. The failure to warn handbook. Hanrow Press. Columbia, MD; 1986.

Hammer W. Product safety management and engineering. Second Edition; Des Plaines, IL; American Society of Safety Engineers Press: 1993.

Kolb J, Ross S. Product safety and liability. New York, NY; McGraw-Hill: 1980.

Krieger G, Montgomery J. Accident prevention manual for business and industry — engineering & technology, 11th Ed. Itasca, IL; National Safety Council. 1997; 4-14.

Laing P. Product safety - management guidelines. Chicago, IL; National Safety Council. 1989; 40-48.

McGuire EP. The product safety function: organization and operation. New York, NY; The Conference Board Inc.; 1979.

Miller K. Myth surrenders to reality: design defect litigation in Iowa. Drake Law Review. 2003;51(3).

Petersen D. Techniques of safety management, a systems approach. Goshen, NY; Aloray. 1989: 31.

Forensic Engineering Technology Solutions for Highway Work Zone Temporary Traffic Control Investigations

By Daniel J. Melcher, PE (NAFE 711S) and Rachel E. Keller, PE (NAFE 873M)

Abstract

Incidents or collisions involving pedestrians, bicyclists, motorcycles, automobiles, heavy trucks, or tractor-trailers frequently occur in roadway or roadside areas affected by highway construction projects. When such events arise, the ensuing claims or litigation processes often concern whether or not the temporary traffic control (TTC) system in place at the time was compliant with the applicable standard of care. Due to the short-term and constantly changing nature of construction projects and work zones, the hardest challenge for the forensic engineer is often to determine what was in place at the time and location of the incident. This paper will introduce and expound on the application of modern technology solutions to address these questions. Methods for extraction of useful information from the raw data will be addressed, along with examples demonstrating the engineering application of this data to the underlying legal questions.

Keywords

Forensic engineering, temporary traffic control (TTC), maintenance of traffic (MOT), highway construction work zones, transportation engineering, highway safety, traffic control devices, photogrammetry, animation

Introduction

Construction and maintenance activities occur frequently throughout our nation's transportation network in order to improve function and safety, aid traffic flow, provide new benefits, or keep existing facilities at an adequate level of service:

- As our nation's travel demands grow, roadways continue to be expanded or upgraded. Aging roadways and bridges require rehabilitation and renewal projects.
- Construction of new roadways involves connections with the existing adjacent facilities.
- Expansion of transit systems impacts the surrounding vehicular and pedestrian routes.
- Private property construction activities affect the abutting public roadways and pedestrian routes.
- Our public infrastructure requires routine maintenance activities that alter the normal flow of traffic.
- Utility construction and maintenance work occurs within the public right-of-way.

In these situations (and others), the work to be completed provides an engineering benefit to the public, but a consequence of achieving the project's goals is a temporary alteration to the normal function of the public roadways or private roads open to public travel. These impacts on the transportation environment may include mobile and intermittent operations that are constantly moving, short- and intermediate-term events lasting from minutes to three days, or long-term projects that occupy a portion of roadway or sidewalk for weeks or months.

According to the *Manual on Uniform Traffic Control Devices* (MUTCD), anytime the normal function of a roadway (or private road open to public travel) is suspended by work activities, there needs to be an appropriate implementation of temporary traffic control (TTC) in order to provide continuity of movement for motor vehicles, motorcycles, bicycles, pedestrians, commercial vehicles, and transit (Manual on Uniform Traffic Control Devices 2009). The primary function of

Daniel J. Melcher, PE, 11847 162nd Place North, Jupiter, FL 33478, (813) 909-3418; Daniel@focusforensics.com;
Rachel E. Keller, PE, 133 E. 143rd Avenue, Tampa, FL 33613; Rachel@focusforensics.com

this TTC system is to provide for the reasonably safe and effective movement of road users through or around the work zones while reasonably protecting road users, workers, responders to traffic incidents, and equipment.

As with any permanent transportation facility, a variety of incidents may potentially occur within a TTC area:

- A pedestrian may trip and fall while walking through a temporary pedestrian detour.
- A bicyclist may encounter a pavement discontinuity around a drainage feature.
- A motorcyclist may encounter a vertical height difference within a milling and paving project.
- A passenger vehicle may have an intersection collision with another vehicle, or may depart from the roadway into the work zone and strike a piece of equipment.
- A commercial vehicle may collide with queued vehicles at a flagging station.

There are a nearly infinite variety of potential scenarios for incidents within a work zone or TTC area. Some of these may be coincidental, and have no relationship to the location where the event occurred. Others may have a direct relationship to the work zone, such as a lack of proper advanced warning or devices that were placed incorrectly by the workers (Hintersteiner 2008).

When a collision or incident does occur within a work zone area, it is not uncommon for claims or litigation processes to ensue. These types of cases often involve multiple interested parties, such as the claimants, other motorists, the governmental entity, owner of the project, the engineer designer of record, the prime contractor for the project, traffic control subcontractors, subcontractors conducting specific elements of the project related to the incident, and construction engineering / inspection (CEI) professionals. Though each party has different levels of involvement in the actual incident, all are typically interested in determining whether or not the TTC in place at the time of the incident was consistent with the standard of care and whether or not there was any connection between the existing TTC and the causation of the event. As such, any entity involved in the claim or litigation can benefit from a thorough and detailed forensic engineering evaluation to address the causation of the incident at hand and to help prevent similar incidents.

Despite the breadth of incident types (and the complexity of the highway construction industry), forensic engineers can follow a consistent process to complete an independent analysis of any incident and the TTC issues related to that event:

1. Forensic determination of what TTC system was actually in place at the date and time of the subject incident, including the selection and location of individual traffic control devices and the historical development of the TTC leading up to the date of the incident.
2. Engineering study to determine the applicable guidelines or standards for the work activity that was taking place, including a review of federal, state, local, and project-specific documents and publications.
3. A forensic engineering comparison between the existing TTC and the recommended TTC to identify any deficiencies or discrepancies.
4. If deficiencies or discrepancies existed, identification of the parties involved in the project and their relative responsibility for the condition in question.
5. Coordination of the TTC findings with a forensic engineering collision reconstruction effort, in order to evaluate whether any deficiencies or discrepancies are causally related, or unrelated, to the subject event.

Though Steps 2 through 5 of the methodology are outside the scope of this paper, all of the steps are predicated on first being able to determine (to a reasonable degree of engineering certainty) what was actually in place for the transportation system at the time of the incident. However, the scope of investigation needed for a TTC case is both extensive and complex:

- Geography of data needed: A TTC zone can be as small as a single driveway or sidewalk. Alternately, the areas affected by construction, including advanced warning areas, detours, and TTC devices, can extend for many miles, making

the relevant "scene" of the incident larger than in most forensic engineering cases.

- Quantity of data needed: A thorough investigation would ideally identify and document all aspects of the TTC, including roadway geometry, lane usage, roadside conditions, pedestrian routes, permanent signs, temporary signs, permanent pavement markings, temporary pavement markings, channelizing devices, delineators, barriers, tapers, traffic signalization, sight lines, and any other relevant transportation engineering issue.

- Temporary nature of data needed: The ephemeral nature inherent to TTC zones has long presented difficult obstacles for forensic engineers. Some conditions exist only for a few minutes or hours. In contrast, notice of claims or litigation may not be provided until months or years have passed. In many forensic engineering assignments, the analyst is not contacted until well after the project is completed or has at least transitioned to another stage or phase of construction.

As modern technology develops, there are new techniques and resources that can be utilized to address these fundamental and critical questions for forensic engineering evaluation of TTC projects. Four categories are presented for data acquisition and information-gathering methods:

Engineering Solution 1: Field Investigation

When an involved party becomes aware of a major incident or potential claim situation, the immediate retention of a forensic engineering expert can be extremely beneficial for documentation and data preservation. A rapid response to the scene by the engineering data collection team allows the analyst to capture a snapshot of the TTC system before it has been changed by the ongoing flow of work activities. Specific technology applications for rapid response data collection include:

- Laser mapping (**Figure 1**) — Total station mapping can document the points in 3D space to identify the roadway geometry and locations of key TTC components directly in the area of the collision or incident. This serves as the basis for a scene diagram. However, this technology is not ideal for documenting all advanced warning and devices over miles of roadway.

Figure 1
Laser mapping of scene.

- Photography (**Figure 2**) — Visual documentation of the type, location, and orientation of all TTC devices is imperative. This task includes going back far enough to identify the beginning of the work zone for every direction of travel of an involved vehicle or pedestrian. As the roadway is likely to change as construction continues or is completed, it can be helpful to document photographs with permanent landmarks.

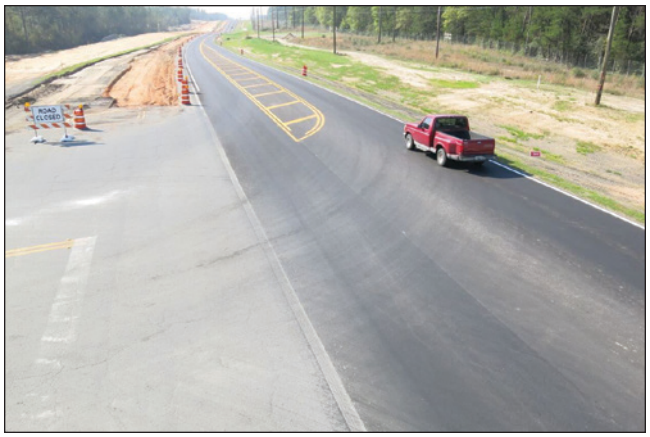

Figure 2
Photographs of scene.

- GPS coordinate data (**Figure 3**) — Collecting GPS coordinates of all TTC devices, along with major landmarks and roadway features, is a useful way to document locations and distances for future reference. This is especially helpful when major projects are going through large changes over time, which will eventually eradicate most visual landmarks or reference points.

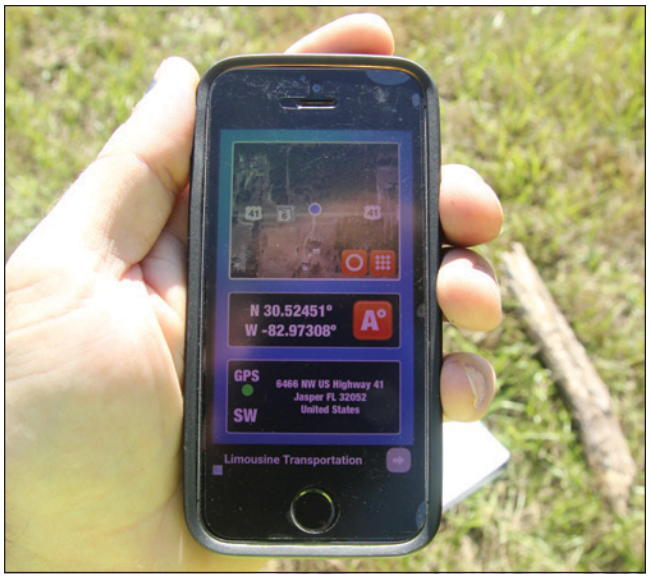

Figure 3
GPS coordinates of key data.

- Videography (**Figure 4**) — Drive-through videos can be a useful method of documenting all of the advanced warning, channelizing devices, and information conveyed by the work zone to motorists or pedestrians for each approach to the scene of the incident. Traffic observational study videos can document how motorists are behaving within the work zone and responding to the traffic control setup.

Figure 4
Scene drive-through video.

- Measurements – When relevant, the heights, widths, offsets, and sizes of TTC devices, work equipment, or sight line obstructions should be documented.

- 3D scanning (**Figure 5**) – Given the size and complexity of TTC systems, a full 3D scan of the entire environment can be an appropriate method for documenting all of the devices and roadway features. Modern 3D scanners create a cloud with millions of data points, which can be utilized for analysis or visualization.

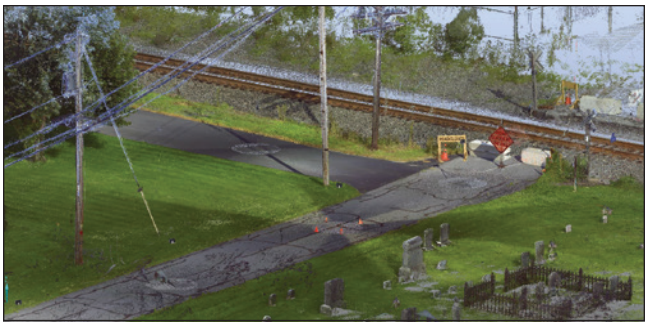

Figure 5
3-dimensional scanning.

- Aerial photography (**Figure 6**) — Some highway construction work zones, such as on major freeways in congested urban areas, cannot be safely documented with other methods. In such circumstances, an airplane or helicopter service (providing aerial photography with high resolution images) can be a source of data collection for roadway layouts and TTC devices (Dilich and Goebelbecker 1996) (Whelchel 2003). This is an especially useful method for projects that are very large or have many miles of TTC system.

Figure 6
Aerial photography of scene.

- Drones (**Figures 7** and **8**) — Remote-controlled high-resolution photography or videography can now be used in certain appropriate circumstances to document a TTC zone, offering many of the same advantages as piloted aerial

Figure 7
Drone photography.

Figure 9
Imprint of sign.

Figure 8
Drone photography.

Figure 10
Obliterated lane lines.

photography. It is expected that this technology will continue to evolve in the near future.

In circumstances when the forensic engineer is notified after there have already been changes made to the temporary condition of the roadway and traffic control devices, field investigation can still prove fruitful. Mapping or 3D scanning of the permanent roadway, landmarks, markings, and signs are an important basis for diagramming the scene, and will be used in combination with later techniques. Often, evidence of previous stages can still be found in the roadway environment. For example, there may be a darkened asphalt area where the base of a drum had been, or dead grass in the area of a portable changeable message sign (PCMS) trailer (**Figure 9**) had been. Obliterated pavement markings can usually be identified and mapped to determine their previous position (**Figure 10**). Station marking paint should also be documented for cross-reference with the project plans. A thorough field investigation may provide extensive insight into the previously existing TTC, even after the completion of the construction project.

Engineering Solution 2: Police and First Responder Materials

Police officers and other first responders have a unique opportunity to document the conditions of the construction project and TTC immediately after an incident occurs. However, the focus of their investigations usually is on the determination of criminal conduct and the provision of emergency and medical services. As such, there is a variety of detail and thoroughness to be found in the investigative materials of first responders.

The main difficulty faced, from a traffic engineering evaluation perspective, is that the first responders tend to be focused directly on the areas of impact and final rest — with little or no documentation of any advanced warning devices or the TTC in the area leading up to the incident location. In many cases, photographs are limited to the area within 100 feet upstream from the area of impact.

First responders sometimes actually create a greater challenge for the forensic engineer in determining the TTC that existed at the time of the incident because it is not uncommon for police or emergency services to either move the TTC devices to gain access with their vehicles and equipment or to move the work zone's TTC devices to provide traffic control around the incident investigation area. This should be considered when evaluating the TTC setup documented in first responder materials.

There may be important evidence and data captured in first responder materials, or there may be nothing of use. Some of the sources of data that can be extremely helpful, if they are available, include:

- Scene photography (**Figure 11**) — Some investigators thoroughly document an entire TTC system on approach, though this is not common. Even if the focus of the photograph is not on TTC, there may be documentation of the roadway and devices visible in the background.

Figure 11
Police scene photographs.

- Mapping and measurements (**Figure 12**) — Especially in serious injury or fatality cases, police investigators may use either a laser or wheel device to document the location of items, including lane markings, tapers, crash attenuators, barrier walls, signs, arrow panels, or channelizing devices. These can be incorporated into the forensic engineering diagram by tying in to a permanent landmark or reference points.

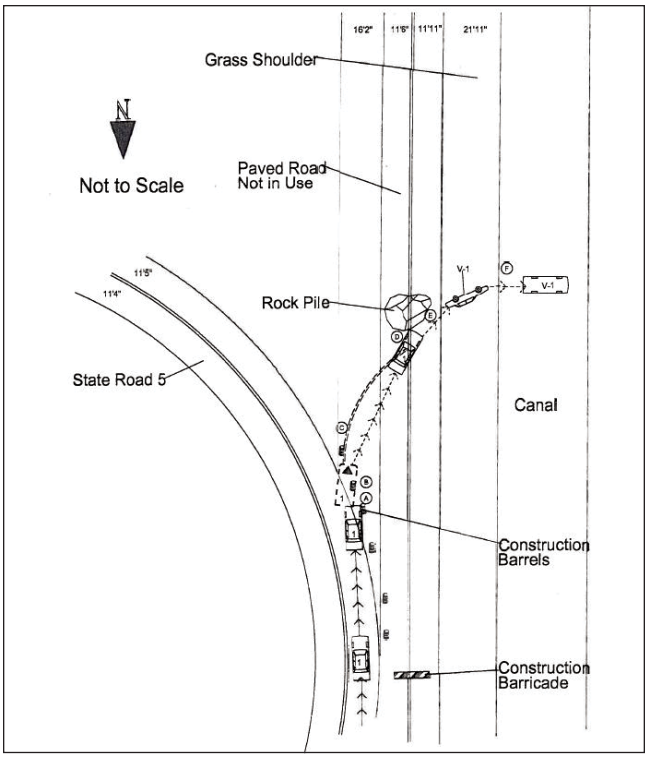

Figure 12
Police investigation measurements.

- Field notes — In some cases, police investigators may do a drive-through of the entire work zone and make written notes about the identification and location of various signs and devices. In other cases, there may be generalized references to signs and other TTC, but without specific locations provided.

- Dash cams (**Figure 13**) — If the police, fire, or emergency vehicles are equipped with a dashboard camera, they may inadvertently document the entire approach to the collision location as a side benefit. Some or all of the advanced warning signs, arrow panels, PCMSs, channelizing devices, taper locations, and other critical TTC information may be identified in the frames of the video as the vehicle proceeds. In some circumstances, the dash cam continues recording after the vehicle comes to a stop, and

Figure 13
Police dash camera footage.

might capture the post-incident relocation of existing TTC setups as first responders adjust to control traffic around the investigation area. One challenge with obtaining this type of documentation is getting a copy of the video footage before it is overwritten by future video.

Engineering Solution 3: Public Sources

With increases in the technologies adopted in our society, there has been a trend toward imagery becoming available from sources entirely unrelated to the subject incident. Many TTC cases have been forensically evaluated thoroughly, thanks to the fortuitous availability of video or photographic evidence. Though not comprehensive, these are some of the categories of public information sources that have been used to collect TTC data:

- Driver, witness, or passerby photography (**Figure 14**) — Whether with a digital camera, film camera, or cell phone, many incidents now have one or more photographs taken by someone other than law enforcement and first responders. Even if the focus of the photograph is not on TTC, there may be documentation of the roadway and devices visible in the background.

- News media (**Figure 15**) — Still photography or videography of an incident scene may be captured by media professionals and published in print, television, or online formats. A search for relevant news imagery may result in useful documentation of a temporary work zone TTC system. This is especially helpful when media crews use elevated camera positions or helicopter-based videographers to document large segments of the roadway.

Figure 14
Photo by unrelated passerby.

Figure 15
Photograph taken by media.

- Surveillance videos and dash cams (**Figure 16**) — Many private businesses and residences are equipped with security or surveillance cameras that may be pointed in a direction of interest for documenting the collision scene or roadway approach. Many commercial and private vehicle owners are choosing to install video camera data recorders in their vehicles, which can be manually triggered or can automatically trigger a recording when internal accelerometers indicate a collision event. Some units have multiple camera views, such as both forward and rearward. The video footage captured may

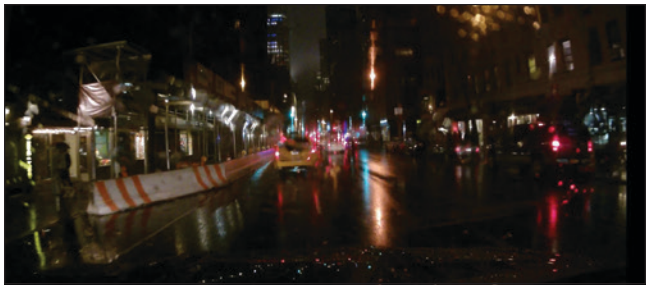

Figure 16
Surveillance / dash cam footage.

inadvertently document the entire approach to the collision location. Some or all of the advanced warning signs, arrow panels, PCMSs, channelizing devices, taper locations, and other critical TTC information may be identified in the frames of the video as the vehicle proceeds.

- Historical dated aerials (**Figure 17**) — Rectified aerial photographs of roadway environments are available from numerous public sources, including Google Earth, Microsoft Bing, TerraServer, and local government agencies (Wirth et al. 2015). Published research has indicated that these sources are typically adequately precise for taking scaled measurements. As most images are dated, it is possible to either find an aerial that captured the sequence of construction and the TTC in place for that phase, or at least to bracket the date of the incident with aerials from both before and after. Depending on the resolution of the imagery, it can be difficult in satellite aerial imagery to identify the legends of specific signs, but usually the pavement markings, channelizing devices, and large devices such as PCMS or arrow panels are well documented.

Figure 17
Dated aerial image.

- Historical dated photographs (**Figure 18**) — Services including Google and Bing also continue to publish photographs that are not from directly overhead, but instead from an orthogonal angle or from street level. These images, many of which are dated, provide a better opportunity to view the faces of signs and the locations of traffic signal heads, while also documenting the pavement markings, roadway geometry, and other TTC devices.

Figure 18
Dated street view image.

- Social media (**Figure 19**) — Occasionally, a private individual posts photos or videos of a roadway on social media sites such as YouTube. Sometimes passersby are documenting the incident aftermath. In one case, a motorcyclist videotaped his drive-through along a segment of roadway that happened to occur on the same day as a collision event. That video was not intended to investigate the TTC, but it captured each sign location along the way.

Figure 19
Social media footage.

Engineering Solution 4: Project Documents and Resources

Numerous documents are typically produced and retained as part of ongoing highway construction or building construction projects. Many of these documents also provide useful information in a forensic engineering context. Whether gathered directly from a client or through the court-directed production process, a thorough study of the documents should be

conducted to glean engineering data. Items of interest may include the stage of construction, the duration of a work phase, the location of work activities, the identity of individuals involved in specific tasks or inspections, the timing of TTC implementation, and the specific devices and locations for the TTC system. The following sources may provide engineering data relevant to the investigation:

- Contractor emergency response (**Figure 20**) — Some highway construction companies, construction engineer / inspection (CEI) firms, or governmental agency engineers respond to the scene of a major incident if they are aware of it occurring within their work zone. These individuals may photograph the location of the incident and the surrounding roadway environment in order to develop safety improvements and countermeasures — and in order to preserve this information in case of later claims or litigation.

Figure 20
Contractor emergency response image.

- Contractor drive-through videos (**Figure 21**) — Some contractors or governmental agencies routinely videotape drive-throughs of their large projects to document the ongoing work activities and TTC devices.

- Contractor progress aerials (**Figure 22**) — For major construction projects, an aerial photography company may be hired to conduct weekly or monthly routine progress aerials, documenting the stage of construction as well as the TTC system.

Figure 21
Contractor drive-through video.

Figure 22
Progress aerial.

- Contractor work photographs (**Figure 23**) — When issues arise with a construction activity, or major accomplishments are completed, some contractors or subcontractors will choose to photograph their work for documentation. If the TTC is visible in the background, these photos can be helpful as well for the forensic engineer.

Figure 23
Contractor work photographs.

- Post-collision reports (**Figures 24**) — Some state agencies require an investigation to be conducted following a known incident within a work zone. For example, the Florida Department of Transportation (FDOT) issues a standard form called "Engineer's Maintenance of Traffic Evaluation at Crash Site," which should be completed by the state's project engineer or their retained CEI professional. This document can include diagrams, measurements, data logs, or narrative descriptions.

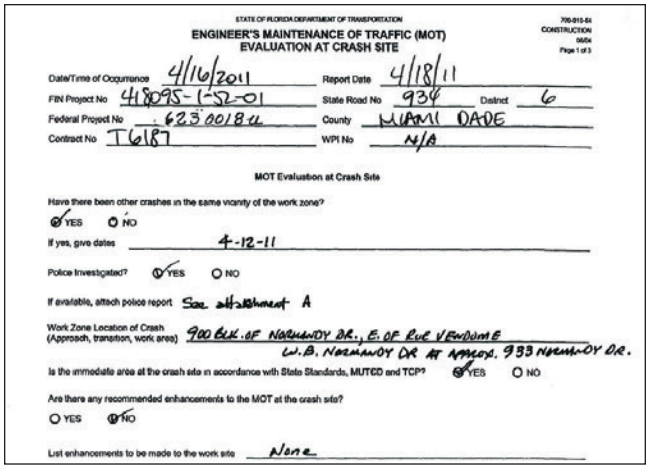

STATE OF FLORIDA DEPARTMENT OF TRANSPORTATION

700-010-04
CONSTRUCTION
09/04
Page 1 of 3

ENGINEER'S MAINTENANCE OF TRAFFIC (MOT) EVALUATION AT CRASH SITE

Date/Time of Occurrence: 4/16/2011 Report Date: 4/18/11
FIN Project No: 418095-1-52-01 State Road No: 934 District: 6
Federal Project No: 6230018A County: MIAMI DADE
Contract No: T6187 WPI No: N/A

MOT Evaluation at Crash Site

Have there been other crashes in the same vicinity of the work zone? (✓) YES ( ) NO
If yes, give dates: 4-12-11
Police Investigated? (✓) YES ( ) NO
If available, attach police report: See attachment A
Work Zone Location of Crash (Approach, transition, work area): 900 BLK. OF NORMANDY DR., E. OF RUE VENDOME
W.B. NORMANDY DR AT APPROX. 933 NORMANDY DR.
Is the immediate area at the crash site in accordance with State Standards, MUTCD and TCP? (✓) YES ( ) NO
Are there any recommended enhancements to the MOT at the crash site? ( ) YES (✓) NO
List enhancements to be made to the work site: None

Figure 24
Construction project post-collision evaluation.

- Daily reports of construction or daily time sheets (**Figure 25**) — Most governmental agencies require daily accounting of the work activities by all contractors, subcontractors, and equipment. This usually includes the location of work (either with general descriptions or station numbering), a description of the work, a numerical tabulation of quantities, and information about any discrepancies or unusual situations encountered.

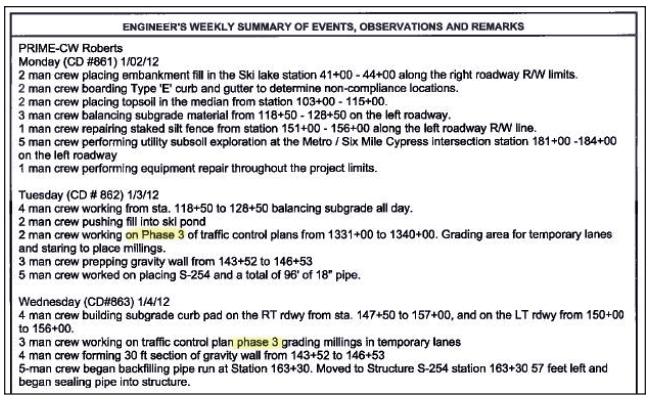

ENGINEER'S WEEKLY SUMMARY OF EVENTS, OBSERVATIONS AND REMARKS

PRIME-CW Roberts
Monday (CD #861) 1/02/12
2 man crew placing embankment fill in the Ski lake station 41+00 - 44+00 along the right roadway R/W limits.
2 man crew boarding Type 'E' curb and gutter to determine non-compliance locations.
2 man crew placing topsoil in the median from station 103+00 - 115+00.
3 man crew balancing subgrade material from 118+50 - 128+50 on the left roadway.
1 man crew repairing staked silt fence from station 151+00 - 156+00 along the left roadway R/W line.
5 man crew performing utility subsoil exploration at the Metro / Six Mile Cypress intersection station 181+00 -184+00 on the left roadway
1 man crew performing equipment repair throughout the project limits.

Tuesday (CD # 862) 1/3/12
4 man crew working from sta. 118+50 to 128+50 balancing subgrade all day.
2 man crew pushing fill into ski pond
2 man crew working on Phase 3 of traffic control plans from 1331+00 to 1340+00. Grading area for temporary lanes and staring to place millings.
3 man crew prepping gravity wall from 143+52 to 146+53
5 man crew worked on placing S-254 and a total of 96' of 18" pipe.

Wednesday (CD#863) 1/4/12
4 man crew building subgrade curb pad on the RT rdwy from sta. 147+50 to 157+00, and on the LT rdwy from 150+00 to 156+00.
3 man crew working on traffic control plan phase 3 grading millings in temporary lanes
4 man crew forming 30 ft section of gravity wall from 143+52 to 146+53
5-man crew began backfilling pipe run at Station 163+30. Moved to Structure S-254 station 163+30 57 feet left and began sealing pipe into structure.

Figure 25
Contractor daily report of construction.

- Project plans and specifications (**Figure 26**) — In situations with temporary detours or temporary roadway construction, the project plans can provide information about the roadway geometry of the temporary facility even if the temporary asphalt has been destroyed prior to being documented by the forensic engineer. The project plans also provide insight into the general phasing of the construction project, the traffic control setup intended by the design engineer, and context for the forensic engineer to consider when evaluating the overall TTC system.

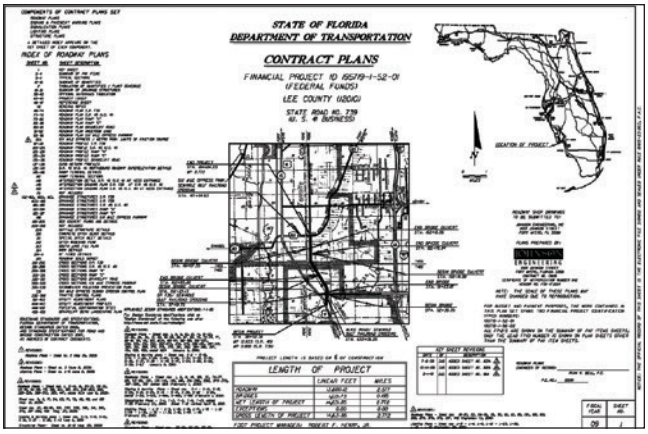

STATE OF FLORIDA
DEPARTMENT OF TRANSPORTATION

CONTRACT PLANS

FINANCIAL PROJECT ID 65719-1-52-01
(FEDERAL FUNDS)
LEE COUNTY (100G)
STATE ROAD NO. 739
(U. S. 41 BUSINESS)

LENGTH OF PROJECT

	LINEAR FEET	MILES
TOTAL LENGTH OF PROJECT		
LESS LENGTH OF BRIDGES		
NET LENGTH OF PROJECT		

Figure 26
Project plans and specifications.

Analyzing the TTC Data

As described in the introduction, the purpose of the forensic engineering data collection efforts is to generate a comprehensive understanding of the transportation system that existed for users at the time of a past incident. In order to be able to evaluate the information available to motorists, the effectiveness of the traffic control devices — and the appropriateness of the overall TTC system — the forensic engineer needs to complete a tabulated list of TTC devices and a graphical representation of the roadway environment. The goal is a thorough and accurate scaled diagram, depicting all of the aspects of the transportation system through the TTC zone (**Figure 27**).

After gathering data using the engineering solutions listed above, engineering processing and analysis of the data is still necessary to convert raw data into a usable format. For example, photographs of roads and signs are useful data, but they need to be processed to convert the information into spatial coordinates. Some photographic data is easily incorporated into a scene diagram based on permanent landmark references or

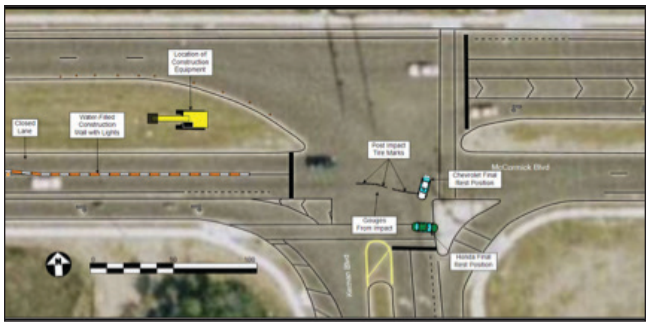

Figure 27
Scaled diagram of TTC zone.

photo-matching methods. In complex scenes, greater precision can be accomplished utilizing one of multiple photogrammetry techniques (Fenton and Kerr 1997) (Hicks 1999) (Ziernicki 2000) (Fenton et al. 2001) (Danaher and Ziernicki 2007) (Randles et al. 2010). Many forms of photogrammetry are reliant upon known locations of existing structures in the photographs and videos. Examples of these existing structures include lane lines lengths and widths, trees, permanent signage, or buildings. Once the positions of known objects within a photograph or video are determined, the TTC devices that were temporary and no longer available for documentation can still be located within 3-dimensional space. There are numerous computer programs that will assist an analyst in performing the photogrammetry analysis, such as Photomodeler (from Eos Systems Inc.) or iWitness (from DCS Inc.), or the analysis can be done in some circumstances by hand, utilizing parallel lines and similar triangles. In especially complicated cases, the entire geometry of a temporary roadway, which may have existed only for a short period of time during one phase of a construction project, can be re-created in 3-dimensional space utilizing photogrammetry processing.

After all the photographic, coordinate, and narrative data has been compiled from all available sources, the final product is a to-scale scene diagram. This creates the overall visual reference for subsequent steps of the forensic engineering analysis of the TTC system, including evaluating whether safety countermeasures can be developed, and whether the work zone was in compliance with applicable plans, guidelines, and standards at the time of the incident. First, the diagram should include "re-building" the roadway geometry as it was at the time of the incident, including historical aerials in the background. The diagram should extend sufficiently far in every direction to incorporate the relevant transportation engineering context, and should include related items such as hills, curves, intersections, interchanges, sight distance obstructions, and roadside obstacles. Additional data that can be added to the diagram, if available, include police measurements, to-scale police diagrams, and laser scene mapping of roadway geometry and temporary traffic control devices. Coordinates of items developed through photogrammetry analysis of photos or videos can be added as another layer of data, including signs and markings, channelizing devices, traffic signals, or other TTC devices. If coordinating with a collision reconstruction, the transportation engineer can include pertinent information from the subject collision in the overall diagram, such as points of impact, sight lines, critical decision points, and a distance-time line to evaluate the information available to each motorist as they traversed the work zone prior to impact. In addition to assisting with the analysis process for the engineer, a completed diagram serves as a visual communications tool for educating clients, juries, attorneys and claims personnel regarding the roadway environment and TTC system as it existed on the date of the subject incident.

Another communication technique that can be especially effective for these temporary roadway conditions is a 3-dimensional recreation of the scene, either as a static image 3D rendering or in the form of a real-time moving animation (**Figure 28**). In many cases, this is the only way to visually depict the actual TTC condition as it existed at the time of the incident, since everything was changed prior to documentation. An animation brings together the vehicle motions from the collision reconstruction with the forensic engineering evaluation of the TTC setup, and places the viewer in a position to see a realistic perspective from various viewpoints in real time (**Figure 29**). For example, the animation may depict the viewpoint of an involved driver as he or she passes by each of the advanced warning signs and continues without slowing down before ultimately crashing into a queue of stopped vehicles ahead. The type of animation selected will vary widely based on case-specific facts, but can be a very effective tool for demonstrating the final opinions and conclusions of the forensic engineer when based on a thoroughly documented process described above for collecting and analyzing data from new technology sources.

Figure 28
3D Visualization of TTC zone.

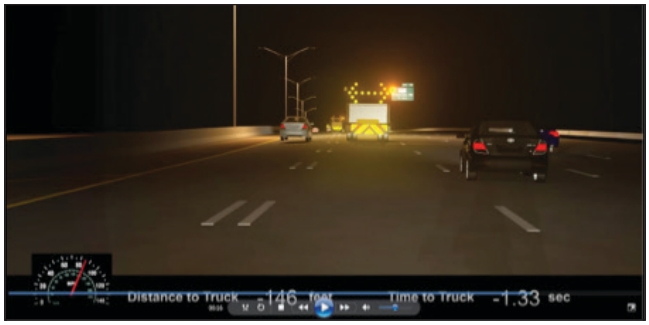

Figure 29
3D Visualization of TTC zone.

Conclusion

Forensic engineering cases involving the evaluation of temporary traffic control issues are inherently challenging due to the changeability and short-term nature of the scenes. They are further complicated by the large-scale geography, complexity, and multi-party aspects of the claims. However, many of the new technological developments that were presented throughout this paper can be leveraged to the advantage of the forensic engineer in order to gather data, process geospatial information, and accomplish a thorough re-creation of how the roadway environment and TTC system existed at the time of the subject incident. Use of these technologies improves opportunities to develop safety improvements, identify deficiencies, or develop professional engineering conclusions regarding the work zone's role in a specific incident.

Additional technologies and methodologies have also been developed to aid in the engineering analysis and the final communication of opinions and conclusions. Moving forward, it is likely that more sources of video and still imagery will proliferate, making these techniques critical for the effective forensic engineering evaluation of transportation safety incidents.

Bibliography

Danaher D, Ziernicki R. Forensic engineering evaluation of physical evidence in accident reconstruction. Journal of the National Academy of Forensic Engineers. 2007;24(2):1.

Dilich M, Goebelbecker J. Accident investigation and reconstruction mapping with aerial photography. SAE Technical Paper 960894. Warrendale, PA; Society of Automotive Engineers: 1996.

Fenton S, Kerr R. Accident scene diagramming using new photogrammetric technique. SAE Technical Paper 970944. Warrendale, PA; Society of Automotive Engineers: 1997.

Fenton S, Neale W, Rose N, Hughes C. Determining crash data using camera-matching photogrammetric technique. SAE Technical Paper 2001-01-3313. Warrendale, PA; Society of Automotive Engineers: 2001.

Hicks J. Examples of the use of photogrammetry in forensic engineering and accident reconstruction. Journal of the National Academy of Forensic Engineers. 1999;16(2).

Hintersteiner R. Forensic engineering: highway construction work zone accidents. Journal of the National Academy of Forensic Engineers. 2008;25(1).

Manual on uniform traffic control devices. Washington DC; Federal Highway Administration: 2009.

Randles B, Jones B, Welcher J, Szabo T, Elliott D, MacAdams C. The accuracy of photogrammetry vs. hands-on measurement techniques used in accident reconstruction. SAE Technical Paper 2010-01-0065. Warrendale, PA; Society of Automotive Engineers: 2010.

Whelchel M. Forensic engineering use of aerial photography in accident reconstruction. Journal of the National Academy of Forensic Engineers. 2003;20(1).

Wirth J, Bonugli E, Freund M. Assessment of the accuracy of Google Earth imagery for use as a tool in accident reconstruction. SAE Technical Paper 2015-01-1435. Warrendale, PA; Society of Automotive Engineers: 2015.

Ziernicki R. Forensic engineering comparison of two & three dimensional photogrammetric accident analysis. Journal of the National Academy of Forensic Engineers. 2000;17(1).